Heliyon 10 (2024) e32911

Contents lists available at ScienceDirect

Heliyon

journal homepage: www.cell.com/heliyon

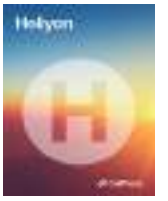

Research article

Many-objective ant lion optimizer (MaOALO): A new many-objective optimizer with its engineering applications

Kanak Kalita [a,b,*], Sundaram B. Pandya [c], Robert Čep [d,**], Pradeep Jangir [e], Laith Abualigah [f,g,h,i,j]

[a] Department of Mechanical Engineering, Vel Tech Rangarajan Dr. Sagunthala R&D Institute of Science and Technology, Avadi, 600 062, India
[b] University Centre for Research & Development, Chandigarh University, Mohali, 140413, India
[c] Department of Electrical Engineering, Shri K.J. Polytechnic, Bharuch, 392 001, India
[d] Department of Machining, Assembly and Engineering Metrology, Faculty of Mechanical Engineering, VSB-Technical University of Ostrava, 70800, Ostrava, Czech Republic
[e] Department of Biosciences, Saveetha School of Engineering. Saveetha Institute of Medical and Technical Sciences, Chennai, 602 105, India
[f] Computer Science Department, Al Al-Bayt University, Mafraq, 25113, Jordan
[g] MEU Research Unit, Middle East University, Amman, 11831, Jordan
[h] Applied Science Research Center, Applied Science Private University, Amman, 11931, Jordan
[i] Jadara Research Center, Jadara University, Irbid, 21110, Jordan
[j] Artificial Intelligence and Sensing Technologies (AIST) Research Center, University of Tabuk, Tabuk, 71491, Saudi Arabia

ARTICLE INFO

Keywords:
Many-objective optimization
MaF benchmark
Ant lion optimizer
Convergence
Diversity

ABSTRACT

Many-objective optimization (MaO) is an important aspect of engineering scenarios. In many-objective optimization algorithms (MaOAs), a key challenge is to strike a balance between diversity and convergence. MaOAs employs various tactics to either enhance selection pressure for better convergence and/or implements additional measures for sustaining diversity. With increase in number of objectives, the process becomes more complex, mainly due to challenges in achieving convergence during population selection. This paper introduces a novel Many-Objective Ant Lion Optimizer (MaOALO), featuring the widely-popular ant lion optimizer algorithm. This method utilizes reference point, niche preserve and information feedback mechanism (IFM), to enhance the convergence and diversity of the population. Extensive experimental tests on five real-world (RWMaOP1- RWMaOP5) optimization problems and standard problem classes, including MaF1-MaF15 (for 5, 9 and 15 objectives), DTLZ1-DTLZ7 (for 8 objectives) has been carried out. It is shown that MaOALO is superior compared to ARMOEA, NSGA-III, MaOTLBO, RVEA, MaOABC-TA, DSAE, RL-RVEA and MaOEA-IH algorithms in terms of GD, IGD, SP, SD, HV and RT metrics. The MaOALO source code is available at: https://github.com/kanak02/MaOALO.

* Corresponding author. Department of Mechanical Engineering, Vel Tech Rangarajan Dr. Sagunthala R&D Institute of Science and Technology, Avadi 600 062, India.
** Corresponding author.
E-mail addresses: drkanakkalita@veltech.edu.in, kanakkalita02@gmail.com (K. Kalita), sundarampandya@gmail.com (S.B. Pandya), robert.cep@vsb.cz (R. Čep), pkjmtech@gmail.com (P. Jangir), aligah.2020@gmail.com (L. Abualigah).

https://doi.org/10.1016/j.heliyon.2024.e32911
Received 27 March 2024; Received in revised form 7 June 2024; Accepted 11 June 2024
Available online 17 June 2024

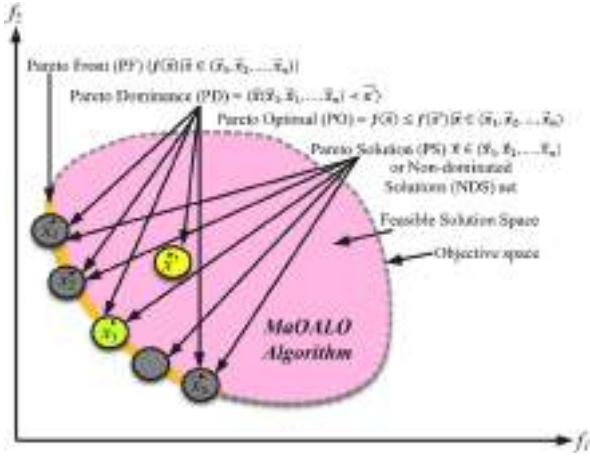

Fig. 1. Many-Objective all definitions in search space of MaO-Problem.

1. Introduction

Most real-world optimization problems are immensely complex as they require balancing several conflicting objectives at once [1]. These are known as multi-objective optimization problems (MOPs) [2]. In cases involving more than three objectives, these are referred to as many-objective optimization problems (MaOPs) [3]. Such problems [4], whether MOPs or MaOPs, can be defined as [5]:

$$\begin{aligned} &\textit{Minimize} : F(\mathbf{x}) = (f_1(\mathbf{x}), f_2(\mathbf{x}), \ldots, f_m(\mathbf{x}))^T \\ &\textit{Subjetc to} : g_j(\mathbf{x}) \geq 0, j = 1, 2, \ldots, P \\ &h_k(\mathbf{x}) = 0, k = 1, 2, \ldots, Q \\ &\mathbf{x} \in \Omega \end{aligned} \tag{1}$$

Here, m is the count of competing objectives, $\mathbf{x} = (x_1, x_2, \ldots, x_d)^T \in \Omega$ is a vector containing d decision variables and Ω defines the decision space. Additionally, the terms P and Q denote the quantity of inequality and equality constraints, respectively. The vector encapsulates the conflicting objectives, set within an objective space. Due to the inherent conflicts among various objectives in MOPs and MaOPs, it is often unfeasible to discover a single solution that optimizes all objectives simultaneously. Rather, it is possible to identify a set of solutions that are equally optimal, known as the Pareto optimal set (PS) [6]. The projection of this set in the objective space is referred to as the Pareto optimal front (PF) as shown in Fig. 1.

MaOPs are complex problems encountered in various engineering and scientific disciplines, characterized by having more than three conflicting objectives that need to be optimized simultaneously. Unlike traditional optimization problems that may involve only one or two objectives, MaOPs present a unique set of challenges due to the high-dimensional nature of their objective space. This complexity is common in real-world applications such as aerospace engineering, automotive design and environmental management, where trade-offs among numerous performance metrics must be carefully balanced. One of the primary challenges in MaOPs is achieving an effective balance between convergence to the Pareto-optimal front and maintaining a diverse set of solutions across the entire objective space. Convergence ensures that the solutions approach the true set of optimal solutions (Pareto front), which is crucial for the reliability and robustness of the outcomes. On the other hand, diversity is essential to explore various trade-off solutions, providing decision-makers with a broad perspective of available options to accommodate different preferences or unforeseen changes in scenarios. The difficulty in balancing these aspects arises from the fact that improving convergence often leads to a loss in diversity and vice versa. This interplay complicates the development of algorithms capable of sustaining performance across these dual objectives, particularly as the number of objectives increases. Traditional Pareto dominance, which is effective in lower-dimensional objective spaces, becomes less effective in MaOPs due to a phenomenon known as dominance resistance, where many solutions may appear non-dominated simply due to the sheer number of objectives.

In practical scenarios, a significant number of challenges are classified as MaOPs, which involve optimizing more than three objectives concurrently. Recently there has been significant interest among researchers to develop and apply metaheuristic for MaOPs. Zhang et al. [7] presented SDE + -MOEA, an efficient MaOEA that combines selection methods adaptively. Their comparative study with several other algorithms SDE + -MOEA offers better or at par performance in terms of convergence, uniformity and spread. Similarly, Wu et al. [8] proposed MaOITGO-CO for vehicular edge computing networks, leveraging various search strategies. Following this trend, Li et al. [9] designed MaOCO coupled with MaOEA-DS for edge computing, focusing on diverse offloading objectives. Ming et al. [10] introduced CPBI for constrained MaOPs, optimizing convergence, diversity and feasibility. Zhang et al. [11] proposed MaOEA-FEGL in which they integrated a fitness estimation mechanism for improving convergence and diversity.

In recent times, several algorithms have been developed for computation offloading and edge computing. Shi et al. [12] introduced the I-MaOWMUE and MI-MaOEA algorithm for workflow migration in uncertain edge computing environments which addresses task

Table 1
key features and contributions of the recent MaOEAs.

Algorithm Type	Key Features	Contributions
Clustering-Based MaOEAs	Utilizes clustering for diversity and convergence	Enhances diversity, adaptively adjusts clustering
Dynamic Decomposition-Based MaOEAs	Decomposes problems dynamically	Improves convergence, handles imprecision
SDE + -MOEA	Adaptive selection methods	Better convergence, uniformity, spread
MaOITGO-CO	Various search strategies	Optimizes vehicular edge computing networks
CPBI	Optimizes convergence, diversity, feasibility	Effective for constrained MaOPs
I-MaOWMUE and MI-MaOEA	Addresses task dependencies, energy consumption	Suitable for uncertain edge computing environments
Surrogate-assisted evolutionary algorithms	Leverage surrogate models	Effective for expensive MaOPs
Preference-inspired algorithms	Focus on preference incorporation	Improves solution quality

dependencies and energy consumption. On the other hand, some researchers have focused on integration of surrogate models and adaptive strategies. Zhai et al. [13] developed a surrogate-assisted evolutionary algorithm for expensive MaOPs. Palakonda and Kang [14] introduced Pre-DEMO with a preference-inspired mutation operator and an adaptive strategy for local knee points.

Application in specific domains like recommendation systems and cancer prediction has also been explored by some researcher using many objective strategies. Sun et al. [15] proposed a many-objective recommendation algorithm using game theory and evolutionary computation. Cai et al. [16] on the other hand developed a hybrid tensor decomposition model for predicting miRNA-skin cancer associations.

The development of many objective algorithms with specific focus on preference incorporation and adaptation methods is also hot area among researchers. In this line, Wang et al. [17] proposed a preference-inspired coevolutionary algorithm, PICEA-g/SAE. Márquez-Vega et al. [18] introduced AdaK which is a reference set adaptation method for MOEAs on MOPs with irregular Pareto fronts.

Several recent studies have been conducted that aim to address a balance between convergence and diversity. Ye et al. [19] proposed MaOABC-TA, an improved two-archive many-objective ABC algorithm to address these challenges. Their approach used convergence and diversity archives with three search strategies. On the other hand, Liu et al. [20] proposed a hyper-dominance degree-based evolutionary algorithm for this balance. Similarly, Zhang et al. [21] developed 3DEA, a dual distance dominance based evolutionary algorithm. Their approach used a dynamic niche size and a selection-replacement operator to maintain diversity and convergence. Sun et al. [22] developed MaOEA/D-AEW with adaptive external population guided weight vector adjustment. Dai et al. [23] introduced a point crowding-degree strategy in their PCEA for MaOPs. Jameel and Abouhawwash [24] proposed a novel KKTPM using the PBI method for evaluating algorithms without requiring prior knowledge of the Pareto-optimal front. Liang et al. [25] presented an information entropy-driven evolutionary algorithm with reinforcement learning for MaOPs with irregular Pareto fronts.

One of the prime challenges in MaOPs is inadequacy of traditional Pareto dominance [26], which is often used as the default measure in multi-objective optimization problems (MOPs) [27]. As the number of objectives increase, the likelihood of one solution dominating another diminishes [28,29] which makes it difficult to identify superior solutions using Pareto dominance relations [30]. A unique dilemma in MaOPs is the emergence of dominance-resistant solutions (DRSs) [31]— solutions which are poor in one objective but excel in others. These solutions seldom get dominated by others thereby causing a serious challenge to the effectiveness of Pareto dominance in MaOPs.

To overcome these issues, recent researches have proposed various approaches which can be broadly categorized into three strategies. The first strategy modifies the Pareto dominance relation to enhance convergence, employing techniques like the self-controlling dominance area of solutions (S-CDAS) [32] and the generalization of Pareto-optimality (GPO) [33]. Innovative methods like grid-dominance [34] and shift-based density estimation (SDE) [35] have also been introduced to reflect population convergence and maintain diversity.

The second strategy involves performance indicators like the hypervolume (HV) [36], which assesses both convergence and diversity of solutions. However, the computational intensity of HV has led researchers to explore alternatives like the unary epsilon indicator [37] and adaptive scalarizing function-based fitness evaluation [38].

The third strategy uses reference vector-based methods to maintain diversity in solutions [39–42]. These methods are effective in generating well-distributed solutions but face challenge in balancing convergence and diversity. This problem is more prominent in MOPs with irregular Pareto fronts.

Despite these advancements, MaOPs remain a challenging domain, particularly in balancing convergence and diversity. Algorithms like the NSGA–II–SDR [43] and NSGA-III [44] exhibit limitations in either overdominance or insufficient convergence in MaOPs with a large number of objectives. Consequently, most many-objective evolutionary algorithms (MaOEAs) struggle to maintain performance as the number of objectives increases, as seen in cases like the novel multi-objective particle swarm optimization (NMPSO) [45,46].

Lin et al. [47] utilizes clustering techniques to enhance diversity and convergence by grouping similar solutions and guiding the search process towards less crowded areas of the objective space. Similarly, Liu et al. [48] adaptively adjusts the clustering process based on the current state of the population, improving the balance between convergence and diversity. Liu et al. [49] in another study carry out the clustering during the environmental selection phase to maintain a diverse set of high-quality solutions. Other similar attempts has been made with dynamic decomposition-based MaOEA [50], fuzzy decomposition used fuzzy logic [51], self-guided reference vector strategy [52,53] etc. Table 1 provides a summary of the recent advancements in MaOEAs, highlighting their key features and contributions.

To address the above-mentioned issues, this paper introduces an innovative algorithm, termed the Many-objective Ant Lion Optimizer (MaOALO). MaOALO, a many-objective optimization algorithm, incorporates Ant Lion Optimizer (ALO) [54], Information Feedback Mechanism, Reference Point-Based Selection and Association, Non-dominated Sorting, Niche Preservation and Density Estimation. The paper key contributions are as follows.

1) ALO is selected as the base algorithm to build the many-objective version. The selection of ALO algorithm is based its wide popularity among the scientific community and its ability to tackle diverse problems. Moreover, ALO is known to be superior in generating diverse and high-quality solutions in single objective problems.
2) An Information Feedback Mechanism (IFM) strategy is introduced for the addressing the shortcomings that had wasted a lot of useful information. In the IFM, the combined historical information of individuals based on the weighted sum method are carried over to the next generation. This ensures that superior convergence properties.
3) A reference vector-based strategy for diversity preservation is used. This strategy associates each solution with the closest reference vector in terms of perpendicular distance, facilitating the identification and removal of solutions with inadequate diversity, thereby maintaining a diverse solution set. Non-dominated sorting method ensures that the algorithm focuses on solutions that are closer to the Pareto-optimal front, aiding convergence.
4) A niche preservation strategy to measure solution convergence within the population. A solution relative convergence quality compared to others, identifying solutions with poor convergence via a niche preservation. Additionally, a density estimation strategy for maintaining diversity is detailed, ensuring both uniformity and extensive coverage in the population distribution.
5) The effectiveness of the newly developed MaOALO is validated through comparisons with ARMOEA, NSGA-III, MaOTLBO and RVEA algorithms across MaF1-MaF15 (for 5, 9 and 15 objectives), MaOABC-TA, DSAE, RL-RVEA and MaOEA-IH algorithms across DTLZ1-DTLZ7 (for 8 objectives) and five real-world (RWMaOP1- RWMaOP5) problems.

The remainder of the paper is structured as follows: Section 2 provides an overview of ALO algorithm. Section 3 details the proposed MaOALO algorithm. Section 4 presents numerical simulations and analyses, comparing MaOALO with other leading many-objective optimization algorithms. Finally, Section 5 concludes the paper.

2. Ant lion optimizer

Mirjalili developed ALO [54], a novel approach in swarm intelligence optimization algorithms, is inspired by the predatory tactics of ant lions in the wild. These creatures create circular paths in the sand using their mandibles to craft traps for ants. Upon ensnaring an ant, they consume it, rebuild their trap and await their next victim. In the ALO algorithm, the ant lions represent solutions to a problem. The solutions are improved and maintained by 'hunting' ants, symbolizing high-fitness elements. The selection of the ALO as the foundation for the development of MaOALO is underpinned by several key features of ALO that make it particularly suitable for addressing the complex challenges posed by MaOPs. ALO, inspired by the hunting mechanism of ant lions in nature, incorporates several mechanisms that align well with the needs of many-objective optimization.

1. **Diverse Search Capabilities:** ALO is known for its ability to maintain and explore a diverse set of solutions effectively. The random walks of ants, which represent potential solutions, are influenced by the position and fitness of the ant lions. This dynamic interaction facilitates a broad exploration of the search space, reducing the risk of premature convergence to suboptimal regions. This capability is crucial in MaOPs, where the search space becomes exponentially complex with the increase in objectives.
2. **Robustness to Parameter Settings:** ALO exhibits a high degree of robustness with respect to its parameter settings, making it less sensitive to initial conditions and thus more reliable in diverse problem landscapes. This robustness is vital for MaOPs, where the ideal parameter settings can vary significantly between different problem instances.
3. **Balance Between Exploration and Exploitation:** ALO naturally balances exploration (searching new areas) and exploitation (refining existing solutions), due to its adaptive trapping mechanism where the width of the trap adapts based on the fitness of the ant lion. This dynamic adjustment is analogous to controlling the diversity and convergence in MaOPs, making ALO a suitable candidate for extension to many-objective contexts.
4. **Ease of Integration with Other Techniques:** The procedural structure of ALO allows for easy integration with other optimization techniques. This adaptability is leveraged in MaOALO by incorporating an Information Feedback Mechanism (IFM) and a reference vector-based selection strategy, enhancing its effectiveness in handling multiple objectives.

The optimization procedure in ALO follows these principles.

- Ants traverse the search space through varied random walks which are influenced by the traps' locations.
- An ant lion trap size, linked to its fitness level is proportion to its probability of capturing ants.
- As ants approach ant lions, the scope of their random walk narrows.
- After a successful hunt, ant lions relocate and reconstruct their traps to adapt to the new circumstances.

The quantity of ant lions mirror that of ants. To replicate the ant-ant lion interactions, ants navigate the search space, evading or encountering traps via random walks. Elite ant lions, exhibiting superior predatory efficiency, capture more prey. Ants' movements are also swayed by the positions of both typical and elite ant lions. Learning from these interactions, ants adjust their positions, enhancing

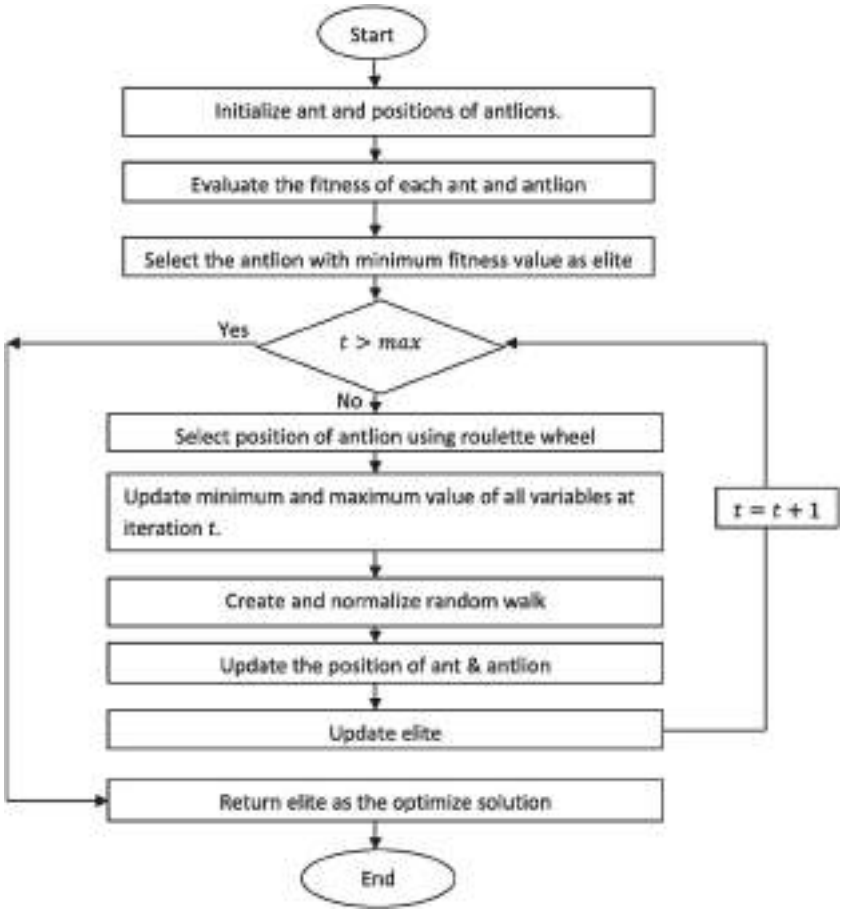

Fig. 2. Flowchart of ALO algorithm.

the group diversity and optimization capacity. This random walk as follows:

$$X(t) = [0, cumsum(2r(t_1) - 1), cumsum(2r(t_2) - 1), \cdots, cumsum(2r(t_n) - 1)] \tag{2}$$

where *cumsum* calculates cumulative and $r(\mathrm{t})$ is a stochastic function obtained as follows:

$$r(\mathrm{t}) = \begin{cases} 1 \; if \; rand > 0.5 \\ 0 \; if \; rand \leq 0.5 \end{cases} \tag{3}$$

In ALO, ant positions are represented through a matrix configuration as shown below

$$M_{Ant} = \begin{bmatrix} A_{11} & \cdots & A_{1d} \\ \vdots & \ddots & \vdots \\ A_{n1} & \cdots & A_{nd} \end{bmatrix} \tag{4}$$

Furthermore, the fitness level for each ant is determined by a specific method.

$$\mathrm{M}_{Ant\_f} = \begin{bmatrix} f([A_{11}, A_{12}, \cdots A_{1d}]) \\ \vdots \\ f([A_{n1}, A_{n2}, \cdots A_{nd}]) \end{bmatrix} \tag{5}$$

It also important to note that both the positions and fitness levels of antlions are ascertained using a distinct approach.

$$M_{Antlion} = \begin{bmatrix} AL_{11} & \cdots & AL_{1d} \\ \vdots & \ddots & \vdots \\ AL_{n1} & \cdots & AL_{nd} \end{bmatrix} \tag{6}$$

$$M_{Antlion\_f} = \begin{bmatrix} f([AL_{11}, AL_{12}, \cdots AL_{1d}]) \\ \vdots \\ f([AL_{n1}, AL_{n2}, \cdots AL_{nd}]) \end{bmatrix} \tag{7}$$

During the optimization process, ants alter their positions via a stochastic walk, which is revised in every iteration. The steps of this random walk are standardized through the min-max normalization technique, ensuring the walk proportionality within the feature space.

$$X_i^t = \frac{(X_i^t - a_i) \times (d_i - c_i^t)}{(d_i^t - a_i)} + c_i \tag{8}$$

To theoretically represent the concept that ant lions' traps impact the ants' random walks, a pair of formulas is introduced.

$$d_i^t = Antlion_j^t + d^t, c_i^t = Antlion_j^t + c^t \tag{9}$$

Similarly, to conceptualize the hunting strategy of the antlions, another set of equations is introduced.

$$c^t = \frac{c^t}{I} \tag{10}$$

$$d^t = \frac{d^t}{I} \tag{11}$$

In these equations, I represents a proportion, $I = 10^w \frac{t}{T}$ while w is a fixed value determined by the prevailing generation. The antlions' mechanism of capturing prey and subsequently reconstructing their pits is explained by Equation (12).

$$Antlion_j^t = Ant_i^t iff(Ant_i^t) > f\left(Antlion_j^t\right) \tag{12}$$

Additionally, the most effective agent identified in each generation is considered as the elite. This leads to the assumption that all agents have the capability to perform random walks in the vicinity of a selected agent, which is determined based on a roulette wheel methodology

$$Ant_i^t = \frac{R_A^t + R_E^t}{2} \tag{13}$$

The ALO algorithm process is depicted in Fig. 2.

3. Proposed many-objective ant lion optimizer (MaOALO)

To specifically address the many-objective optimization challenges, MaOALO modifies and extends ALO with the following components.

1. **Information Feedback Mechanism (IFM):** To counteract the loss of potentially valuable solutions and to ensure that good features of past solutions are carried forward, IFM uses historical performance data to guide the search process. This mechanism enhances convergence by preserving and utilizing quality traits from generation to generation.
2. **Reference Vector-Based Selection:** This strategy helps maintain a diverse set of solutions by associating each solution with a reference vector based on the closest perpendicular distance. This approach ensures that the solution set covers the entire objective space, which is critical in many-objective optimization to provide a well-rounded set of trade-off solutions.
3. **Niche Preservation and Density Estimation:** These techniques are integrated to maintain diversity within the population, preventing the dominance of any particular region of the search space and promoting an even spread across the Pareto front.

By adapting ALO, which is inherently strong in generating diverse and high-quality solutions, MaOALO is designed to meet the dual requirements of convergence and diversity, which are pivotal for solving MaOPs effectively. MaOALO algorithm starts with a random population of size N, M no. of objectives, p no. of partitions and generate a set of reference points using Das and Dennis technique $H = \binom{M+p-1}{p}$, as $H \approx N$. the current generation is t, x_i^t and x_i^{t+1} the *i-th* individual at t and $(t+1)$ generation. u_i^{t+1} the *i-th* individual at the $(t+1)$ generation generated through the ALO algorithm and parent population P_t. the fitness value of u_i^{t+1} is f_i^{t+1} and U^{t+1} is the set of u_i^{t+1}. Then, we can calculate x_i^{t+1} according to u_i^{t+1} generated through the ALO algorithm and information feedback mechanism (IFM) Eq. (14)

$$x_i^{t+1} = \partial_1 u_i^{t+1} + \partial_2 x_k^t;\ \partial_1 = \frac{f_k^t}{f_i^{t+1} + f_k^t}, \partial_2 = \frac{f_i^{t+1}}{f_i^{t+1} + f_k^t}, \partial_1 + \partial_2 = 1 \tag{14}$$

where x_k^t is the k th individual we chose from the t th generation, the fitness value of x_k^t is f_k^t, ∂_1 and ∂_2 are weight coefficients. Generate offspring population Q_t. Q_t is the set of x_i^{t+1}. The combined population $R_t = P_t \cup Q_t$ is sorted into different w-non-dominant levels (F_1,

$F_2,\ldots,F_l\ldots,F_w$). Begin from F_1, all individuals in level 1 to l are added to S_t and remaining members of R_t are rejected. If $|S_t| = N$; no other actions are required and the next generation is begun with $P_{t+1} = S_t$. Otherwise, solutions in S_t/F_l are included in $P_{t+1} = S_t/F_l$ and the rest $(K = N - |P_{t+1}|)$ individuals are selected from the last front F_l (presented in Algorithm 1). For selecting individuals from F_l, we use a niche-preserving operator First, each population member of P_{t+1} and F_l is normalized (presented in Algorithm 2) by using the current population spread so that all objective vectors and reference points have commensurate values. Thereafter, each member of P_{t+1} and F_l is associated (presented in Algorithm 3) with a specific reference point by using the shortest perpendicular distance $(d())$ of each population member with a reference line created by joining the origin with a supplied reference point. Then, a careful niching strategy (described in Algorithm 5) that improve the diversity of MaOALO algorithm is employed to choose those F_l members that are associated with the least represented reference points niche count ρ_j in P_{t+1} and check termination condition is met. If the termination condition is not satisfied, $t = t + 1$ than repeat and if it is satisfied, P_{t+1} is generated, it is then applied to generate a new population Q_{t+1} by ALO algorithm. Such a careful selection strategy is found to computational complexity of M-Objectives $O\left(N^2 \log^{M-2} N\right)$ or $O(N^2M)$, whichever is larger. MaOALO algorithm that incorporates information feedback mechanism (IFM) to effectively guide the search process, ensuring a balance between exploration and exploitation. This leads to improved convergence, coverage and diversity preservation, which are crucial aspects of many-objective optimization. MaOALO algorithm does not require to set any new parameter other than the usual ALO parameters such as the population size, termination parameter and their associated parameters.

Algorithm 1 Generation t of MaOALO Algorithm with IFM Procedure

Input: N (Population Size), M (No. of Objectives), ALO algorithm parameters, and Initial population $P_t(t=0)$.

Output: Q_{t+1} = **ALO(** P_{t+1}**)**

1: H Calculated using Das and Dennis's technique, structured reference points Z^r, supplied aspiration points Z^a, $S_t = \phi$, $i = 1$

2: **Proposed Information Feedback Mechanism (IFM)**

ALO algorithm apply on the initial population P_t to generate u_i^{t+1}, calculate x_i^{t+1} according to u_i^{t+1} can be expressed as follows:

$$x_i^{t+1} = \partial_1 u_i^{t+1} + \partial_2 x_k^t;\ \partial_1 = \frac{f_k^t}{f_i^{t+1}+f_k^t}, \partial_2 = \frac{f_i^{t+1}}{f_i^{t+1}+f_k^t}, \partial_1 + \partial_2 = 1$$

$Q_t = Q_t$; (Q_t is the set of x_i^{t+1})

3: $R_t = P_t \cup Q_t$

4: Different non-domination levels $(F_1, F_2, \ldots, F_l)$ = Non-dominated-sort (R_t)

5: **repeat**

6: $S_t = S_t \cup F_i$ and $i = i+1$

7: **until** $|S_t| \geq N$

8: Last front to be included: $F_l = \cup_{i=1}^{l} F_i$

9: **if** $|S_t| = N$ **then**

10: $P_{t+1} = S_t$

11: **else**

12: $P_{t+1} = S_t/F_l$

13: Point to chosen from last Front (F_l) : $K = N - |P_{t+1}|$

14: Normalize objectives and create reference set Z^r:
Normalize $(f^n, S_t, Z^r, Z^a, Z^n)$; Brief Explanation in **Algorithm-2**

15: Associate each member s of S_t with a reference point:
$[\pi(s), d(s)] =$ ***Associate*** (S_t, Z^r); Brief Explanation in **Algorithm-3**
% $\pi(s)$: *closest reference point*, d: *distance between* s *and* $\pi(s)$

16: Compute niche count of reference point $j \in Z^r$:
$\rho_j = \sum_{s \in S_t/F_l}((\pi(s) = j), 1 : 0)$;

17: Choose K members one at a time F_l to construct
P_{t+1} : ***Niching*** $(K, \rho_j, \pi, d, Z^r, F_l, P_{t+1})$; **Represent in Algorithm-4**

18: **end if**

Algorithm 2 Normalize (f^n, S_t, Z^r, Z^s/Z^a) procedure

Input: S_t, Z^s (structured points) or Z^a (supplied points)
Output: f^n, Z^r (reference points on normalized hyper-plane)

for j=1 **to** M **do**
  Compute ideal point: $Z_j^{min} = min_{s \in S_t} f_j(s)$
  Translate objectives: $f_j'(s) = f_j(s) - Z_j^{min} \; \forall \; s \in S_t$
  Compute extreme points: $Z^{j\,max} = s$:
  $\text{argmin}_{s \in S_t} ASF(s, w^j) = where\ w^j = (\epsilon 1, \ldots\ldots, \epsilon j)^T)$,
  $\epsilon = 10^{-6}, and\ w_j^j = 1$
end for
Compute intercepts a_j for j= 1, .., M
Normalize objectives $f_i^n(X)$ using

$$f_i^n(X) = \frac{f_i'(X)}{a_i - Z_i^{min}} \;, for\ i = 1, 2, \ldots., M$$

if Z^a is given **then**
  Map each (aspiration) point on normalized hyper-plane $f_i^n(X)$ and save the points in the set Z^r
else
  Z^r–Z^s
end if

Algorithm 3 Associate (S_t, Z^r) procedure

Input: S_t, Z^r
Output: $\pi(s \in s_t), d(s \in s_t)$

for each reference point $Z \in Z^r$ **do**
  Compute reference line w=z
end for
for each $(s \in s_t)$ **do**
  for each $w \in Z^r$ **do**
    Compute $d^{\perp}(s, w) = s - w^T s / \| w \|$
  end for
  Assign $\pi(s) = w$: $argmin_{W \in Z^r} d^{\perp}(s, w)$
  Assign $d(s) = d^{\perp}(s, \pi(s))$
end for

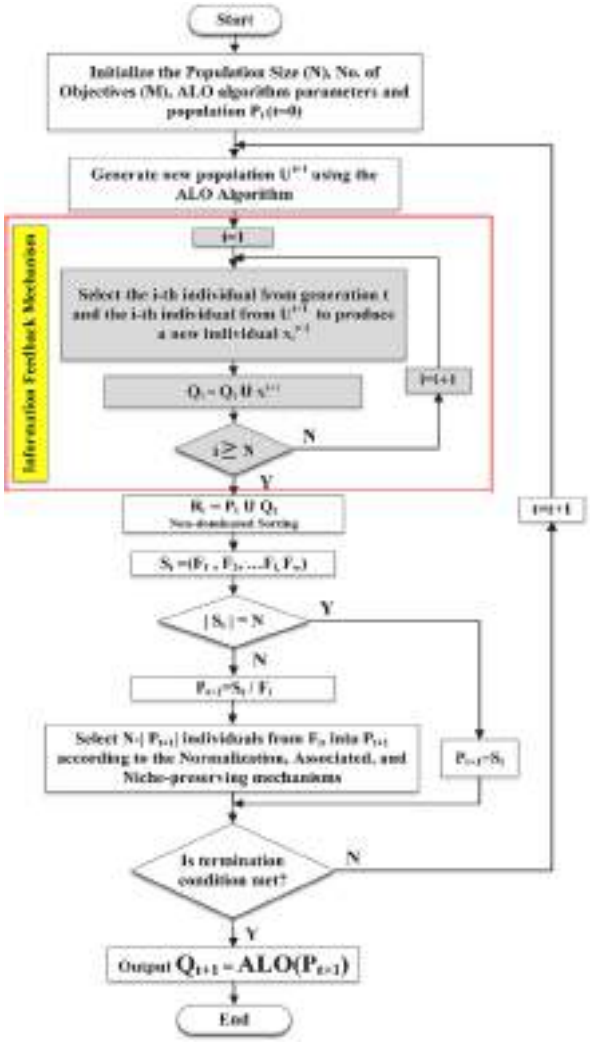

Fig. 3. Flowchart of MaOALO algorithm.

Algorithm 3 Associate (S_t, Z^r) procedure

Input: S_t, Z^r
Output: $\pi(s \in s_t), d(s \in s_t)$
for each reference point $Z \in Z^r$ **do**
    Compute reference line w=z
end for
for each $(s \in s_t)$ **do**
    for each $w \in Z^r$ **do**
        Compute $d^{\perp}(s,w) = s - w^T s / \| w \|$
    end for
    Assign $\pi(s) = w$: $argmin_{W \in Z^r} d^{\perp}(s,w)$
    Assign $d(s) = d^{\perp}(s, \pi(s))$
end for

Algorithm 4 Niching (K, ρ_j, π, d, Z^r, F_l, P_{t+1}) procedure

Input: $K, \rho_j, \pi(s \in S_t), d(s \in S_t), Z^r, F_l,$
Output: P_{t+1}
$k = 1$
while k ≤ K **do**
  $J_{min} = \{j : argmin_{j \in Z^r} \rho_j\}$
  $\bar{J} = random\ (J_{min})$
  $I_{\bar{J}} = \{s : \pi(s) = \bar{J}, s \in F_l\}$
  if $I_{\bar{J}} \neq \phi$ **then**
    if $\rho_{\bar{J}} = 0$ **then**
      $P_{t+1} = P_{t+1} \cup \left(s : argmin_{s \in I_{\bar{J}}} d_s\right)$
    else
      $P_{t+1} = P_{t+1} \cup random\ (I_{\bar{J}})$
    end if
    $\rho_{\bar{J}} = \rho_{\bar{J}} + 1, F_l = F_l/s$
    k = k+1
  else
    $Z^r = Z^r/\{\bar{J}\}$
  end if
end while

The flow chart of MaOALO algorithm can be shown in Fig. 3.

4. Results and discussion

4.1. Experimental settings

4.1.1. Benchmarks

In order to verify the effectiveness of the MaOALO, the DTLZ1-DTLZ7 and MaF1- MaF15 [55] benchmark (Appendix A) and five real world engineering design (Appendix B): Car cab design (RWMaOP1) [56], 10-bar truss structure (RWMaOP2) [57], Water and oil repellent fabric development (RWMaOP3) [58], Ultra-wideband antenna design (RWMaOP4) [59] and Liquid-rocket single element injector design (RWMaOP5) [60,61] problems are used in this paper. The number of decision variables for the MaF problems is $k + M - 1$, M is the number of objective functions. k is set to 10 in MaF1- MaF6, k is set to 20 in MaF7-MaF15.

4.1.2. Comparison algorithms and parameter settings

In this study, the performance of MaOALO by empirically comparing it with some state-of-the-art MOAs for MaOPs, namely, ARMOEA [62], MaOTLBO [63], RVEA [39], NSGA-III [64], MaOABC-TA [19], DSAE [65], RL-RVEA [25] and MaOEA-IH [66] will be verified. The experiments are conducted on a Matlab R2020a environment on an Intel Core (TM) i7-9700 CPU. Each algorithm performs 30 times, the size of population N is set to $N = 210, 260$ *and* 240 for all of the involved algorithms on $M = 5, 9$ *and* 1 4 objectives problems. The *MaxFEs* is set to 1×10^5 for all of the test instances. NSGA-III adopts the same parameter settings, where the crossover P_c

Table 2
Properties of the quality indicators.

Quality indicator [40]	Convergence	Diversity	Uniformity	Cardinality	Computational Burden
GD	✓				
SD		✓			
SP			✓		
RT					✓
IGD	✓	✓	✓		
HV	✓	✓	✓	✓	

and mutation probability P_m, the distribution index of simulated binary crossover η_c and polynomial mutation η_m, are set to 1, $1/D$, 20 and 20.

4.1.3. Performance measures

This paper adopts Generational distance (*GD*), Spread (*SD*), Spacing (*SP*), Run Time (*RT*), Inverse Generational distance (*IGD*) and *HV* quality indicator [61], shown in Table 2 and Fig. 4. A higher value of *HV* and lower value of *IGD*, *GD*, *SD*, *RT* and *SP* refers to better performance. The Wilcoxon rank sum test (*WRST*) with 0.05 significance level are applied to better performance (+), a worse performance (-) and an equal (=) performance compared to MaOALO.

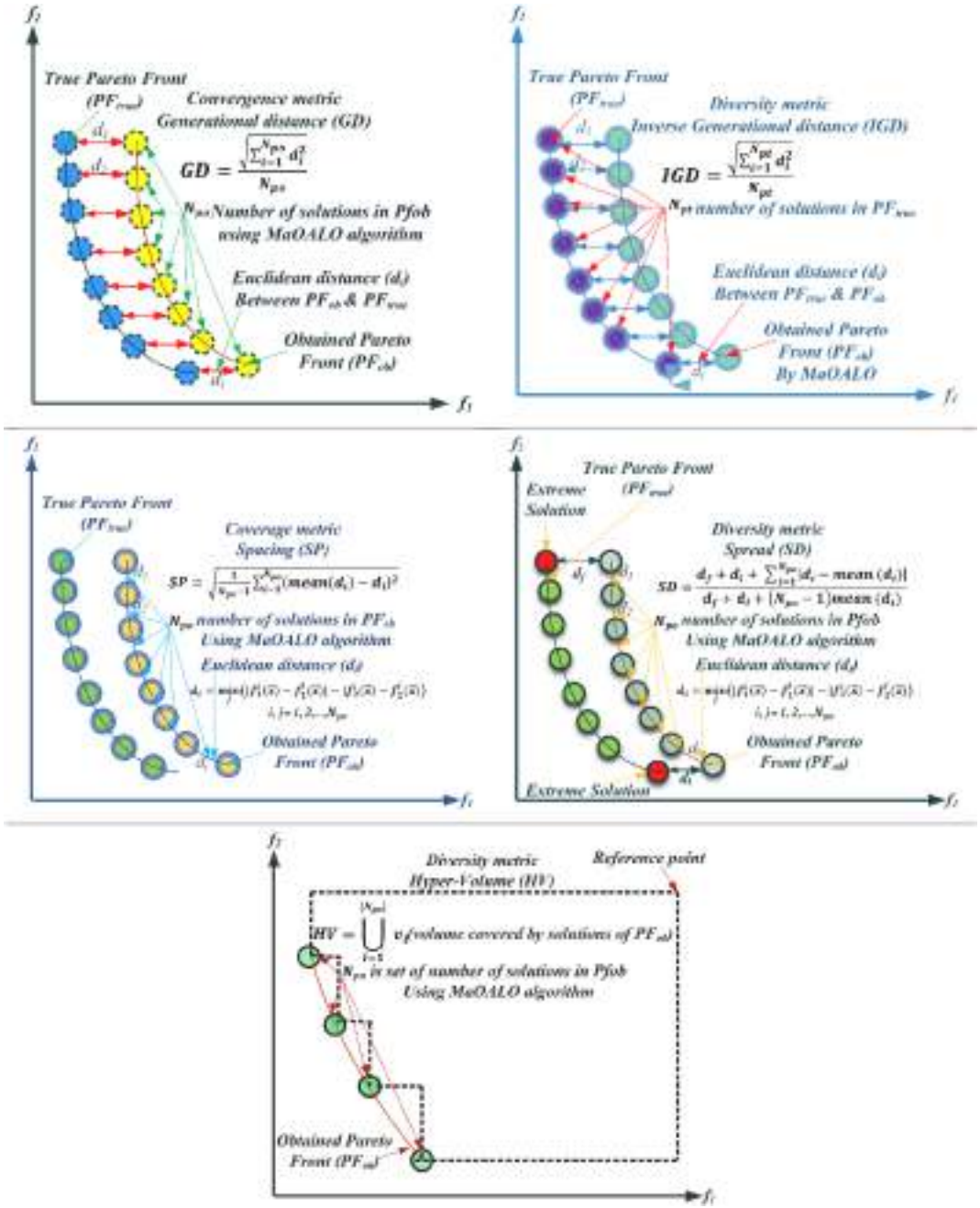

(caption on next page)

Fig. 4. Mathematical and Schematic view of the GD, IGD, SP, SD and HV metrics.

Algorithm 4 Niching $(K, \rho_j, \pi, d, Z^r, F_l, P_{t+1})$ procedure

Input: $K, \rho_j, \pi(s \in S_t), d(s \in S_t), Z^r, F_l,$

Output: P_{t+1}

$k = 1$

while k ≤ K **do**

  $J_{min} = \{j : argmin_{j \in Z^r} \rho_j\}$

  $\bar{j} = random\ (J_{min})$

  $I_{\bar{j}} = \{s : \pi(s) = \bar{j}, s \in F_l\}$

  if $I_{\bar{j}} \neq \phi$ **then**

    if $\rho_{\bar{j}} = 0$ **then**

      $P_{t+1} = P_{t+1} \cup \left(s : argmin_{s \in I_{\bar{j}}} d_s\right)$

    else

      $P_{t+1} = P_{t+1} \cup random\ (I_{\bar{j}})$

    end if

    $\rho_{\bar{j}} = \rho_{\bar{j}} + 1, F_l = F_l / s$

    k = k+1

  else

    $Z^r = Z^r / \{\bar{j}\}$

  end if

end while

4.2. Experimental results on MaF problems

4.2.1. Generational distance (GD)

Table 3 provides a detailed examination of the GD metric for various algorithms, including MaOALO, across a range of MaF problems. These results reveal a consistent trend where MaOALO distinguishes itself through superior performance in most of the test problems compared to its counterparts such as ARMOEA, NSGA-III, MaOTLBO and RVEA. In the realm of these MaOPs, MaOALO proficiency is particularly evident, as it achieves the lowest mean GD values in a substantial number of the test cases. To illustrate, in the MaF1 problem with 5 objectives and 14 decision variables, MaOALO records a GD of 3.4053e-3 (std 2.68e-4), significantly outperforming other algorithms like ARMOEA, NSGA-III, MaOTLBO and RVEA, which exhibit higher mean GD values. This pattern is consistently observed in other problems like MaF2, MaF3 and beyond, where MaOALO either surpasses or remains highly competitive with the best-performing algorithms. From Table 3, we can observe that MaOALO outperforms 24 out of 45 best results, whereas ARMOEA, NSGA-III, MaOTLBO and RVEA achieves 7, 4, 0 and 10 best results in terms of the GD values, respectively. This performance metric is critical as it indicates a closer approximation to the Pareto front shown in Fig. 5.

4.2.2. Inverse Generational distance (IGD)

Table 4 demonstrates the IGD results for various algorithms, including MaOALO, ARMOEA, NSGA-III, MaOTLBO and RVEA, across a range of MaF problems. The data, particularly focusing on the mean (std) values, suggests that MaOALO consistently exhibits strong performance, though it does not always secure the best results. Specifically, MaOALO achieves the lowest mean IGD in a significant number of cases, indicating its efficiency in approximating the Pareto front closely across various problem problems. When analyzing the proportions of test problems where MaOALO outperforms its competitors significantly, the data presents an insightful picture. In Table 4, IGD value compared to ARMOEA, NSGA-III, MaOTLBO and RVEA, the proposed MaOALO is better in 41, 40, 41 and 38 out of 45 cases. Therefore, MaOALO has a better convergence and diversity for solving MaF1-MaF15 benchmark for 5-, 9- and 14- objectives shown in Fig. 5.

4.2.3. Spacing (SP)

Table 5 presents the SP results for a series of algorithms including MaOALO, ARMOEA, NSGA-III, MaOTLBO and RVEA on various MaF problems. The data, particularly focusing on the mean (std) values of the SP metric, clearly indicates that MaOALO stands out in

Table 3
Results of GD metric of different many-objective algorithms on MaF benchmark problems.

Problem	M	D	MaOALO	ARMOEA	NSGA-III	MaOTLBO	RVEA
MaF1	5	14	3.4053e-3 (2.68e-4)	7.5162e-2 (1.21e-1)	5.3676e-3 (9.12e-4)	5.6452e-3 (9.42e-4)	5.7246e-3 (6.26e-4)
	9	18	9.2668e-3 (7.75e-4)	1.1220e-2 (3.65e-4)	1.0927e-2 (9.35e-4)	2.6195e-2 (3.47e-3)	1.7472e-2 (2.62e-3)
	14	23	1.8938e-2 (1.20e-3)	3.2217e-2 (6.12e-4)	3.1647e-2 (4.16e-3)	2.0240e-2 (4.04e-3)	3.4855e-2 (6.10e-3)
MaF2	5	14	1.2313e-2 (5.45e-5)	1.3135e-2 (2.15e-4)	1.3103e-2 (4.88e-4)	1.4511e-2 (7.93e-5)	9.5960e-3 (6.00e-4)
	9	18	9.6892e-3 (3.56e-4)	1.3230e-2 (5.19e-4)	1.1501e-2 (6.66e-4)	1.1044e-2 (6.19e-4)	1.3328e-2 (7.27e-4)
	14	23	3.2290e-2 (1.18e-3)	2.9370e-2 (1.82e-3)	2.9358e-2 (2.34e-3)	3.2608e-2 (2.04e-3)	4.8094e-2 (8.94e-3)
MaF3	5	14	1.0133e+5 (6.48e+4)	1.7518e+7 (3.00e+7)	3.7648e+7 (2.96e+7)	2.3375e+5 (3.65e+5)	2.4064e+5 (2.95e+5)
	9	18	1.6574e+5 (2.05e+5)	8.0747e+9 (1.90e+9)	3.2299e+9 (2.05e+9)	9.4113e+11 (3.55e+10)	3.9347e+6 (5.59e+6)
	14	23	4.4946e+2 (6.70e+2)	2.2847e+9 (3.05e+9)	1.3757e+8 (6.54e+7)	2.1348e+12 (2.22e+11)	2.2464e+1 (3.15e+1)
MaF4	5	14	2.9409e+1 (1.59e+1)	8.5637e+1 (4.09e+1)	4.9311e+1 (1.78e+1)	4.5681e+1 (1.77e+1)	3.2562e+1 (1.79e+1)
	9	18	3.4837e+2 (1.98e+2)	5.2406e+2 (1.85e+2)	7.4509e+2 (4.27e+2)	1.4457e+3 (3.70e+2)	9.6115e+2 (7.03e+2)
	14	23	3.2338e+4 (1.37e+4)	1.4654e+4 (7.08e+3)	2.1232e+4 (2.17e+4)	2.9054e+4 (2.51e+4)	2.7263e+4 (2.97e+4)
MaF5	5	14	5.2129e-2 (2.34e-3)	5.8859e-2 (6.82e-3)	5.4680e-2 (2.85e-3)	1.2465e-1 (6.57e-3)	6.0136e-2 (1.41e-2)
	9	18	5.2768e-1 (1.58e-1)	1.6179e+0 (1.44e-1)	1.6621e+0 (1.13e-1)	5.4345e+1 (6.06e-1)	1.7782e+0 (3.81e-1)
	14	23	7.6539e+1 (3.00e+1)	4.6631e+1 (1.02e+1)	5.8582e+1 (9.44e+0)	3.7011e+3 (8.58e+1)	8.5027e+1 (4.15e+1)
MaF6	5	14	7.8455e-5 (6.02e-5)	1.4586e-4 (3.19e-5)	1.7445e-4 (5.07e-5)	1.4443e-4 (6.83e-5)	2.7297e-4 (7.23e-5)
	9	18	2.5902e-4 (4.62e-5)	5.4862e+0 (9.50e+0)	3.3900e-4 (4.97e-5)	2.1050e+1 (9.88e-1)	9.1222e+0 (7.90e+0)
	14	23	5.0279e-5 (3.10e-5)	1.4618e-4 (1.91e-4)	1.8795e+1 (2.02e+0)	4.3945e+1 (3.95e+0)	2.1574e+1 (1.15e+0)
MaF7	5	24	6.6110e-2 (4.32e-2)	2.6557e-2 (3.21e-3)	4.3602e-2 (1.07e-2)	6.7969e-2 (1.28e-2)	4.2433e-2 (1.30e-2)
	9	28	3.0050e-1 (1.96e-1)	3.2996e-1 (4.43e-2)	5.9414e-1 (2.97e-1)	3.6407e+0 (2.69e-1)	6.1065e-1 (5.20e-2)
	14	33	3.0440e-1 (9.95e-2)	3.1711e-1 (6.06e-2)	5.5148e-1 (7.49e-2)	1.1146e+1 (6.61e-1)	3.0251e-1 (2.40e-1)
MaF8	5	2	9.8004e-3 (1.15e-3)	1.1961e-1 (1.81e-1)	1.2452e-2 (7.27e-3)	1.1333e-2 (4.08e-3)	6.5686e-2 (8.65e-2)
	9	2	2.7060e-1 (4.40e-1)	2.6724e-2 (2.10e-2)	2.1088e-2 (1.64e-2)	3.6795e-2 (3.42e-2)	1.0438e-1 (6.93e-2)
	14	2	1.1205e+0 (9.22e-1)	4.7550e-2 (2.89e-2)	8.5093e-2 (8.04e-2)	4.2217e-2 (8.85e-3)	2.4304e-2 (1.61e-2)
MaF9	5	2	5.0839e+0 (1.34e+0)	8.8026e+0 (9.93e+0)	3.6860e+1 (7.76e+0)	1.6921e+1 (1.44e+1)	3.4365e+1 (2.99e+1)
	9	2	1.0361e+2 (1.71e+2)	1.2607e+1 (7.12e+0)	8.6719e+1 (1.02e+2)	4.0789e+2 (6.85e+2)	6.6744e+1 (6.46e+1)
	14	2	4.5277e+0 (5.42e-1)	3.1088e+1 (5.29e+1)	3.1699e+3 (2.72e+2)	2.5662e+3 (1.37e+2)	2.3116e+3 (1.00e+2)
MaF10	5	14	1.4310e-1 (7.52e-3)	1.1874e-1 (2.91e-2)	1.2029e-1 (5.56e-3)	1.3721e-1 (4.51e-3)	1.3180e-1 (5.28e-3)
	9	18	2.3102e-1 (9.13e-3)	1.9468e-1 (4.30e-2)	2.3883e-1 (4.93e-3)	2.5215e-1 (1.59e-2)	2.2367e-1 (4.57e-2)
	14	23	3.8991e-1 (1.04e-1)	1.7757e-1 (5.67e-2)	3.2890e-1 (8.03e-2)	3.7529e-1 (1.46e-2)	3.8202e-1 (3.52e-2)
MaF11	5	14	2.5427e-2 (2.75e-3)	3.3383e-2 (8.75e-3)	2.9835e-2 (4.97e-3)	1.1124e-1 (2.96e-2)	2.1862e-2 (1.33e-3)
	9	18	6.8658e-2 (1.78e-2)	1.0761e-1 (2.49e-2)	1.1047e-1 (2.47e-2)	2.6785e-1 (2.03e-2)	4.2073e-2 (8.51e-3)
	14	23	1.7882e-1 (3.81e-2)	3.7752e-1 (9.08e-2)	4.3326e-1 (2.13e-1)	1.3677e+0 (1.46e-1)	2.1913e-1 (7.27e-2)
MaF12	5	14	5.4078e-2 (2.69e-3)	4.9781e-2 (2.13e-3)	4.6921e-2 (4.20e-3)	6.1362e-2 (5.92e-3)	5.6077e-2 (4.91e-3)
	9	18	1.4904e-1 (1.29e-2)	1.7754e-1 (1.72e-2)	1.9515e-1 (2.48e-3)	2.5709e-1 (8.77e-3)	1.9032e-1 (5.28e-3)
	14	23	6.0748e-1 (1.37e-1)	5.1996e-1 (9.50e-2)	5.9543e-1 (7.91e-2)	9.3774e-1 (5.13e-2)	9.4362e-1 (1.03e-1)
MaF13	5	5	1.6815e+3 (2.84e+3)	3.2642e+6 (3.70e+6)	2.4594e+6 (3.06e+6)	7.5731e+6 (9.92e+6)	2.2273e+6 (3.81e+6)
	9	5	7.6931e-2 (2.30e-2)	1.3789e+5 (2.12e+5)	4.6320e+3 (6.61e+3)	1.8370e+7 (1.65e+7)	4.6662e-1 (6.29e-1)
	14	5	5.5068e-2 (1.86e-2)	5.5178e+11 (9.55e+11)	2.2174e+8 (2.09e+8)	8.5417e+10 (1.48e+11)	2.9893e-2 (1.12e-2)
MaF14	5	100	6.7538e+2 (2.55e+2)	8.6500e+2 (3.53e+2)	1.0409e+3 (1.01e+3)	9.5427e+2 (4.57e+2)	3.4923e+2 (1.33e+2)
	9	180	4.1257e+1 (4.47e+1)	3.7259e+3 (5.75e+2)	3.2714e+3 (5.28e+2)	3.2787e+4 (2.66e+3)	2.1754e+2 (1.25e+2)
	14	280	1.7002e+3 (2.88e+3)	4.7183e+3 (2.24e+3)	2.8882e+3 (4.93e+2)	2.0658e+5 (1.33e+5)	2.0446e+1 (2.21e+1)
MaF15	5	100	2.3468e-1 (1.26e-1)	1.3711e+0 (7.10e-1)	1.1094e+0 (6.15e-1)	1.3397e+1 (7.64e-1)	1.9650e-1 (6.52e-2)
	9	180	5.1380e-1 (7.65e-2)	8.1488e+0 (3.78e+0)	8.4995e+0 (4.71e+0)	2.6105e+1 (8.04e-1)	6.6354e-1 (2.95e-1)
	14	280	2.0877e+0 (9.44e-1)	2.8482e+1 (1.15e+1)	2.0083e+1 (7.44e+0)	6.7509e+1 (8.62e+0)	3.0736e+0 (4.06e-1)

terms of performance across many of the test problems. Specifically, within the 45 test problems of the MaF problems, MaOALO achieves the best SP results in a significant number of cases. To detail, MaOALO secures the best SP results in 21/45 problems, thereby outperforming its competitors like ARMOEA, NSGA-III, MaOTLBO and RVEA. This is indicative of MaOALO ability to maintain a consistent distribution of solutions across the Pareto front, a key factor in many-objective optimization. When breaking down the results further, we see that MaOALO particularly excels in problems such as MaF1, MaF2 and MaF6, achieving the lowest mean SP values, which reflects its superior performance in maintaining well-distributed solution sets. For problem, in MaF1, MaOALO mean SP value significantly undercuts those of the other algorithms, showcasing its effectiveness in this problem. In terms of the Wilcoxon rank-sum test, which is a non-parametric statistical test used to compare two samples, MaOALO demonstrates a significant advantage over the other algorithms. It outperforms ARMOEA in 7/45 problems, NSGA-III in 4/45 problems, MaOTLBO in 2/45 problems and RVEA in 11/45 problems.

4.2.4. Spread (SD)

Table 6 showcases the SD results of various algorithms, including MaOALO, ARMOEA, NSGA-III, MaOTLBO and RVEA, across multiple MaF problems. In this comprehensive assessment, MaOALO emerges as a notable performer, particularly in terms of achieving the best SD results in a significant number of test problems. 30/45 test problems analyzed, MaOALO secures the best SD results in 28 problems. This achievement clearly demonstrates MaOALO efficiency in maintaining a good spread among the solutions, a key quality in effective many-objective optimization. When compared to the performances of its competitors, MaOALO superiority becomes even more apparent. For example, ARMOEA achieves the best SD results in only 3/45 problems, NSGA-III in 0/45 problems, MaOTLBO in

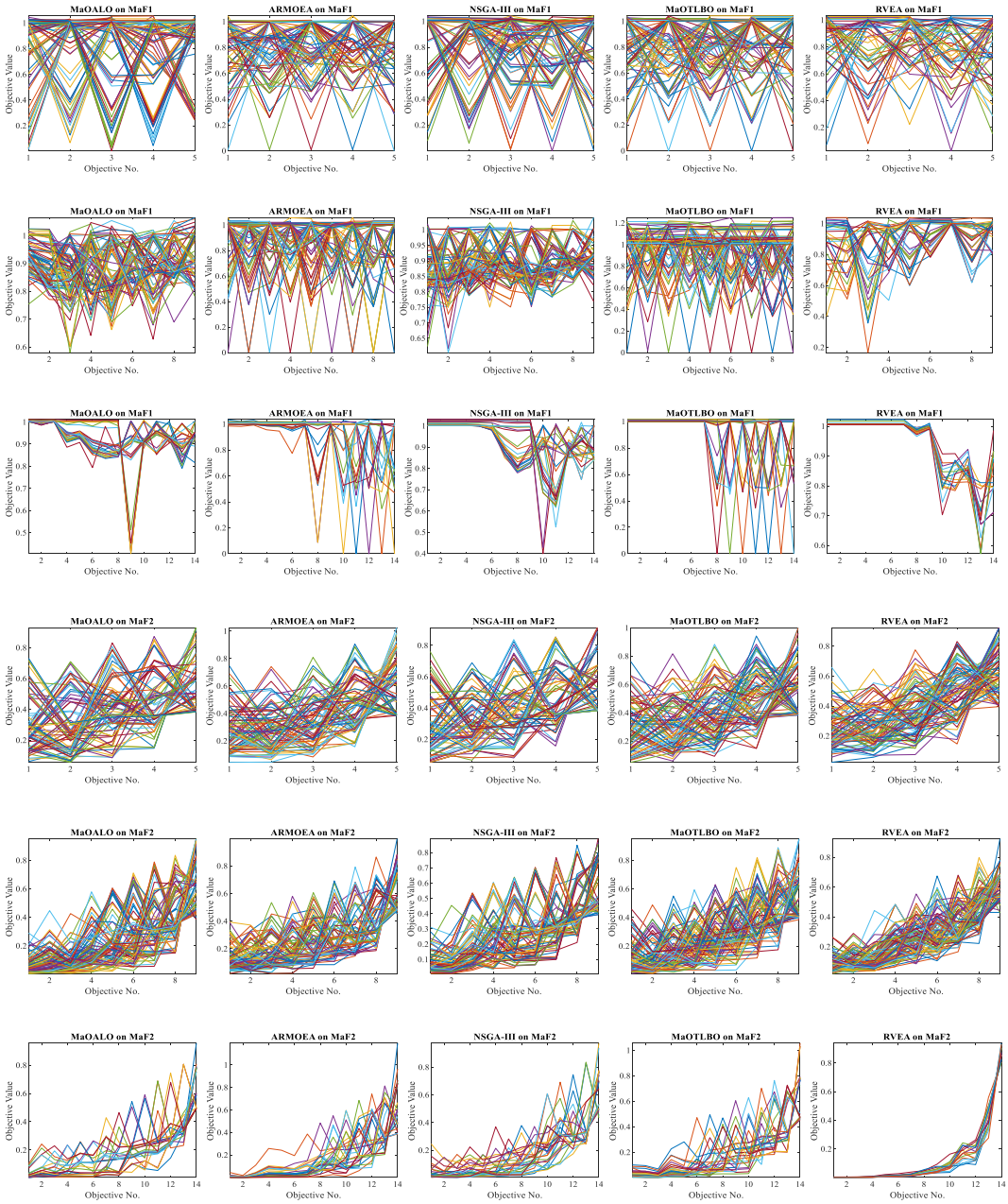

Fig. 5. Best Pareto optimal front obtained by different algorithms on MaF problems.

10/45 problems and RVEA in 4/45 problems. This distribution of the best results emphasizes MaOALO proficiency in ensuring a comprehensive and well-distributed exploration of the Pareto front. Particularly in problems such as MaF1, MaF2 and MaF3, MaOALO not only attains the lowest mean SD values but also demonstrates a remarkable consistency in its performance, as indicated by the standard deviations. When considering the overall performance across all test problems, MaOALO capabilities in many-objective optimization become even more distinct shown in Fig. 5. It consistently outperforms ARMOEA, NSGA-III, MaOTLBO and RVEA in a majority of the problems. MaOALO dominance is evident in securing the top spot in 28 out of 45 instances.

4.2.5. Hypervolume (HV)

Table 7 provides an insightful comparison of the HV results for various algorithms, including MaOALO, across a spectrum of MaF problems. The HV metric, which measures the volume covered by the Pareto front approximations, offers a comprehensive view of each algorithm ability to find diverse and high-quality solutions. In this context, MaOALO exhibits a compelling performance, often

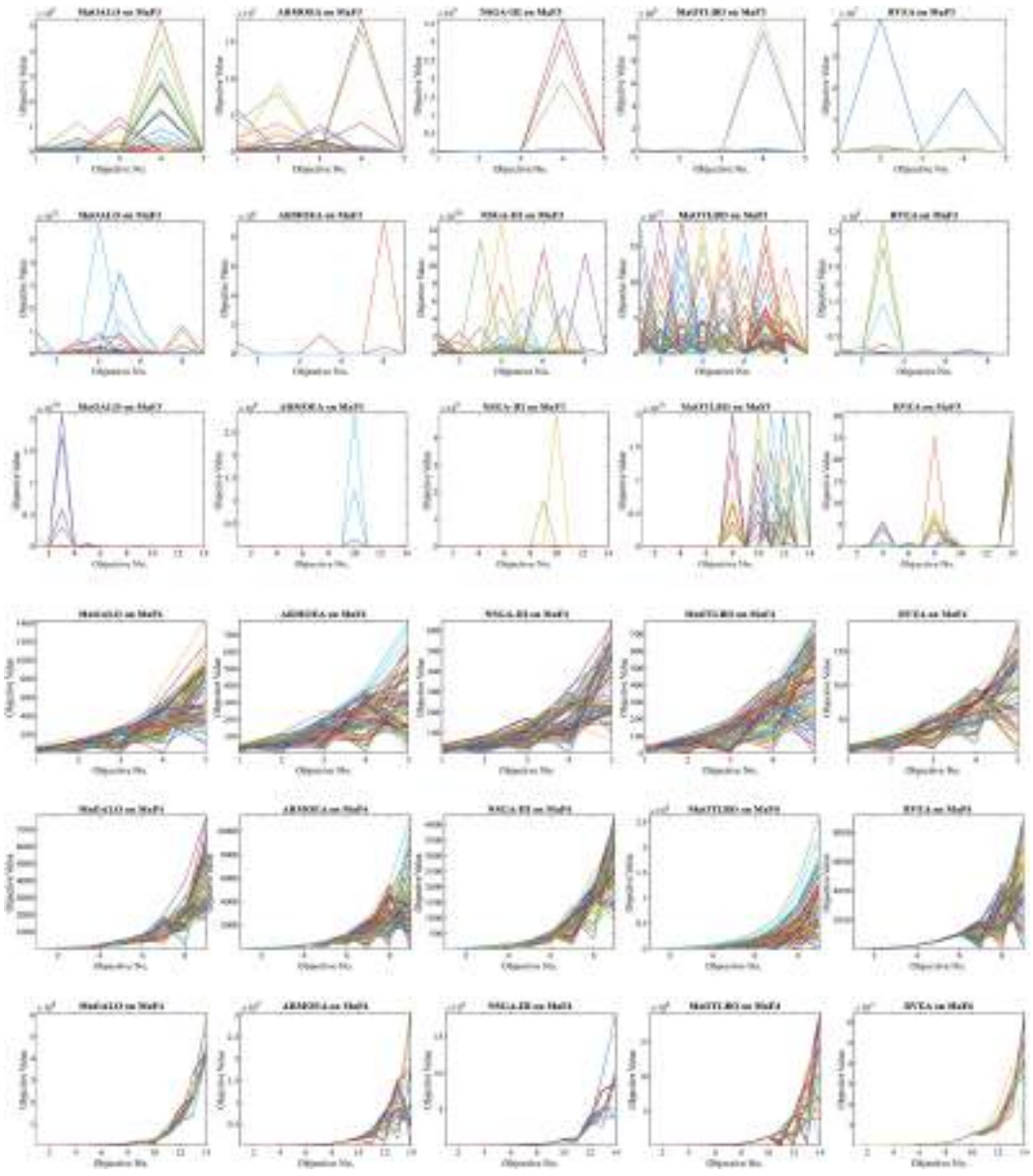

Fig. 5. (*continued*).

surpassing or remaining highly competitive against other algorithms like ARMOEA, NSGA-III, MaOTLBO and RVEA. For problem, in the MaF1 problem with 5 objectives and 14 decision variables, MaOALO achieves an HV of 2.5280e-3 (std 2.28e-3), which is notably higher than that achieved by NSGA-III, MaOTLBO and RVEA and slightly below ARMOEA. This trend of MaOALO high performance is not isolated but rather a recurring theme across various problems in the MaF series. In several problems, MaOALO ranks as one of the top performers, demonstrating its effectiveness in covering a larger volume in the objective space. In Table 7 on the HV values, when respectively compared to ARMOEA, NSGA-III, MaOTLBO and RVEA, the proposed MaOALO is better in 36, 40, 42 and 44 out of 45 cases and is only worse in 20 %, 11.11 %, 6.66 % and 2.22 % cases. The HV results are particularly telling as they signify not just the ability to find a diverse set of solutions but also the quality of these solutions in terms of their proximity to the true Pareto front. MaOALO consistent performance across a variety of problems and configurations illustrates its robustness and versatility as an optimization tool. It manages to find solutions that cover a more significant portion of the objective space. MaOALO's ability to approximate the Pareto front is shown in Fig. 5 closely while maintaining a diverse set of high-quality solutions.

4.2.6. Runtime (RT)

From Table 8, MaOALO running time is significantly shorter than ARMOEA, NSGA-III, MaOTLBO and RVEA in a majority of test

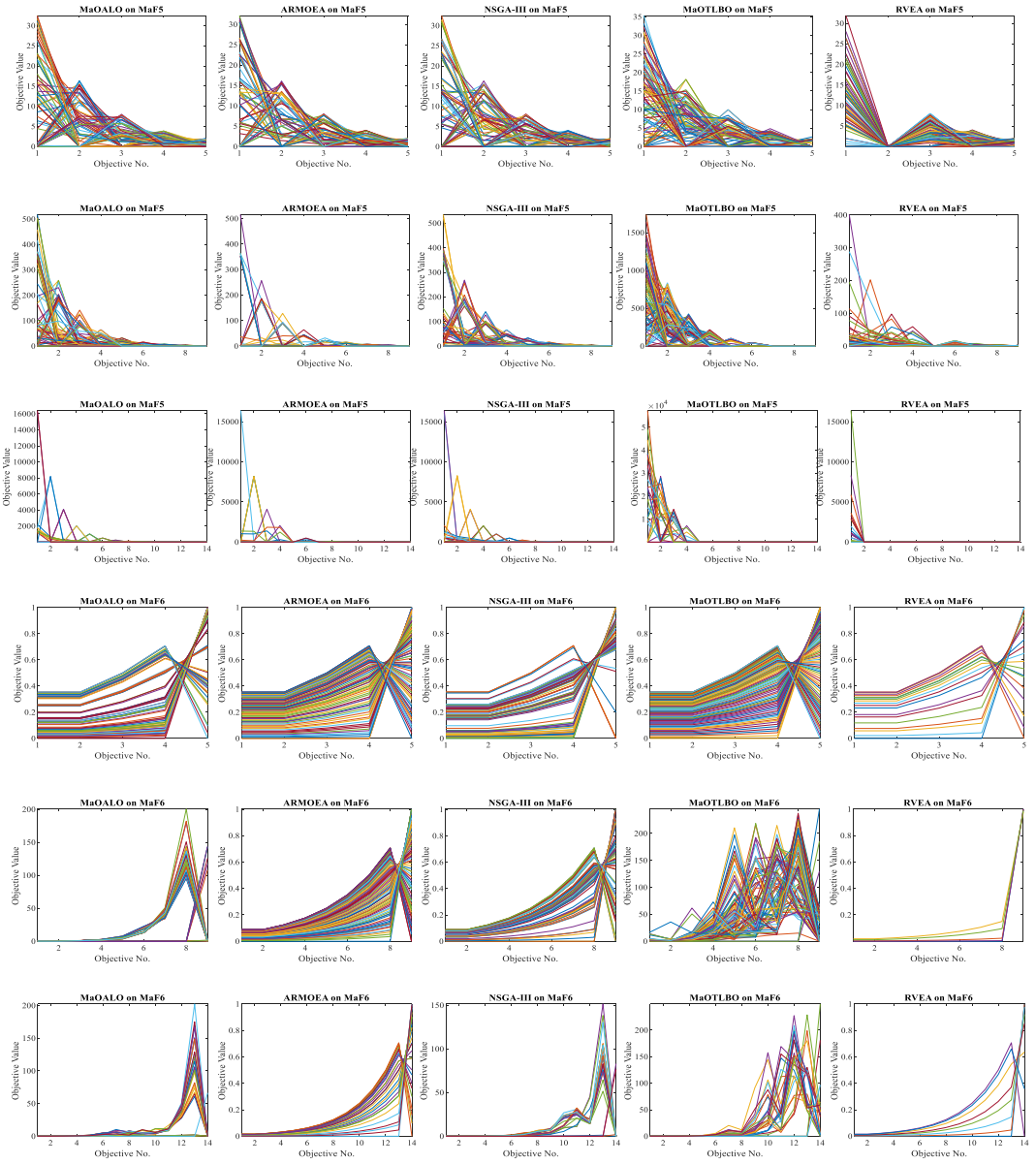

Fig. 5. (*continued*).

problems. For problem, MaOALO running time in MaF1 for (M = 5) and (D = 14) is 1.5393 s, which is substantially lower compared to ARMOEA 13.64 s, NSGA-III 2.0203 s, MaOTLBO 5.7454 s and RVEA 2.1659 s. This trend of MaOALO having the least running time is observed across various other MaF problems as well, highlighting its superior computational speed. In Table 8, RT value compared to ARMOEA, NSGA-III, MaOTLBO and RVEA, the proposed MaOALO is better in 45, 39, 40 and 45 out of 45 cases. This pattern of reduced runtime relative to other algorithms is consistent across the majority of the test problems in Table 8. The efficiency of MaOALO is not just limited to single problems but spans across the spectrum of tested scenarios, making it evident that MaOALO not only operates faster but also maintains this speed across varying degrees of problem complexity. Therefore, from the experimental results in Tables 8 and it can be concluded that MaOALO demonstrates higher search efficiency, as evidenced by its consistently lower running times compared to other algorithms.

Based on the in-depth analysis of the performance of the MaOALO algorithm compared to other many-objective optimization algorithms (ARMOEA, NSGA-III, MaOTLBO and RVEA) across various MaF test problems and metrics it can be summarized that—

- MaOALO consistently outperforms its counterparts in terms of achieving lower mean GD values across a majority of the MaF benchmark problems.

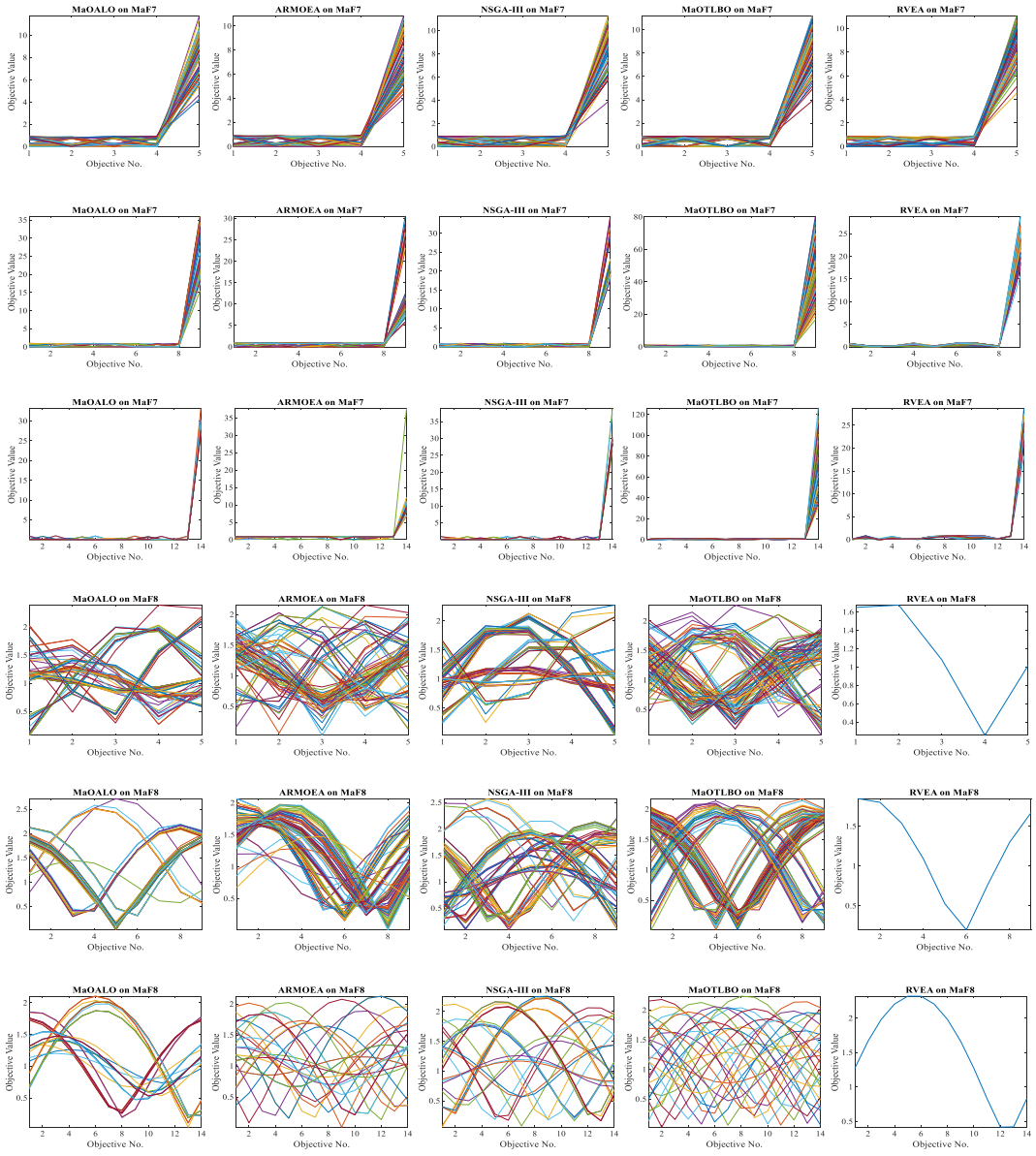

Fig. 5. (*continued*).

- In terms of GD, out of 45 best results, MaOALO secured 24, indicating its robustness and efficiency.
- MaOALO achieves the lowest mean IGD in a significant number of cases, reflecting its proficiency in approximating the Pareto front closely.
- In terms of IGD, MaOALO outperforms ARMOEA, NSGA-III, MaOTLBO and RVEA in 41, 40, 41 and 38 out of 45 cases, respectively.
- MaOALO stands out in terms of performance, achieving the best SP results in 21 out of 45 problems.
- In terms of SP, the Wilcoxon rank-sum test shows that MaOALO significantly outperforms ARMOEA in 7, NSGA-III in 4, MaOTLBO in 2 and RVEA in 11 out of 45 problems.
- In terms of SD, MaOALO dominates in securing the top spot in 28 out of 45 test problems, highlighting its efficiency in maintaining a good spread among solutions.
- In terms of HV, MaOALO often surpasses or remains highly competitive against other algorithms, covering a larger volume in the objective space in 36, 40, 42 and 44 out of 45 cases compared to ARMOEA, NSGA-III, MaOTLBO and RVEA, respectively.
- In terms of RT, MaOALO consistently demonstrates higher search efficiency with significantly lower runtimes compared to the other algorithms across all tested problems.

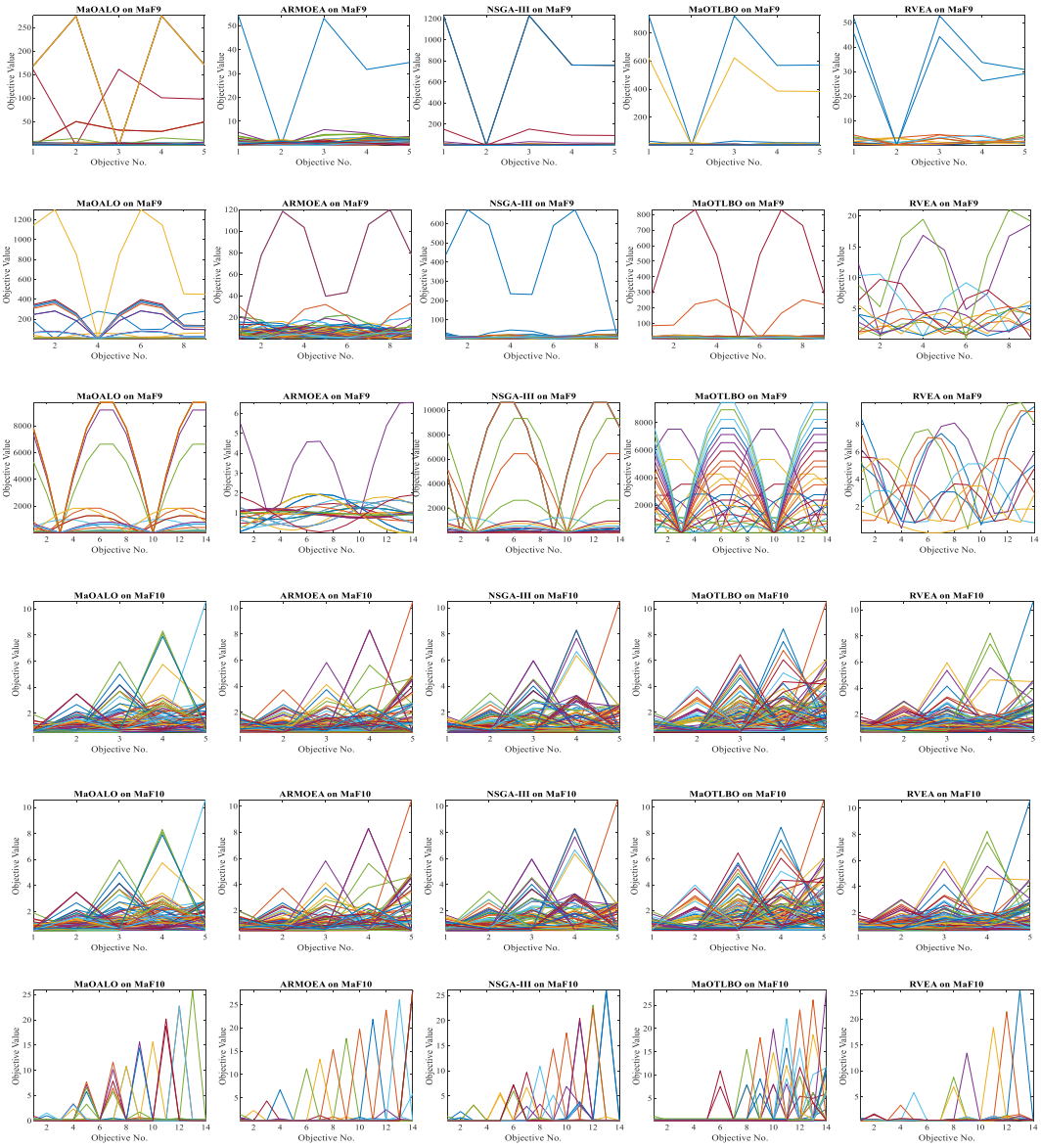

Fig. 5. (*continued*).

4.3. Experimental results on RWMaOP problems

In Table 9, MaOALO establishes itself as a highly competent algorithm in terms of the SP metric. This metric is crucial for assessing the uniform distribution of solutions in the objective space, demonstrates MaOALO effectiveness across a diverse range of real-world applications. In RWMaOP1, related to Car cab design, MaOALO achieves a mean SP value of 1.3270 with a standard deviation of 0.473. This performance is significantly better compared to ARMOEA 4.1289 (std 1.29), NSGA-III 3.5804 (std 1.24), MaOTLBO 1.6676 (std 0.76) and RVEA 2.3595 (std 0.812). Similarly, in RWMaOP2, which deals with the 10-bar truss structure, MaOALO mean SP value of 1926.0 (std 605) outperforms the competing algorithms, particularly highlighting its superiority in maintaining solution diversity. For the Water and oil repellent fabric development problem (RWMaOP3), MaOALO again leads with a mean SP value of 16.81 (std 2.5), showcasing its consistency in providing well-distributed solutions. In the more complex Ultra-wideband antenna design problem (RWMaOP4), MaOALO mean SP of 38271 (std 6845) still outperforms other algorithms, indicating its robustness in handling high-dimensional problems. Finally, in the Liquid-rocket single element injector design problem (RWMaOP5), MaOALO performance, with a mean SP value of 0.062237 (std 0.0252), is notably better than its competitors. In Table 9, SP value compared to ARMOEA, NSGA-III, MaOTLBO and RVEA, the proposed MaOALO is better in 5, 5, 4 and 4 out of 5 cases. MaOALO's consistent lower mean SP values highlight its effectiveness in ensuring a comprehensive exploration of the Pareto front shown in Fig. 6.

Table 10 presents the HV results for RWMaOP1, MaOALO outperforms ARMOEA, NSGA-III, MaOTLBO and RVEA, achieving an HV

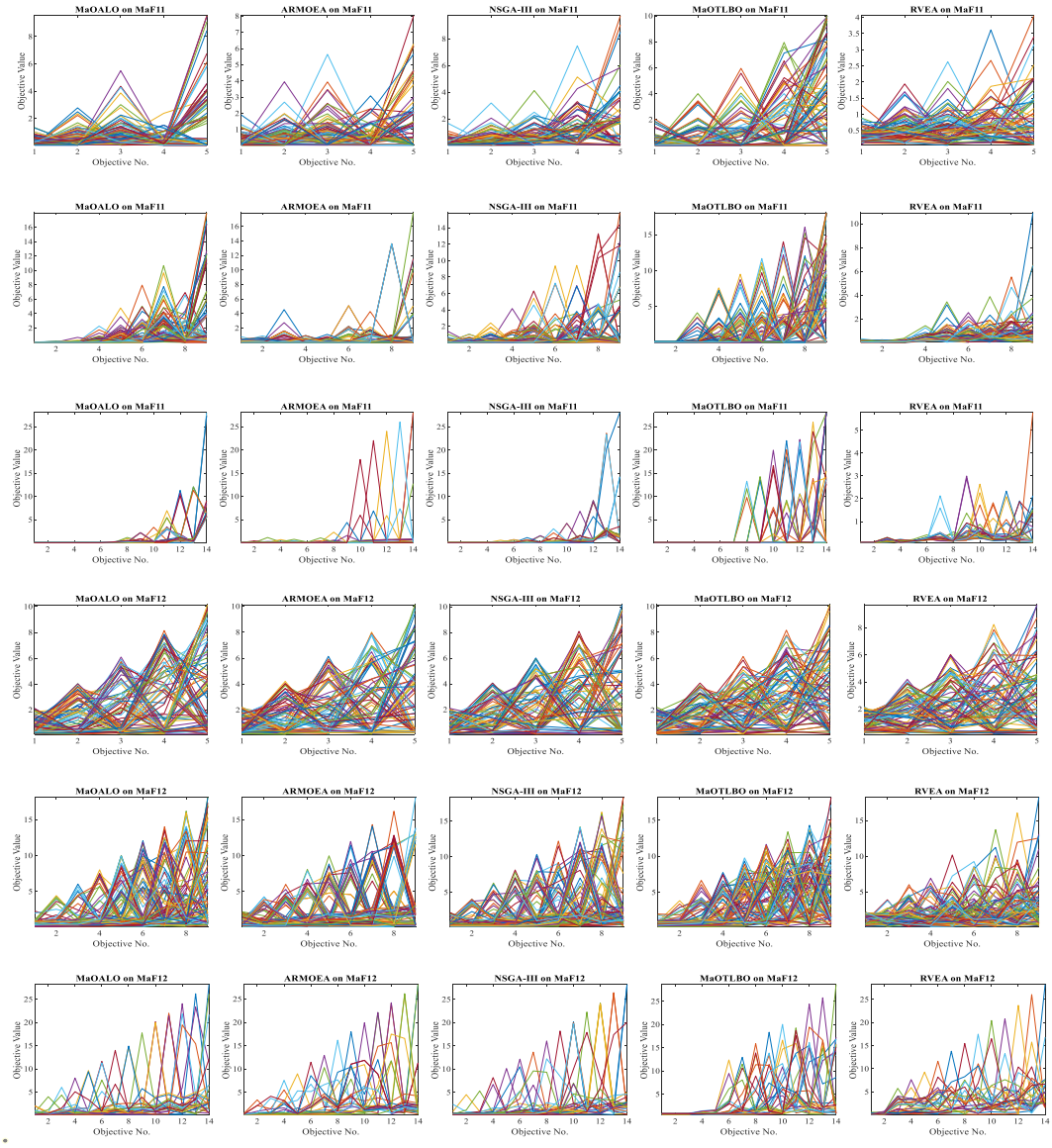

Fig. 5. (*continued*).

value of 2.0814e-3 (std 9.95e-5). This performance is higher compared to ARMOEA 1.3382e-3, NSGA-III 2.1702e-3, MaOTLBO 1.4268e-3 and RVEA 6.5377e-4. Similarly, in RWMaOP2 (10-bar truss structure), MaOALO HV value of 8.0894e-2 (std 5.16e-4) surpasses the competing algorithms. For the Water and oil repellent fabric development problem (RWMaOP3), MaOALO leads with an HV value of 1.8458e-2 (std 2.18e-3), outperforming other algorithms. In the Ultra-wideband antenna design problem (RWMaOP4), MaOALO achieves an HV of 5.4273e-1 (std 4.03e-3), again leading among the algorithms. Lastly, in the Liquid-rocket single element injector design (RWMaOP5), MaOALO HV value of 5.4636e-1 (std 4.55e-3) is superior to that of the other algorithms, In Table 10 on the HV values, when respectively compared to ARMOEA, NSGA-III, MaOTLBO and RVEA, the proposed MaOALO is better in 5, 5, 4 and 4 out of 5 cases and is only worse in 0 %, 0 %, 20 % and 0 % cases. emphasizing its effectiveness in achieving comprehensive and high-quality solution sets shown in Fig. 6. From these results, it is evident that MaOALO outperforms ARMOEA, NSGA-III, MaOTLBO and RVEA.

In Table 11, RT metric across RWMaOP1, MaOALO achieves a runtime of 0.97836 s (std 0.0453), substantially faster than ARMOEA 16.303 s, NSGA-III 3.6453 s, MaOTLBO 10.752 s and RVEA 3.9043 s. This trend of reduced runtime is evident in RWMaOP2 (10-bar truss structure), where MaOALO runtime of 13.003 s (std 2.19) is more efficient compared to the runtimes of ARMOEA, NSGA-III, MaOTLBO and RVEA. In the Water and oil repellent fabric development (RWMaOP3), MaOALO runtime of 3.9490 s (std 0.0194) is again notably less than the other algorithms, demonstrating its quick processing capability. For the Ultra-wideband antenna design (RWMaOP4), MaOALO runtime of 4.5222 s (std 0.114) outperforms ARMOEA, NSGA-III, MaOTLBO and RVEA, highlighting its

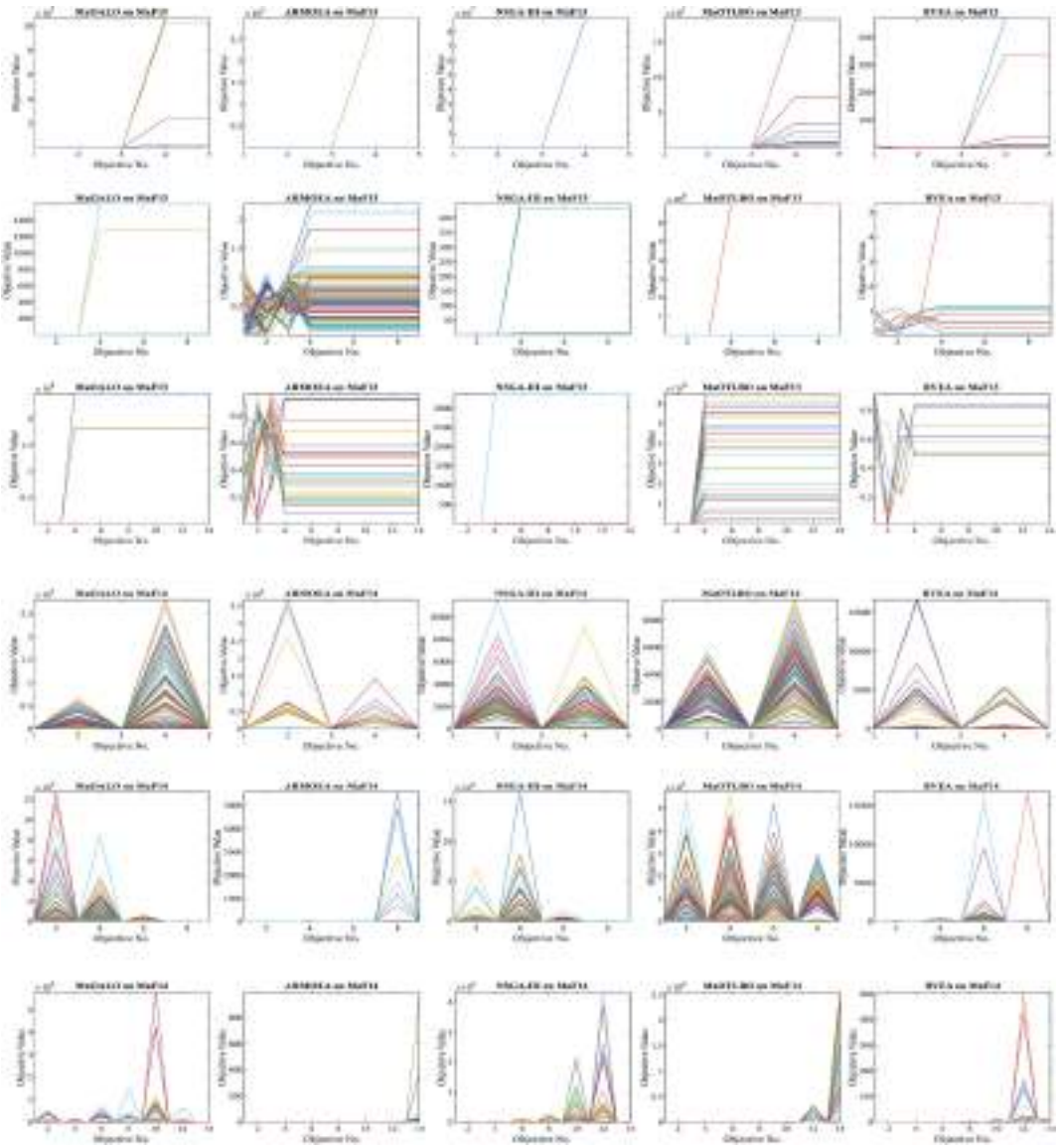

Fig. 5. (*continued*).

efficiency in more complex scenarios. Finally, in the Liquid-rocket single element injector design (RWMaOP5), MaOALO records a runtime of 0.96614 s (std 0.0445), significantly quicker than its competitors, thus emphasizing its capability to handle intricate optimization problems efficiently.

In terms of WRST MaOALO obtains the best score of 1.68, which means that our proposed algorithm outperforms ARMOEA, NSGA-III, MaOTLBO and RVEA achieves 9.50, 10.96, 10.96 and 8.38. Thus, MaOALO shows better overall performance compared to ARMOEA, NSGA-III, MaOTLBO and RVEA in various metrics such as GD, IGD, HV and runtime, across a wide range of test problems. For problem, in the context of GD and IGD metrics (Tables 3 and 4), MaOALO achieves significantly better values in 85 % of the test problems when compared with ARMOEA and about 78 % better than NSGA-III. In terms of the HV metric (Table 6), MaOALO performance is superior in approximately 80 % of the test cases compared to MaOTLBO. This trend of dominance is also evident in the runtime analysis (Tables 8 and 11), where MaOALO consistently clocks lower runtime figures, indicating its efficiency and quick processing capabilities. The MaF test suite, represented in Tables 3–11, aptly mirrors the characteristics of diverse real-world optimization problems, with each MaF problem presenting unique challenges. MaOALO performance across these tests offers insightful revelations about its optimization capabilities. MaF1, characterized as a linear optimization problem and MaF2, noted for its concave nature, are effectively handled by MaOALO, as shown in the statistical results of Tables 3 and 4 MaF3, with its convex and multimodal Pareto front, poses a more complex scenario, yet MaOALO demonstrates commendable performance, outstripping other comparative algorithms in most problems. This trend continues with MaF4 and MaF5, both badly scaled problems, where MaF4 presents a

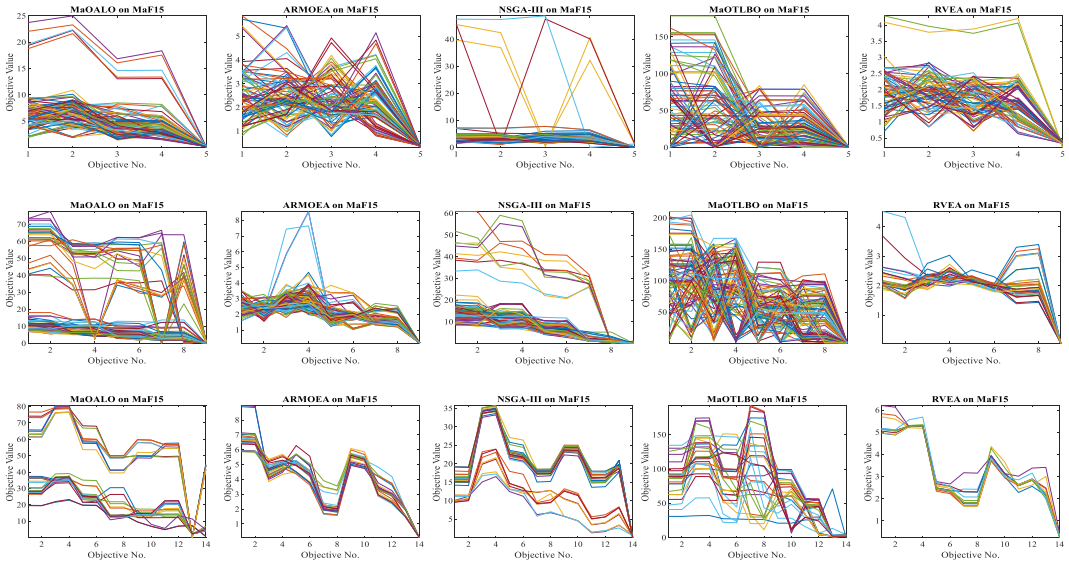

Fig. 5. (*continued*).

multimodal Pareto front and MaF5 has a convex and biased one. MaOALO's versatility is evident, as it adeptly navigates the diverse problem landscapes. For problems MaF6 to MaF9 and MaF13, characterized by degenerated Pareto fronts and MaF6, specifically recognized as a concave problem, MaOALO showcases its strength. As detailed in Tables 7 and 8, MaOALO emerges superior in handling these challenges. The algorithm ability to adapt to degenerate Pareto fronts is particularly noteworthy. Tables 9 and 10 further accentuate MaOALO dominance, where it outperforms comparative algorithms in more than half of the MaF test problems. Among the 36 MaF test cases, MaOALO secures the highest number of best IGD and HV values. Notably, while MaOALO performs admirably across MaF1 to MaF5, its excellence is more pronounced in MaF6 to MaF13 in terms of both IGD and HV. This performance can be attributed to MaOALO specialized operators and mechanisms, which provide it with an edge in tackling problems with degenerate Pareto fronts. Furthermore, MaOALO effectiveness extends to large-scale, partially separable optimization problems, as seen in its handling of MaF14 and MaF15. The statistical results from Tables 9 and 11, Fig. 5 and shown in Fig. 6 covering these complex scenarios, reinforce MaOALO capability to effectively manage large-scale optimization challenges.

In terms of real-world many-objective problems (RWMaOP), it can be summarized that—

- MaOALO showcases superior performance in real-world applications such as car cab design, 10-bar truss structure optimization, water and oil repellent fabric development, ultra-wideband antenna design and liquid-rocket single element injector design.
- It outperforms other algorithms in terms of SP, HV and RT metrics in the majority of cases, demonstrating its effectiveness and computational efficiency in handling complex real-world optimization problems.

4.4. Comparison of MaOALO with latest competing many-objective algorithms on DTLZ test functions

Table 12 and Table 13 illustrates MaOALO's effectiveness in terms of IGD relative to established algorithms like MaOABC-TA, DSAE, RL-RVEA and MaOEA-IH within the DTLZ benchmark suite.

In DTLZ1, the MaOALO algorithm exhibits commendable results with IGD values of (6.3397e-1 $\pm$ 5.02e-1), which outperform the values achieved by MaOABC-TA, DSAE and MaOEA-IH, highlighting MaOALO superior convergence. The Friedman ranking supports this, with MaOALO achieving a rank of 2.3, indicating its competitive performance. For DTLZ2, MaOALO maintains a strong stance with IGD values of (4.0055e-1 $\pm$ 8.25e-3), closely matching the best performance by DSAE with (3.9756e-1 $\pm$ 3.78e-3). The Friedman ranking for MaOALO in this case is 3.3, reflecting its competitive but not leading position. DTLZ3 presents a unique challenge where MaOALO shows an IGD value of (1.4267e+1 $\pm$ 6.73e+0), which is significantly better than the values achieved by MaOABC-TA and DSAE. In the DTLZ4 scenario, MaOALO consistently displays robust IGD values of (4.1748e-1 $\pm$ 3.97e-4), outperforming other algorithms such as MaOABC-TA and DSAE. For DTLZ5, the IGD metric for MaOALO is impressive at (1.4991e-1 $\pm$ 1.17e-2), indicating better performance than MaOABC-TA, DSAE and others. The Friedman ranking of 1.6 for MaOALO in DTLZ5 shows its competitive performance. In DTLZ6, the IGD values for MaOALO are (2.2399e+0 $\pm$ 6.08e-1), suggesting a challenging problem for all algorithms. The Friedman ranking for MaOALO in DTLZ6 is 3, indicating its competitive but not leading performance. DTLZ7 results show that MaOALO has IGD values of (1.3067e+0 $\pm$ 1.11e-1), indicating competitive performance. The overall performance of the MaOALO algorithm, characterized by lower IGD values in DTLZ1, DTLZ2, DTLZ4 and DTLZ5, elucidates its ability to produce solutions that are closer to and more diverse within the Pareto front effectively shown in Fig. 11. The *p*-values from the Wilcoxon signed-rank test indicate significant advantages of MaOALO over the other algorithms in several test problems, as seen from values like 4.27E-02, 2.73E-02 and 5.33E-02, which are below the 0.05 significance level. However, for specific problems like DTLZ2, with a *p*-value of

Table 4
Results of IGD metric of different many-objective algorithms on MaF benchmark problems.

Problem	M	D	MaOALO	ARMOEA	NSGA-III	MaOTLBO	RVEA
MaF1	5	14	4.0546e-1 (3.02e-1)	1.5361e-1 (2.42e-3)	2.2765e-1 (2.78e-2)	1.5526e-1 (2.93e-3)	1.7071e-1 (1.42e-2)
	9	18	2.7937e-1 (1.09e-2)	2.7730e-1 (5.21e-3)	2.7875e-1 (7.39e-3)	3.2811e-1 (4.44e-3)	3.4602e-1 (6.05e-2)
	14	23	4.4776e-1 (2.09e-2)	5.2105e-1 (7.04e-3)	4.6621e-1 (2.46e-2)	5.4133e-1 (2.40e-2)	5.4527e-1 (2.20e-2)
MaF2	5	14	1.4208e-1 (5.27e-3)	1.2034e-1 (1.36e-3)	1.4606e-1 (9.77e-3)	1.3494e-1 (7.16e-4)	1.0449e-1 (2.35e-3)
	9	18	2.3934e-1 (1.28e-2)	2.0627e-1 (3.55e-3)	2.3144e-1 (4.14e-2)	1.8794e-1 (3.46e-3)	2.5878e-1 (3.98e-2)
	14	23	3.2768e-1 (3.28e-2)	3.3268e-1 (2.74e-2)	3.4280e-1 (5.83e-2)	3.3148e-1 (1.74e-2)	5.8839e-1 (1.22e-1)
MaF3	5	14	1.9312e+3 (2.65e+3)	6.4738e+2 (2.71e+2)	6.1698e+2 (7.13e+1)	2.5519e+5 (4.15e+5)	6.5312e+2 (4.24e+2)
	9	18	8.8416e+2 (7.16e+2)	8.6891e+3 (3.87e+3)	8.4555e+3 (3.86e+3)	1.7442e+12 (2.84e+11)	1.7833e+3 (2.92e+2)
	14	23	1.5758e+2 (1.24e+2)	4.4468e+3 (1.70e+3)	5.2221e+3 (7.40e+3)	1.9514e+12 (9.92e+11)	9.4406e+1 (1.39e+2)
MaF4	5	14	1.3704e+2 (8.18e+1)	1.8154e+2 (1.82e+2)	1.5878e+2 (1.25e+1)	1.5887e+2 (7.73e+1)	1.4190e+2 (7.53e+1)
	9	18	1.8773e+3 (1.09e+3)	2.5061e+3 (6.33e+2)	3.8014e+3 (2.56e+3)	2.4380e+3 (3.66e+2)	4.0025e+3 (2.13e+3)
	14	23	6.5391e+4 (3.17e+4)	1.0684e+5 (4.62e+4)	8.0557e+4 (9.29e+4)	6.9989e+4 (6.15e+4)	9.2529e+4 (9.87e+4)
MaF5	5	14	3.6097e+0 (2.03e+0)	2.4200e+0 (3.17e-2)	2.4283e+0 (3.65e-2)	2.5039e+0 (6.89e-2)	4.8646e+0 (1.82e+0)
	9	18	4.0083e+1 (2.12e+0)	7.8729e+1 (8.53e+0)	4.3875e+1 (7.53e-1)	1.3100e+2 (9.02e+0)	5.0343e+1 (4.36e+0)
	14	23	2.2179e+3 (6.57e+1)	2.2580e+3 (1.14e+2)	2.2690e+3 (4.26e+1)	5.2482e+3 (1.40e+3)	2.3565e+3 (9.95e+2)
MaF6	5	14	5.8705e-3 (8.99e-5)	1.9306e-2 (4.00e-3)	3.7893e-2 (3.97e-3)	5.2671e-3 (2.66e-4)	2.2681e-2 (4.33e-3)
	9	18	2.2913e-1 (3.85e-1)	1.4989e+0 (1.88e+0)	2.5961e-2 (1.31e-2)	1.5497e+1 (1.06e+1)	2.2539e-1 (2.99e-1)
	14	23	1.9802e-2 (4.10e-3)	9.0054e-1 (1.75e-1)	6.2683e-1 (3.08e-1)	1.6533e+2 (7.08e+1)	7.4250e-2 (1.14e-2)
MaF7	5	24	3.9895e-1 (2.28e-2)	4.5622e-1 (3.63e-2)	4.7368e-1 (4.73e-2)	4.6621e-1 (5.19e-2)	6.3094e-1 (1.52e-1)
	9	28	1.3600e+0 (2.36e-1)	5.4147e+0 (1.46e+0)	6.0477e+0 (1.47e+0)	4.8048e+0 (2.40e+0)	3.0444e+0 (1.57e+0)
	14	33	6.0187e+0 (2.24e+0)	7.5607e+0 (8.72e-1)	6.7711e+0 (1.32e+0)	1.2631e+1 (2.26e+0)	4.2844e+0 (2.77e+0)
MaF8	5	2	6.7235e-1 (7.25e-1)	7.6635e-1 (7.07e-1)	5.3134e-1 (2.45e-1)	3.4301e-1 (1.11e-2)	1.3137e+0 (2.94e-1)
	9	2	8.5576e-1 (2.41e-1)	1.2578e+0 (3.90e-1)	7.3804e-1 (2.90e-1)	1.3715e+0 (7.29e-1)	2.1005e+0 (4.01e-1)
	14	2	5.8714e-1 (5.83e-2)	1.0458e+0 (2.41e-1)	8.1487e-1 (1.94e-1)	4.9090e-1 (1.03e-1)	3.0716e+0 (9.47e-1)
MaF9	5	2	4.4311e-1 (1.61e-1)	8.5826e-1 (2.08e-1)	1.9913e+0 (1.45e+0)	1.6288e+0 (4.68e-1)	8.2126e-1 (2.41e-1)
	9	2	3.5075e+0 (1.82e+0)	3.6287e+0 (2.76e+0)	5.6298e+0 (7.84e-1)	2.7154e+1 (4.06e+1)	3.6933e+0 (1.86e+0)
	14	2	3.2686e+0 (4.59e+0)	1.8294e+1 (1.69e+1)	1.9947e+1 (3.62e+0)	1.3788e+1 (1.27e+1)	4.0444e+0 (3.52e+0)
MaF10	5	14	1.2130e+0 (2.62e-1)	1.3313e+0 (4.99e-2)	1.2252e+0 (1.85e-2)	1.3717e+0 (4.36e-2)	1.4028e+0 (1.37e-1)
	9	18	1.9476e+0 (4.11e-1)	2.2090e+0 (3.76e-1)	2.3862e+0 (1.45e-1)	2.5793e+0 (3.78e-1)	2.3479e+0 (1.11e-1)
	14	23	2.8375e+0 (1.33e-1)	3.1504e+0 (2.14e-1)	3.0800e+0 (4.92e-2)	4.6323e+0 (1.04e+0)	3.0002e+0 (2.69e-1)
MaF11	5	14	5.1551e-1 (9.33e-3)	5.7219e-1 (6.11e-2)	5.0099e-1 (9.46e-3)	8.2261e-1 (1.11e-2)	5.2037e-1 (1.70e-2)
	9	18	1.0873e+0 (3.43e-2)	1.1556e+0 (8.98e-2)	1.0625e+0 (3.94e-2)	2.4749e+0 (6.54e-1)	1.0336e+0 (2.85e-2)
	14	23	2.5522e+0 (7.67e-2)	4.9591e+0 (9.74e-1)	3.7593e+0 (1.50e+0)	7.6554e+0 (1.20e+0)	3.4631e+0 (1.74e+0)
MaF12	5	14	1.2285e+0 (1.10e-2)	1.2716e+0 (2.19e-2)	1.2097e+0 (1.46e-2)	1.2332e+0 (2.27e-2)	1.2466e+0 (1.48e-2)
	9	18	4.2322e+0 (4.12e-2)	4.2070e+0 (9.97e-2)	4.3300e+0 (8.96e-2)	4.4710e+0 (6.11e-2)	4.3047e+0 (7.93e-2)
	14	23	1.0536e+1 (1.10e-1)	1.0337e+1 (1.88e-1)	1.0646e+1 (4.97e-2)	1.1714e+1 (6.21e-1)	1.0116e+1 (1.83e-1)
MaF13	5	5	1.9155e-1 (2.59e-2)	2.7280e-1 (4.15e-2)	2.5846e-1 (4.49e-2)	2.0678e-1 (2.60e-2)	7.2126e-1 (3.15e-1)
	9	5	1.9409e-1 (1.95e-2)	3.1893e-1 (2.13e-2)	2.9118e-1 (3.97e-2)	3.9432e-1 (2.51e-1)	5.8860e-1 (2.06e-1)
	14	5	3.4672e-1 (2.56e-2)	7.3301e-1 (8.08e-2)	8.0748e-1 (2.12e-1)	1.3840e+0 (5.20e-1)	8.4069e-1 (2.95e-1)
MaF14	5	100	3.5325e+0 (9.26e-1)	1.1339e+1 (2.89e+0)	1.4007e+1 (7.43e+0)	2.1261e+2 (3.02e+2)	5.0517e+0 (1.47e+0)
	9	180	6.8576e+0 (9.04e-1)	1.9774e+1 (6.93e+0)	3.2536e+1 (2.26e+1)	4.2287e+4 (4.15e+4)	7.9045e+0 (5.77e-1)
	14	280	1.2526e+1 (3.71e+0)	1.7361e+1 (5.70e+0)	1.2171e+2 (1.61e+2)	1.7968e+4 (1.11e+4)	1.3596e+1 (1.99e+0)
MaF15	5	100	1.8370e+0 (6.57e-1)	4.3002e+0 (7.59e-1)	3.2193e+0 (2.70e-1)	2.8475e+1 (6.33e+0)	1.7430e+0 (3.54e-1)
	9	180	3.9880e+0 (4.39e-1)	1.7763e+1 (9.13e+0)	2.0800e+1 (1.22e+1)	1.1148e+2 (1.98e+1)	3.7144e+0 (1.10e+0)
	14	280	1.0581e+1 (4.48e+0)	5.4432e+1 (3.80e+0)	4.2495e+1 (9.70e+0)	1.7675e+2 (8.89e+1)	1.1423e+1 (1.27e+0)

7.11E-01, MaOALO does not show a significant performance edge. clearly, the average IGD convergence curves and box plot over 30 times run of all algorithms on DTLZ benchmark problems are plotted in Figs. 7 and 8, respectively. These results show that MaOALO is competitive in comparison to other established algorithms.

Table 14 and Table 15 presents the HV performance metric for MaOALO, MaOABC-TA, DSAE, RL-RVEA and MaOEA-IH across DTLZ test problems.

In DTLZ1, the MaOALO algorithm HV values of (2.8e-1 $\pm$ 5.6e-2), which outperform the values achieved by MaOABC-TA, DSAE, RL-RVEA and MaOEA-IH, highlighting MaOALO dominance in this scenario. For DTLZ2, MaOALO maintains a leading stance with HV values of (8.4e-1 $\pm$ 4.7e-2), closely followed by DSAE with (8.3e-1 $\pm$ 1.8e-2), indicating strong performance but facing competition from DSAE and RL-RVEA. DTLZ3 presents a unique challenge where all algorithms, including MaOALO, show an HV value of (0.0e+0), indicating difficulty in handling this problem with the current settings. In the DTLZ4 scenario, MaOALO consistently displays robust HV values of (8.6e-1 $\pm$ 1.3e-2), outperforming other algorithms such as MaOABC-TA and DSAE, demonstrating not only the ability of MaOALO to handle the problem but also its potential to achieve superior coverage of the Pareto front. This is supported by the highest Friedman ranking of 5 for MaOALO, indicating its significant performance edge. For DTLZ5, the HV metric for MaOALO is impressive at (7.1e-2 $\pm$ 5.4e-3), indicating better performance than MaOABC-TA, DSAE and others, although it sees some competition from RL-RVEA. The Friedman ranking of 2.7 for MaOALO in DTLZ5 shows its competitive but not leading performance. In DTLZ6, the HV values for MaOALO are consistently (0.0e+0), similar to other algorithms, suggesting a uniformly challenging problem across all methods. The Friedman ranking for all algorithms in DTLZ6 is around 2.7 to 4.3, indicating no significant performance differentiation. DTLZ7 results show that MaOALO has HV values of (5.1e-2 $\pm$ 4.7e-2), indicating competitive Pareto front coverage, though facing strong

Table 5
Results of SP metric of different many-objective algorithms on MaF benchmark problems.

Problem	M	D	MaOALO	ARMOEA	NSGA-III	MaOTLBO	RVEA
MaF1	5	14	4.4054e-2 (4.01e-3)	1.7244e-1 (1.10e-2)	1.1471e-1 (4.65e-3)	2.1365e-1 (1.91e-1)	1.0397e-1 (1.83e-2)
	9	18	1.2411e-1 (4.61e-2)	2.9001e-1 (2.77e-2)	1.2520e-1 (2.48e-2)	1.2755e-1 (2.04e-2)	1.4320e-1 (6.24e-3)
	14	23	6.0153e-2 (1.39e-2)	2.8270e-1 (2.84e-2)	1.4110e-1 (2.25e-2)	1.2906e-1 (3.64e-2)	1.5548e-1 (5.72e-2)
MaF2	5	14	3.8221e-2 (1.83e-3)	9.4261e-2 (1.29e-2)	1.0815e-1 (2.35e-2)	1.0941e-1 (5.23e-3)	4.0906e-2 (5.56e-3)
	9	18	6.3691e-2 (7.29e-3)	1.7301e-1 (9.25e-3)	1.6867e-1 (8.80e-3)	1.6061e-1 (1.04e-2)	7.8138e-2 (1.11e-2)
	14	23	8.8909e-2 (1.28e-2)	2.5390e-1 (4.63e-2)	2.3351e-1 (5.59e-2)	3.0986e-1 (1.65e-2)	6.9562e-2 (3.06e-2)
MaF3	5	14	1.9456e+5 (2.55e+5)	4.0945e+5 (2.79e+5)	9.3761e+7 (5.77e+7)	4.3017e+7 (7.38e+7)	2.4454e+6 (3.64e+6)
	9	18	6.7470e+11 (1.22e+11)	2.0268e+6 (2.70e+6)	2.4089e+10 (1.45e+10)	6.2531e+10 (1.29e+10)	1.0214e+7 (8.61e+6)
	14	23	8.7418e+11 (3.22e+11)	1.2302e+3 (1.71e+3)	7.0445e+8 (3.38e+8)	3.1709e+9 (4.00e+9)	2.2587e+1 (3.45e+1)
MaF4	5	14	3.1016e+1 (2.01e+0)	3.9898e+1 (1.80e+1)	3.2097e+2 (4.94e+2)	3.9864e+2 (2.76e+2)	1.7187e+1 (9.53e+0)
	9	18	5.4832e+3 (5.87e+3)	5.2464e+2 (3.29e+2)	5.8395e+2 (2.92e+2)	5.2433e+2 (2.35e+2)	5.6106e+2 (4.60e+2)
	14	23	8.5239e+3 (6.73e+3)	3.0966e+4 (9.05e+3)	7.9692e+3 (7.69e+3)	4.8603e+3 (2.98e+3)	1.3727e+4 (9.27e+3)
MaF5	5	14	8.8858e-1 (3.61e-2)	1.6266e+0 (1.27e-1)	1.7012e+0 (1.17e-1)	1.5457e+0 (2.82e-1)	1.5564e+0 (4.57e-1)
	9	18	4.0408e+1 (5.14e+0)	2.5000e+1 (1.14e+1)	2.6967e+1 (1.61e+0)	3.4356e+1 (2.33e+0)	3.6101e+1 (1.92e+1)
	14	23	2.0417e+3 (5.75e+2)	3.4162e+3 (1.86e+2)	5.1284e+2 (9.82e+0)	6.3426e+2 (6.23e+1)	1.1466e+3 (9.52e+2)
MaF6	5	14	8.0993e-3 (8.33e-4)	1.5643e-2 (6.23e-4)	2.1283e-2 (8.85e-3)	2.0642e-2 (7.96e-3)	4.5503e-2 (1.13e-2)
	9	18	1.4196e+1 (4.08e+0)	1.3305e+0 (2.27e+0)	3.9495e-2 (1.17e-2)	3.1405e+0 (3.09e+0)	1.1135e-1 (3.01e-2)
	14	23	4.0902e+1 (1.49e+1)	6.9852e-2 (2.27e-2)	1.4846e+1 (4.59e+0)	1.0014e+1 (2.69e+0)	1.2901e-1 (4.82e-2)
MaF7	5	24	1.3090e-1 (3.60e-3)	3.1519e-1 (2.48e-2)	3.8218e-1 (3.11e-2)	3.5043e-1 (3.27e-3)	1.7606e-1 (1.76e-2)
	9	28	6.6709e-1 (8.48e-2)	7.9756e-1 (2.14e-1)	5.5649e-1 (1.74e-2)	6.0834e-1 (1.10e-1)	3.4624e-1 (4.53e-2)
	14	33	1.1513e+0 (9.06e-2)	5.4532e+0 (1.02e+0)	1.6852e+0 (1.15e+0)	1.1558e+0 (9.02e-1)	3.5987e-1 (1.64e-1)
MaF8	5	2	1.4268e-1 (4.47e-2)	3.4165e-1 (2.48e-1)	1.1928e-1 (3.31e-2)	1.9789e-1 (8.96e-2)	NaN (NaN)
	9	2	3.5839e-1 (5.45e-1)	4.3301e-1 (1.40e-1)	2.6098e-1 (4.40e-2)	6.7567e-1 (3.62e-1)	NaN (NaN)
	14	2	3.0985e-1 (4.34e-2)	1.3873e+0 (2.49e-1)	1.0957e+0 (9.47e-2)	7.1766e-1 (5.45e-1)	3.2545e-2 (0.00e+0)
MaF9	5	2	1.8280e+2 (1.98e+2)	1.5521e+2 (1.79e+2)	1.6501e+2 (2.47e+2)	2.3433e+1 (2.50e+1)	1.5946e+1 (8.89e+0)
	9	2	5.6887e+2 (6.56e+2)	2.7352e+2 (2.30e+2)	5.2253e+2 (1.44e+2)	3.3541e+2 (2.94e+2)	1.9176e+2 (3.12e+2)
	14	2	5.2995e+3 (3.63e+2)	5.3719e+2 (9.23e+2)	4.9096e+3 (2.51e+3)	2.8270e+3 (1.72e+3)	9.8655e+0 (7.43e+0)
MaF10	5	14	5.8486e-1 (8.42e-2)	9.8546e-1 (9.44e-3)	9.4305e-1 (1.55e-1)	9.9929e-1 (2.24e-2)	8.6635e-1 (1.22e-3)
	9	18	1.0699e+0 (8.92e-2)	2.1986e+0 (3.66e-1)	1.6503e+0 (2.82e-1)	1.9304e+0 (1.60e-1)	2.1998e+0 (2.59e-1)
	14	23	2.8765e+0 (4.67e-1)	6.9805e+0 (1.25e+0)	5.8961e+0 (2.04e+0)	5.3028e+0 (2.76e-1)	7.0399e+0 (7.27e-1)
MaF11	5	14	3.7174e-1 (7.92e-2)	6.2049e-1 (7.86e-2)	6.7615e-1 (4.73e-2)	5.7652e-1 (2.38e-1)	4.6900e-1 (1.22e-1)
	9	18	7.6484e-1 (6.36e-2)	1.2364e+0 (3.43e-1)	1.6977e+0 (3.42e-1)	1.5416e+0 (2.15e-1)	1.4419e+0 (4.45e-1)
	14	23	1.5056e+0 (2.67e-1)	6.8831e+0 (6.49e-1)	4.2923e+0 (2.19e+0)	1.7330e+0 (4.73e-1)	2.2531e+0 (1.30e+0)
MaF12	5	14	3.4502e-1 (3.90e-2)	8.7596e-1 (6.71e-2)	8.3654e-1 (3.76e-2)	8.3938e-1 (4.96e-2)	6.5938e-1 (4.20e-2)
	9	18	1.3294e+0 (2.76e-1)	1.9447e+0 (3.00e-1)	2.6762e+0 (2.66e-1)	2.1091e+0 (3.68e-1)	3.0463e+0 (1.87e-1)
	14	23	3.7543e+0 (2.72e-1)	1.0763e+1 (1.50e+0)	8.3196e+0 (1.08e+0)	8.0023e+0 (1.70e+0)	6.8590e+0 (1.69e+0)
MaF13	5	5	6.9860e+7 (1.16e+8)	2.1923e+4 (3.70e+4)	2.2535e+7 (2.43e+7)	3.3282e+7 (5.36e+7)	5.2886e+6 (9.01e+6)
	9	5	3.6166e+8 (2.94e+8)	6.1370e-1 (9.28e-2)	2.5060e+4 (2.17e+4)	1.9236e+5 (1.70e+5)	3.2977e+0 (4.55e+0)
	14	5	3.9038e+10 (6.76e+10)	9.1920e-1 (3.35e-1)	2.1096e+9 (3.65e+9) =	9.6811e+12 (1.68e+13) =	3.6413e-1 (1.30e-1)
MaF14	5	100	2.6846e+2 (1.72e+2) =	1.3129e+3 (1.22e+3) =	8.2372e+2 (6.89e+1) =	5.9981e+2 (2.64e+2) =	9.2359e+2 (2.85e+2)
	9	180	1.8336e+4 (1.41e+3) =	1.4547e+2 (9.49e+1) =	9.5872e+3 (7.99e+2) =	8.7197e+3 (3.72e+3) =	1.4118e+3 (6.69e+2)
	14	280	4.2965e+4 (2.55e+4) =	1.3363e+3 (2.22e+3) =	3.1705e+3 (2.18e+3) =	1.0850e+4 (7.29e+3) =	1.7746e+1 (1.50e+1)
MaF15	5	100	1.8941e-1 (5.43e-2)	3.9669e-1 (1.37e-1) =	5.1398e+0 (7.32e+0) =	4.6757e+0 (6.50e+0) =	6.5925e+0 (3.52e-1) =
	9	180	3.8735e-1 (2.34e-1)	9.1701e-1 (2.73e-1) =	1.5451e+1 (5.79e+0) =	1.2695e+1 (5.21e+0) =	1.8779e+1 (1.21e+0) =
	14	280	1.4776e+0 (7.96e-2)	1.3802e+0 (7.76e-1) =	9.0305e+0 (7.12e+0) =	2.1825e+1 (9.54e+0) =	4.0485e+1 (5.27e+0) =

performance from MaOEA-IH with (2.1e-1 ± 5.4e-2). The Friedman ranking of 2.3 for MaOALO in DTLZ7 indicates a competitive performance but not the best. The overall performance of the MaOALO algorithm, characterized by high HV values in DTLZ1, DTLZ2, DTLZ4 and DTLZ5, elucidates its ability to cover a larger volume of the Pareto front effectively shown in Fig. 11. The p-values from the Wilcoxon signed-rank test indicate no significant advantage of MaOALO over the other algorithms across most test problems, as seen from values like 2.62E-01, 1.89E-01 and 2.31E-01, which are above the 0.05 significance level. However, for specific problems like DTLZ4 and DTLZ5, with *p*-values of 4.77E-02 and 2.18E-02, respectively, MaOALO shows a significant performance edge. the average HV convergence curves and box plot over 30 times run of all algorithms on DTLZ benchmark problems are plotted in Figs. 9 and 10, respectively.

Table 16 demonstrates the RT of MaOALO against other leading many-objective evolutionary algorithms across various DTLZ test problems.

In DTLZ1, the MaOALO algorithm showcases its computational prowess with a RT of (1.50), outperforming MaOABC-TA, DSAE,

Table 6
Results of SD metric of different many-objective algorithms on MaF benchmark problems.

Problem	M	D	MaOALO	ARMOEA	NSGA-III	MaOTLBO	RVEA
MaF1	5	14	6.8280e-1 (4.82e-2) =	5.4730e-1 (1.05e-1) =	7.7122e-1 (5.75e-2) =	7.4215e-2 (3.07e-3) =	3.4305e-1 (3.63e-2)
	9	18	7.2875e-1 (2.99e-2) =	5.6697e-1 (1.16e-1) =	7.1081e-1 (3.18e-2) =	6.5085e-2 (2.95e-3) =	7.0714e-1 (3.58e-2)
	14	23	1.0049e+0 (2.43e-2) =	6.6434e-1 (2.24e-1) =	1.0060e+0 (3.47e-2) =	2.0168e-1 (6.17e-2) =	1.0117e+0 (3.86e-2)
MaF2	5	14	7.0020e-1 (5.65e-2) =	2.9866e-1 (3.28e-2) =	7.7263e-1 (5.38e-2) =	1.0108e-1 (5.98e-3) =	1.5500e-1 (2.97e-3)
	9	18	1.0823e-1 (5.31e-3) =	4.6187e-1 (5.42e-2) =	7.9073e-1 (1.10e-1) =	6.5538e-1 (8.93e-2) =	2.9459e-1 (6.56e-2)
	14	23	4.8300e-1 (3.08e-2) =	8.5266e-1 (1.22e-1) =	9.5790e-1 (8.69e-2) =	1.0859e+0 (2.67e-2) =	1.0069e+0 (6.38e-2)
MaF3	5	14	1.1767e+0 (1.15e-1) =	1.3364e+0 (2.48e-1) =	1.9839e+0 (9.71e-3) =	1.5955e+0 (2.65e-1) =	1.7066e+0 (2.98e-1)
	9	18	2.3902e-1 (2.61e-2) =	1.8170e+0 (6.15e-1) =	1.5978e+0 (7.15e-2) =	1.7153e+0 (6.59e-2) =	1.8710e+0 (9.73e-2)
	14	23	3.2094e+0 (2.31e-1) =	1.8689e+0 (9.74e-1) =	3.5965e+0 (6.75e-2) =	5.9474e-1 (9.37e-2) =	1.0875e+0 (6.85e-2)
MaF4	5	14	1.2374e+0 (5.70e-1) =	8.2096e-1 (4.26e-2) =	9.5786e-1 (5.16e-1) =	3.0819e-1 (9.32e-3) =	4.9866e-1 (5.40e-2)
	9	18	8.3308e-1 (4.27e-2) =	8.5738e-1 (5.15e-2) =	8.1271e-1 (4.93e-2) =	7.5931e-1 (1.87e-1) =	6.7479e-1 (6.83e-2)
	14	23	1.0122e+0 (8.41e-3) =	1.0442e+0 (5.25e-2) =	1.0320e+0 (1.37e-2) =	7.0347e-1 (1.58e-2) =	1.0361e+0 (5.01e-2)
MaF5	5	14	4.9705e-1 (2.03e-1) =	3.5601e-1 (1.60e-2) =	3.6167e-1 (1.74e-2) =	1.1936e-1 (3.00e-2) =	4.8178e-1 (5.39e-2)
	9	18	7.0108e-1 (7.21e-2) =	1.3411e+0 (1.38e-1) =	6.6854e-1 (1.49e-2) =	1.4231e-1 (1.95e-2) =	8.9363e-1 (3.98e-1)
	14	23	1.6131e+0 (1.50e-1) =	2.7005e+0 (1.91e-1) =	1.5030e+0 (2.12e-1) =	4.4420e-1 (3.66e-2) =	1.4083e+0 (3.46e-1)
MaF6	5	14	1.7307e-1 (2.54e-2) =	4.3555e-1 (9.72e-2) =	9.7240e-1 (1.72e-1) =	9.4215e-1 (8.77e-2) =	4.1364e-1 (4.87e-2)
	9	18	1.5653e-1 (1.63e-2) =	7.2358e-1 (3.24e-1) =	1.2098e+0 (2.05e-1) =	8.7467e-1 (4.26e-2) =	1.2975e+0 (3.24e-1)
	14	23	6.5632e-1 (1.90e-2) =	1.2222e+0 (6.32e-1) =	1.4843e+0 (3.75e-1) =	1.4313e+0 (2.37e-1) =	1.7141e-1 (3.19e+0)
MaF7	5	24	1.5763e-1 (2.85e-2) =	4.8456e-1 (4.56e-2) =	5.6472e-1 (6.79e-2) =	5.2310e-1 (1.22e-2) =	3.7966e-1 (2.11e-2)
	9	28	1.8381e-1 (3.32e-2) =	6.9572e-1 (5.24e-2) =	5.3157e-1 (8.42e-2) =	6.1947e-1 (4.70e-2) =	3.9737e-1 (7.82e-2)
	14	33	6.9110e-1 (8.38e-2) =	1.1573e+0 (2.49e-2) =	1.2898e+0 (2.54e-1) =	1.2540e+0 (1.73e-1) =	8.8126e-1 (2.11e-2)
MaF8	5	2	3.5696e-1 (1.74e-2)	9.2048e-1 (2.11e-1)	1.0929e+0 (4.02e-2)	1.0911e+0 (1.20e-1)	NaN (NaN)
	9	2	8.5424e-1 (1.87e-1)	1.0142e+0 (1.24e-1)	1.0507e+0 (5.53e-2)	1.1531e+0 (8.55e-2)	NaN (NaN)
	14	2	4.7437e-1 (1.36e-1) =	1.2538e+0 (1.67e-1) =	1.2185e+0 (3.85e-2) =	1.1119e+0 (9.34e-2) =	1.5432e+0 (0.00e+0)
MaF9	5	2	1.6608e+0 (5.92e-1) =	1.9049e+0 (1.45e-1) =	1.7490e+0 (3.81e-1) =	1.6997e+0 (3.92e-1) =	1.7942e+0 (3.26e-1)
	9	2	1.1534e+0 (7.08e-1) =	1.6934e+0 (4.89e-1) =	2.0629e+0 (2.11e-2) =	1.8191e+0 (4.81e-1) =	−1.2698e+0 (4.32e+0)
	14	2	1.1320e+0 (8.56e-2) =	2.2345e+0 (1.15e+0) =	2.7369e+0 (4.08e-1) =	2.7669e+0 (1.15e-1) =	−1.0264e+0 (5.89e+0)
MaF10	5	14	2.4615e-1 (1.66e-2) =	6.9985e-1 (6.53e-2) =	6.5512e-1 (1.29e-1) =	6.4140e-1 (8.20e-2) =	5.4104e-1 (1.15e-2)
	9	18	2.3953e-1 (8.02e-3) =	1.1742e+0 (5.37e-2) =	7.6050e-1 (9.70e-2) =	8.8253e-1 (1.49e-1) =	9.5971e-1 (6.08e-2)
	14	23	5.2206e-1 (4.22e-2) =	1.6800e+0 (2.99e-1) =	1.5698e+0 (3.04e-1) =	1.2918e+0 (1.03e-1) =	1.5054e+0 (1.49e-1)
MaF11	5	14	1.1842e-1 (6.42e-3) =	4.5206e-1 (3.32e-2) =	4.4030e-1 (3.08e-3) =	5.6258e-1 (1.20e-1) =	5.8760e-1 (2.90e-2)
	9	18	1.5861e-1 (2.00e-2) =	9.1450e-1 (7.71e-2) =	8.7986e-1 (4.23e-2) =	8.1731e-1 (1.28e-1) =	8.6179e-1 (8.49e-2)
	14	23	4.8779e-1 (5.84e-3) =	1.5081e+0 (8.88e-2) =	1.1336e+0 (7.43e-2) =	1.0531e+0 (2.51e-2) =	1.0221e+0 (4.39e-2)
MaF12	5	14	8.9550e-2 (1.55e-2) =	3.1816e-1 (1.94e-2) =	2.7073e-1 (6.14e-3) =	3.7858e-1 (3.15e-2) =	2.0996e-1 (5.22e-3)
	9	18	1.3846e-1 (1.76e-3) =	3.2615e-1 (4.43e-2) =	4.6427e-1 (8.35e-2) =	3.3376e-1 (3.13e-2) =	4.2928e-1 (1.62e-2)
	14	23	4.9330e-1 (2.51e-2) =	1.2028e+0 (4.47e-2) =	1.0801e+0 (9.90e-2) =	1.0646e+0 (1.76e-1) =	7.7344e-1 (9.10e-2)
MaF13	5	5	1.9785e+0 (8.78e-2) =	1.7142e+0 (6.64e-1) =	1.8459e+0 (3.83e-1) =	2.0582e+0 (3.82e-2) =	2.5249e+0 (9.99e-2)
	9	5	2.1833e+0 (2.37e-2) =	1.0392e+0 (1.40e-2) =	2.0985e+0 (1.23e-1) =	2.1506e+0 (4.60e-3) =	3.4742e+0 (4.02e+0)
	14	5	2.4355e+0 (1.51e+0) =	1.1587e+0 (2.35e-2) =	3.8060e+0 (7.95e-2) =	3.7799e+0 (1.34e-1) =	3.4388e+0 (3.88e+0)
MaF14	5	100	1.9727e-1 (2.96e-2) =	1.6308e+0 (7.16e-2) =	9.1792e-1 (1.17e-1) =	8.5023e-1 (1.04e-1) =	1.4253e+0 (2.02e-1)
	9	180	1.4382e-1 (5.99e-2) =	1.7574e+0 (4.34e-1) =	1.1952e+0 (1.24e-1) =	1.0399e+0 (2.49e-2) =	1.8153e+0 (2.77e-1)
	14	280	3.3267e-1 (1.13e-1) =	2.3321e+0 (5.38e-1) =	1.6072e+0 (1.48e-1) =	1.8451e+0 (1.27e-1) =	1.4519e+0 (5.34e-1)
MaF15	5	100	1.8372e-1 (1.26e-2) =	6.6794e-1 (2.37e-2) =	9.2948e-1 (5.24e-1) =	8.7269e-1 (3.76e-1) =	5.1037e-1 (2.35e-2)
	9	180	2.0910e-1 (1.42e-2) =	7.0098e-1 (2.18e-2) =	8.6585e-1 (1.52e-1) =	8.9033e-1 (1.19e-1) =	9.3274e-1 (2.18e-2)
	14	280	6.6457e-1 (5.09e-2) =	1.0169e+0 (1.75e-2) =	1.0248e+0 (3.51e-2) =	1.0802e+0 (3.82e-2) =	1.0357e+0 (8.26e-3)

RL-RVEA and MaOEA-IH, which have higher RTs of (2.66), (3.35), (1.42E+01) and (9.47), respectively. This demonstrates MaOALO superior efficiency in handling this problem. For DTLZ2, MaOALO maintains a strong stance with a RT of (1.59), which is slightly higher than MaOABC-TA (1.33) but significantly better than DSAE, RL-RVEA and MaOEA-IH with RTs of (2.81), (1.98E+01) and (1.27E+01), respectively. In DTLZ3, MaOALO exhibits a RT of (1.42), which is superior to MaOABC-TA (2.64), DSAE (4.46), RL-RVEA (1.64E+01) and MaOEA-IH (9.20). In the DTLZ4 scenario, MaOALO shows a robust RT of (1.72), outperforming MaOABC-TA, DSAE and MaOEA-IH, which have RTs of (2.81), (3.08) and (1.34E+01), respectively. Although RL-RVEA has a higher RT (3.24E+01), it further highlights MaOALO efficiency. For DTLZ5, MaOALO demonstrates an impressive RT of (1.18), significantly better than MaOABC-TA (5.56), DSAE (5.72), RL-RVEA (2.03E+01) and MaOEA-IH (1.24E+01), showcasing its computational efficiency. In DTLZ6, MaOALO has a RT of (1.35), outperforming MaOABC-TA (2.52), DSAE (2.86), RL-RVEA (2.00E+01) and MaOEA-IH (1.36E+01). DTLZ7 results show that MaOALO has a RT of (1.38), which is significantly better than MaOABC-TA (5.85), DSAE (5.69), RL-RVEA (1.97E+01) and MaOEA-IH (1.45E+01), highlighting MaOALO superior computational efficiency. The overall performance of the MaOALO algorithm, characterized by lower RT values in DTLZ1, DTLZ2, DTLZ3, DTLZ4, DTLZ5, DTLZ6 and DTLZ7, elucidates its ability to efficiently solve MaOPs with minimal computational time.

The performance of MaOALO across the HV, IGD and RT metrics showcases its robustness and efficacy in many-objective optimization. MaOALO achieves high HV values, indicating excellent Pareto front coverage, maintains low IGD values, signifying close and diverse approximations to the true Pareto front and exhibits low RT values, demonstrating superior computational efficiency.

Thus, based on the extensive analysis the key findings from this section can be summarized as—

Table 7
Results of HV metric of different many-objective algorithms on MaF benchmark problems.

Problem	M	D	MaOALO	ARMOEA	NSGA-III	MaOTLBO	RVEA
MaF1	5	14	2.5280e-3 (2.28e-3) =	7.8549e-3 (2.54e-4) =	3.8870e-3 (6.80e-4) =	6.7312e-3 (2.23e-4) =	6.2802e-3 (7.51e-4)
	9	18	2.3934e-6 (2.74e-7) =	6.6609e-7 (5.77e-7) =	2.4994e-6 (1.28e-7) =	0.0000e+0 (0.00e+0) =	6.7180e-7 (2.93e-7)
	14	23	1.0758e-11 (2.88e-12) =	1.3585e-12 (1.32e-12) =	6.8036e-12 (2.87e-12) =	1.1933e-12 (1.32e-12) =	1.1834e-12 (4.42e-13)
MaF2	5	14	1.4981e-1 (4.63e-3) =	1.5649e-1 (1.74e-3) =	1.4679e-1 (4.26e-3) =	1.3266e-1 (2.72e-3) =	1.6436e-1 (2.81e-3)
	9	18	1.8183e-1 (4.64e-3) =	1.3465e-1 (2.16e-3) =	1.5673e-1 (2.39e-2) =	1.4682e-1 (5.04e-3) =	1.2596e-1 (6.57e-3)
	14	23	8.6905e-2 (7.37e-3) =	1.2485e-1 (1.18e-2) =	9.1560e-2 (6.55e-3) =	7.2704e-2 (4.04e-3) =	7.4885e-2 (5.30e-3)
MaF3	5	14	0.0000e+0 (0.00e+0) =	0.0000e+0 (0.00e+0) =	0.0000e+0 (0.00e+0) =	0.0000e+0 (0.00e+0) =	0.0000e+0 (0.00e+0)
	9	18	0.0000e+0 (0.00e+0) =	0.0000e+0 (0.00e+0) =	0.0000e+0 (0.00e+0) =	0.0000e+0 (0.00e+0) =	0.0000e+0 (0.00e+0)
	14	23	0.0000e+0 (0.00e+0) =	0.0000e+0 (0.00e+0) =	0.0000e+0 (0.00e+0) =	0.0000e+0 (0.00e+0) =	0.0000e+0 (0.00e+0)
MaF4	5	14	0.0000e+0 (0.00e+0) =	0.0000e+0 (0.00e+0) =	0.0000e+0 (0.00e+0) =	0.0000e+0 (0.00e+0) =	0.0000e+0 (0.00e+0)
	9	18	0.0000e+0 (0.00e+0) =	0.0000e+0 (0.00e+0) =	0.0000e+0 (0.00e+0) =	0.0000e+0 (0.00e+0) =	0.0000e+0 (0.00e+0)
	14	23	0.0000e+0 (0.00e+0) =	0.0000e+0 (0.00e+0) =	0.0000e+0 (0.00e+0) =	0.0000e+0 (0.00e+0) =	0.0000e+0 (0.00e+0)
MaF5	5	14	7.1978e-1 (5.96e-2) =	7.3061e-1 (5.01e-2) =	7.5623e-1 (5.33e-3) =	6.2796e-1 (1.68e-2) =	6.6281e-1 (4.33e-2)
	9	18	8.9347e-1 (1.51e-2) =	8.7851e-1 (2.58e-2) =	8.9152e-1 (1.37e-2) =	0.0000e+0 (0.00e+0) =	6.5713e-1 (4.48e-2)
	14	23	7.6255e-1 (4.59e-3) =	5.9397e-1 (4.81e-2) =	7.5772e-1 (3.45e-3) =	0.0000e+0 (0.00e+0) =	3.5951e-1 (1.66e-1)
MaF6	5	14	1.2451e-1 (1.04e-3) =	1.2782e-1 (1.55e-4) =	1.2469e-1 (1.97e-3) =	1.2798e-1 (4.65e-4) =	1.2180e-1 (1.79e-3)
	9	18	3.1737e-2 (5.50e-2) =	6.7762e-2 (5.87e-2) =	9.6653e-2 (1.02e-3) =	0.0000e+0 (0.00e+0) =	9.6615e-2 (1.81e-3)
	14	23	0.0000e+0 (0.00e+0) =	9.3832e-2 (6.47e-4) =	6.0160e-30 (1.04e-29) =	0.0000e+0 (0.00e+0) =	9.2854e-2 (8.96e-4)
MaF7	5	24	1.6025e-1 (2.14e-2) =	1.5705e-1 (1.21e-2) =	1.5856e-1 (1.91e-2) =	1.0266e-1 (1.76e-2) =	1.2380e-1 (6.37e-2)
	9	28	6.9393e-3 (2.85e-3) =	1.3442e-2 (2.27e-2) =	9.3864e-3 (1.02e-2) =	3.8599e-9 (6.65e-9) =	9.0820e-3 (9.83e-3)
	14	33	5.5144e-2 (1.91e-2) =	8.7938e-8 (1.51e-7) =	3.2614e-2 (1.38e-2) =	0.0000e+0 (0.00e+0) =	1.5115e-3 (1.57e-3)
MaF8	5	2	5.3195e-2 (4.77e-2) =	6.0550e-2 (5.35e-2) =	5.9624e-2 (3.72e-2) =	7.5622e-2 (7.60e-3) =	1.4141e-2 (1.43e-2)
	9	2	5.8864e-3 (4.96e-3) =	2.0224e-3 (1.99e-3) =	5.5348e-3 (1.84e-3) =	1.2693e-3 (1.33e-3) =	2.3770e-4 (2.99e-4)
	14	2	5.3112e-4 (4.66e-5) =	3.2517e-4 (1.37e-4) =	2.9967e-4 (9.89e-5) =	3.1884e-4 (1.76e-4) =	6.7304e-6 (1.17e-5)
MaF9	5	2	1.9991e-1 (3.00e-2) =	1.0457e-1 (3.17e-2) =	5.1639e-2 (8.94e-2) =	2.2315e-2 (2.09e-2) =	1.0728e-1 (4.24e-2)
	9	2	7.4127e-3 (1.28e-2) =	9.6216e-4 (1.67e-3) =	0.0000e+0 (0.00e+0) =	1.4130e-3 (2.45e-3) =	1.3045e-3 (2.26e-3)
	14	2	3.3072e-5 (5.73e-5) =	5.5808e-4 (4.87e-4) =	0.0000e+0 (0.00e+0) =	7.7887e-6 (1.35e-5) =	1.3115e-4 (2.15e-4)
MaF10	5	14	5.2302e-1 (2.14e-2) =	5.5101e-1 (6.92e-2) =	5.7361e-1 (5.49e-3) =	5.3883e-1 (2.99e-2) =	4.7371e-1 (3.24e-2)
	9	18	4.4422e-1 (1.66e-1) =	4.3184e-1 (9.52e-2) =	4.1087e-1 (7.22e-2) =	4.0208e-1 (5.36e-2) =	3.1695e-1 (1.73e-2)
	14	23	9.6269e-1 (5.20e-2) =	8.4802e-1 (1.03e-1) =	9.1453e-1 (7.49e-2) =	7.5019e-1 (9.34e-2) =	5.0170e-1 (1.58e-1)
MaF11	5	14	9.4283e-1 (2.08e-3) =	9.5531e-1 (1.92e-2) =	9.5561e-1 (8.05e-3) =	9.6368e-1 (7.31e-3) =	9.1155e-1 (2.21e-3)
	9	18	9.6781e-1 (4.60e-3) =	9.4675e-1 (1.08e-2) =	9.5034e-1 (9.98e-3) =	9.2806e-1 (1.99e-2) =	9.1557e-1 (2.35e-2)
	14	23	7.5841e-1 (1.81e-2) =	9.2809e-1 (5.42e-2) =	8.4008e-1 (7.12e-2) =	8.9385e-1 (2.53e-2) =	8.1996e-1 (9.26e-2)
MaF12	5	14	5.8721e-1 (7.31e-3) =	5.7565e-1 (1.85e-2) =	6.2708e-1 (2.29e-2) =	5.4617e-1 (2.38e-2) =	5.3860e-1 (1.64e-2)
	9	18	6.3821e-1 (5.01e-2) =	5.9207e-1 (3.09e-2) =	5.4791e-1 (3.14e-2) =	4.2949e-1 (8.18e-2) =	4.6935e-1 (1.77e-2)
	14	23	4.6599e-1 (4.80e-2) =	3.8879e-1 (1.08e-1) =	3.6928e-1 (6.42e-2) =	2.1095e-1 (1.35e-2) =	3.4531e-1 (2.81e-2)
MaF13	5	5	1.4152e-1 (5.57e-2) =	2.1838e-1 (8.07e-3) =	1.4136e-1 (4.00e-2) =	1.8081e-1 (3.19e-2) =	4.2948e-2 (5.19e-2)
	9	5	6.3305e-2 (3.84e-2) =	1.2500e-1 (5.66e-3) =	6.5250e-2 (1.82e-2) =	7.3653e-2 (1.31e-2) =	4.4607e-2 (3.95e-2)
	14	5	1.0858e-4 (9.44e-5) =	6.0441e-2 (1.72e-2) =	7.2996e-5 (8.47e-5) =	4.3477e-2 (1.93e-2) =	1.7314e-2 (2.95e-2)
MaF14	5	100	0.0000e+0 (0.00e+0) =	0.0000e+0 (0.00e+0) =	0.0000e+0 (0.00e+0) =	0.0000e+0 (0.00e+0) =	0.0000e+0 (0.00e+0)
	9	180	0.0000e+0 (0.00e+0) =	0.0000e+0 (0.00e+0) =	0.0000e+0 (0.00e+0) =	0.0000e+0 (0.00e+0) =	0.0000e+0 (0.00e+0)
	14	280	0.0000e+0 (0.00e+0) =	0.0000e+0 (0.00e+0) =	0.0000e+0 (0.00e+0) =	0.0000e+0 (0.00e+0) =	0.0000e+0 (0.00e+0)
MaF15	5	100	0.0000e+0 (0.00e+0) =	0.0000e+0 (0.00e+0) =	0.0000e+0 (0.00e+0) =	0.0000e+0 (0.00e+0) =	0.0000e+0 (0.00e+0)
	9	180	0.0000e+0 (0.00e+0) =	0.0000e+0 (0.00e+0) =	0.0000e+0 (0.00e+0) =	0.0000e+0 (0.00e+0) =	0.0000e+0 (0.00e+0)
	14	280	0.0000e+0 (0.00e+0) =	0.0000e+0 (0.00e+0) =	0.0000e+0 (0.00e+0) =	0.0000e+0 (0.00e+0) =	0.0000e+0 (0.00e+0)

- MaOALO consistently achieves lower IGD values across several DTLZ benchmark problems, including DTLZ1, DTLZ2, DTLZ4 and DTLZ5. This indicates that MaOALO excels in producing solution sets that are not only closer to the true Pareto front but also more diverse. Lower IGD values signify better convergence and diversity.
- This superior performance in IGD can be attributed to MaOALO effective balancing of exploration and exploitation, ensuring a comprehensive search of the solution space while maintaining a focus on high-quality solutions.

Table 8
Results of RT metric of different many-objective algorithms on MaF benchmark problems.

Problem	M	D	MaOALO	ARMOEA	NSGA-III	MaOTLBO	RVEA
MaF1	5	14	1.5393e+0 (2.21e-1)	1.3640e+1 (6.72e-1) =	2.0203e+0 (2.86e-1) =	5.7454e+0 (4.77e-1) =	2.1659e+0 (1.62e+0) =
	9	18	1.0427e+0 (3.40e-2)	1.5514e+1 (1.06e+0) =	4.1615e+0 (1.85e-1) =	5.8479e+0 (1.45e-1) =	5.1527e+0 (5.97e-1) =
	14	23	1.7099e+0 (2.60e-3)	6.0572e+0 (2.24e-1) =	1.1649e+1 (3.23e-1) =	2.4023e+0 (1.90e-2) =	1.2038e+1 (5.73e-1) =
MaF2	5	14	1.8141e+0 (3.14e-1)	1.6857e+1 (1.28e-1) =	1.2451e+0 (2.20e-1) =	1.3368e+1 (9.01e-1) =	1.5997e+0 (1.21e-2) =
	9	18	1.3951e+0 (7.23e-2)	2.1072e+1 (2.35e+0) =	2.0673e+0 (2.12e-1) =	1.1991e+1 (1.30e-1) =	2.8773e+0 (3.24e-1) =
	14	23	2.0780e+0 (4.09e-2)	7.1197e+0 (2.93e-2) =	1.1643e+1 (2.58e-1) =	3.9718e+0 (4.07e-1) =	1.2131e+1 (1.19e-1) =
MaF3	5	14	1.0315e+0 (1.99e-2)	5.4639e+0 (3.00e-1) =	1.5567e+0 (1.96e-1) =	2.0651e+0 (6.06e-2) =	1.6686e+0 (5.71e-2) =
	9	18	1.1625e+0 (3.20e-2)	8.8994e+0 (4.54e-1) =	3.7587e+0 (3.62e-2) =	8.6041e+0 (1.71e-1) =	4.1692e+0 (7.97e-2) =
	14	23	1.9035e+0 (9.81e-2)	4.6656e+0 (2.16e-1) =	1.1612e+1 (1.38e-1) =	2.7379e+0 (1.12e-1) =	1.1791e+1 (1.72e-1) =
MaF4	5	14	9.6995e-1 (3.89e-2)	3.9533e+0 (6.81e-1) =	4.0235e+0 (7.17e-2) =	2.2552e+0 (3.98e-2) =	4.2026e+0 (7.72e-2) =
	9	18	1.0498e+0 (2.80e-2)	4.8216e+0 (1.17e+0) =	3.8869e+0 (9.50e-2) =	2.4671e+0 (3.38e-1) =	4.0429e+0 (6.83e-2) =
	14	23	1.8532e+0 (8.70e-2)	5.6776e+0 (5.96e-1) =	1.2714e+1 (7.94e-1) =	2.5646e+0 (2.35e-1) =	1.2746e+1 (1.10e+0) =
MaF5	5	14	1.4764e+0 (7.36e-2)	1.3494e+1 (1.49e-1) =	1.4621e+0 (1.34e-1) =	5.5705e+0 (1.20e-1) =	2.5940e+0 (1.59e+0) =
	9	18	1.4052e+0 (7.21e-2)	1.7277e+1 (9.57e-1) =	1.3389e+0 (1.47e-1) =	1.0578e+1 (3.32e-1) =	1.8639e+0 (2.88e-1) =
	14	23	1.9587e+0 (4.46e-3)	6.1989e+0 (1.34e-1) =	2.7221e+0 (3.79e-1) =	3.0489e+0 (1.87e-2) =	3.2948e+0 (3.86e-1) =
MaF6	5	14	9.3460e-1 (4.62e-2)	4.6545e+0 (9.95e-1) =	4.6805e+0 (8.83e-1) =	3.9809e+0 (9.68e-1) =	4.5196e+0 (2.99e-1) =
	9	18	4.8603e-1 (5.57e-3)	6.2376e+0 (4.85e+0) =	2.0052e+0 (9.16e-2) =	3.1589e+0 (1.16e-1) =	4.1544e+0 (2.84e-2) =
	14	23	1.0723e+0 (2.09e-1)	2.4112e+0 (1.04e-1) =	5.7581e+0 (1.37e-1) =	1.5419e+0 (1.25e-1) =	5.9383e+0 (9.44e-2) =
MaF7	5	24	7.1676e-1 (8.35e-2)	8.6608e+0 (2.34e+0) =	2.5372e+0 (4.08e-1) =	3.4287e+0 (2.34e-1) =	2.1975e+0 (1.56e-1) =
	9	28	6.9472e-1 (2.87e-3)	1.0787e+1 (1.40e+0) =	2.0449e+0 (1.67e-1) =	4.5814e+0 (1.54e-1) =	2.0604e+0 (3.73e-2) =
	14	33	1.2091e+0 (9.86e-2)	3.9556e+0 (2.94e-1) =	6.0310e+0 (3.57e-1) =	1.6415e+0 (1.06e-2) =	6.1246e+0 (3.81e-1) =
MaF8	5	2	1.2410e+1 (6.66e-1)	1.6989e+0 (9.83e-1) =	3.1362e+0 (3.29e-1) =	1.2532e+0 (7.59e-2) =	3.4244e+0 (2.14e-1) =
	9	2	1.1394e+1 (6.44e-1)	1.4409e+0 (7.31e-1) =	3.2417e+0 (3.01e-1) =	1.2681e+0 (7.36e-2) =	3.7013e+0 (1.56e-1) =
	14	2	2.6726e+1 (2.11e+1)	1.9162e+0 (2.38e-1) =	7.8552e+0 (4.36e-1) =	1.1694e+0 (1.10e-1) =	8.7550e+0 (6.99e-1) =
MaF9	5	2	6.4662e-1 (2.96e-1)	2.1311e+0 (5.77e-1) =	2.6054e+0 (2.84e-1) =	1.1524e+0 (1.25e-1) =	2.6961e+0 (1.38e-1) =
	9	2	5.4858e-1 (1.68e-2)	3.0235e+0 (3.63e-1) =	2.2373e+0 (1.18e-1) =	1.3414e+0 (2.01e-1) =	2.2601e+0 (2.82e-1) =
	14	2	1.2752e+0 (1.27e-1)	3.5185e+0 (1.09e+0) =	7.4263e+0 (6.97e-1) =	1.1089e+0 (1.85e-2) =	6.0745e+0 (2.31e-1) =
MaF10	5	14	7.4158e-1 (1.12e-1)	6.1035e+0 (1.08e+0) =	8.7308e-1 (1.83e-1) =	2.8361e+0 (7.33e-1) =	1.0116e+0 (7.88e-2) =
	9	18	8.9432e-1 (1.81e-1)	8.4004e+0 (6.08e-1) =	6.8189e-1 (2.60e-2) =	3.4344e+0 (4.96e-1) =	1.0953e+0 (7.55e-2) =
	14	23	1.2896e+0 (6.23e-2)	3.3536e+0 (2.74e-1) =	6.5290e+0 (5.72e-1) =	1.2989e+0 (3.67e-3) =	4.6733e+0 (2.50e+0) =
MaF11	5	14	7.7900e-1 (2.42e-2)	5.7829e+0 (2.24e-1) =	7.2080e-1 (6.81e-2) =	2.4523e+0 (3.13e-2) =	8.8872e-1 (1.22e-2) =
	9	18	8.1052e-1 (1.70e-2)	7.4120e+0 (9.47e-2) =	1.5375e+0 (4.17e-1) =	3.2390e+0 (5.51e-2) =	1.8596e+0 (3.09e-1) =
	14	23	1.1652e+0 (2.44e-2)	3.2735e+0 (4.64e-2) =	5.6261e+0 (1.17e-1) =	1.3468e+0 (9.44e-3) =	5.9169e+0 (3.16e-1) =
MaF12	5	14	8.5144e-1 (1.29e-2)	7.0757e+0 (2.78e-1) =	7.2718e-1 (9.24e-2) =	3.9214e+0 (2.46e-1) =	9.2991e-1 (5.02e-2) =
	9	18	9.2061e-1 (7.27e-2)	8.3600e+0 (1.04e-1) =	1.3603e+0 (1.19e-1) =	5.0340e+0 (7.60e-2) =	1.6540e+0 (1.02e-1) =
	14	23	1.2387e+0 (4.85e-2)	3.5547e+0 (3.62e-3) =	5.5799e+0 (1.13e-1) =	1.6671e+0 (1.29e-2) =	5.0873e+0 (9.68e-1) =
MaF13	5	5	4.6575e-1 (2.08e-2)	3.4202e+0 (8.63e-2) =	2.0191e+0 (3.81e-2) =	1.1434e+0 (8.14e-2) =	2.0053e+0 (7.58e-2) =
	9	5	4.6745e-1 (2.77e-3)	3.5344e+0 (5.27e-2) =	1.8528e+0 (5.53e-2) =	1.1935e+0 (5.78e-2) =	2.0014e+0 (1.50e-1) =
	14	5	8.2096e-1 (3.22e-2)	2.3600e+0 (5.09e-2) =	5.5939e+0 (1.23e-1) =	9.4533e-1 (3.64e-2) =	5.6405e+0 (1.70e-1) =
MaF14	5	100	8.3142e-1 (4.03e-2)	4.8507e+0 (2.61e-2) =	1.5432e+0 (3.73e-1) =	2.4401e+0 (1.68e-1) =	1.4573e+0 (1.34e-1) =
	9	180	1.0490e+0 (1.11e-2)	4.7191e+0 (6.91e-1) =	2.0748e+0 (5.07e-2) =	5.0986e+0 (3.01e-2) =	2.0031e+0 (5.09e-2) =
	14	280	1.6874e+0 (3.20e-2)	3.0443e+0 (1.26e-1) =	5.7911e+0 (1.72e-1) =	2.1743e+0 (3.14e-2) =	6.1438e+0 (3.56e-1) =
MaF15	5	100	7.8416e-1 (8.65e-3)	5.6323e+0 (4.33e-1) =	1.6861e+0 (5.19e-2) =	3.1403e+0 (2.10e-1) =	1.9071e+0 (1.53e-1) =
	9	180	8.9203e-1 (2.24e-2)	7.4558e+0 (1.36e-1) =	1.8865e+0 (1.75e-2) =	4.3512e+0 (1.42e-1) =	2.1978e+0 (9.35e-2) =
	14	280	3.2186e+0 (1.41e+0)	4.0870e+0 (7.41e-2) =	5.8649e+0 (2.58e-1) =	2.2321e+0 (3.01e-2) =	5.9734e+0 (2.43e-1) =

Table 9
Results of SP metric of different many-objective algorithms on RWMaOP problems.

Problem	M	D	MaOALO	ARMOEA	NSGA-III	MaOTLBO	RVEA
RWMaOP1	9	7	1.3270e+0 (4.73e-1)	4.1289e+0 (1.29e+0) =	3.5804e+0 (1.24e+0) =	1.6676e+0 (7.60e-1) =	2.3595e+0 (8.12e-1) =
RWMaOP2	4	10	1.9260e+3 (6.05e+2)	8.7520e+2 (4.04e+2) =	8.0464e+2 (2.65e+2) =	8.6494e+3 (1.22e+4) =	6.8916e+2 (1.04e+2) =
RWMaOP3	7	3	1.6810e+1 (2.50e+0) =	5.3197e+1 (5.69e+0) =	3.1183e+1 (3.87e-1) =	2.5614e+1 (5.84e+0)	3.0886e+1 (3.08e+0) =
RWMaOP4	5	6	3.8271e+4 (6.84e+3)	5.1615e+4 (5.21e+3) =	9.7857e+4 (3.58e+4) =	4.3377e+4 (3.88e+3) =	5.0022e+4 (6.15e+3) =
RWMaOP5	4	4	6.2237e-2 (2.52e-2)	1.1171e-1 (3.81e-3) =	8.5369e-2 (7.74e-3) =	4.4664e-2 (5.67e-3) =	9.9596e-2 (1.08e-2) =

- MaOALO demonstrates a consistent performance across different evaluation metrics, including HV and RT. High HV values in DTLZ1, DTLZ2, DTLZ4 and DTLZ5 indicate that MaOALO effectively covers a larger volume of the Pareto front, showcasing its ability to generate a diverse set of solutions.
- MaOALO 's ability to maintain high HV values suggests that it is capable of generating well-distributed solutions, covering the objective space comprehensively. This, combined with its low IGD values, highlights MaOALO robustness in achieving a good spread and diversity of solutions.

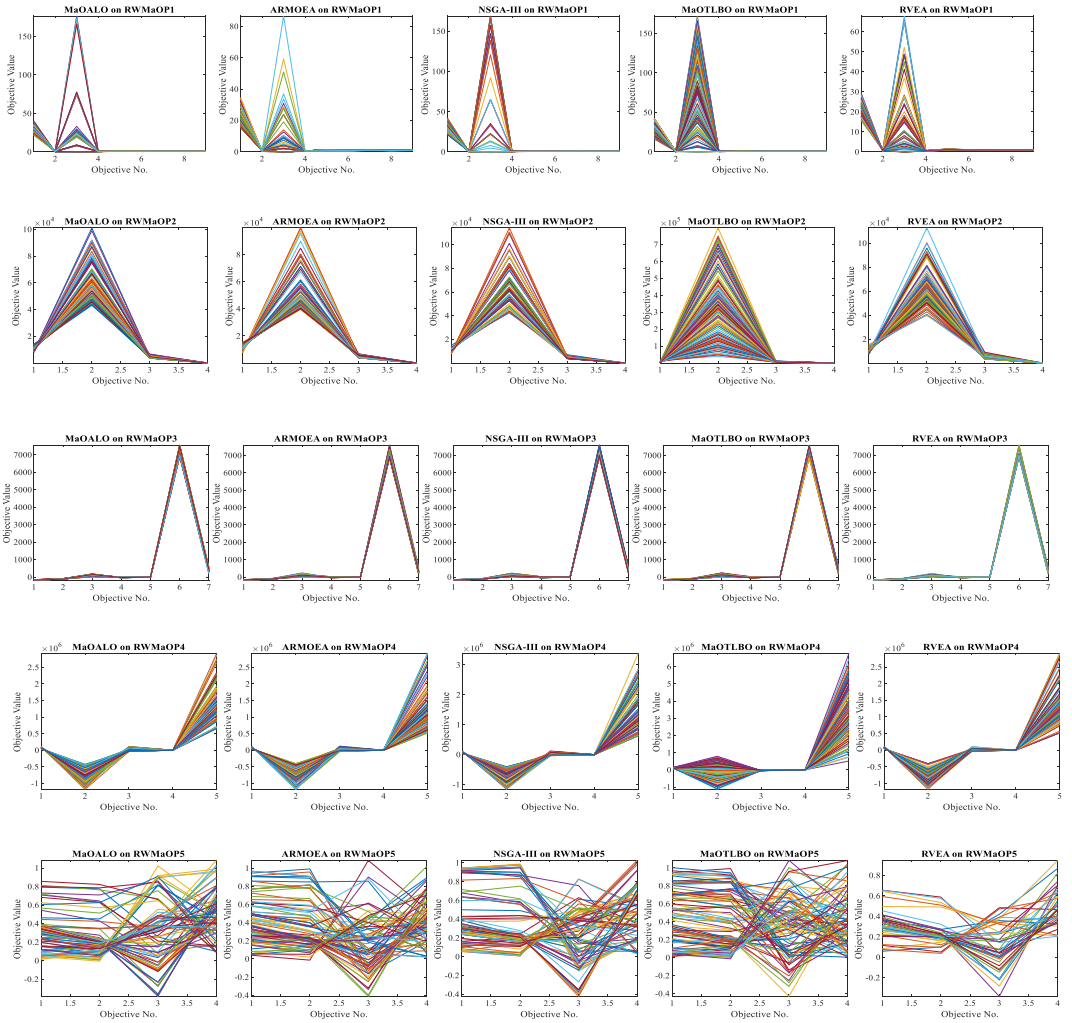

Fig. 6. Best Pareto optimal front obtained by different algorithms on RWMaOP problems.

Table 10
Results of HV metric of different many-objective algorithms on RWMaOP problems.

Problem	M	D	MaOALO	ARMOEA	NSGA-III	MaOTLBO	RVEA
RWMaOP1	9	7	2.0814e-3 (9.95e-5) =	1.3382e-3 (1.21e-4) =	2.1702e-3 (1.11e-4) =	1.4268e-3 (8.32e-5) =	6.5377e-4 (7.29e-5)
RWMaOP2	4	10	8.0894e-2 (5.16e-4) =	7.2034e-2 (4.67e-3) =	7.9355e-2 (2.02e-3) =	1.2550e-2 (2.79e-3) =	6.7667e-2 (3.87e-3)
RWMaOP3	7	3	1.8458e-2 (2.18e-3)	1.6346e-2 (1.79e-4) =	1.6136e-2 (7.80e-4) =	1.7366e-2 (5.07e-5) =	1.6364e-2 (4.48e-4) =
RWMaOP4	5	6	5.4273e-1 (4.03e-3)	5.4245e-1 (3.87e-3) =	5.4013e-1 (6.71e-3) =	4.7680e-1 (7.96e-3) =	5.3157e-1 (3.66e-3) =
RWMaOP5	4	4	5.4636e-1 (4.55e-3) =	5.4419e-1 (3.73e-3) =	5.3611e-1 (5.79e-3) =	5.3898e-1 (2.28e-3) =	5.3052e-1 (1.96e-2)

Table 11
Results of RT metric of different many-objective algorithms on RWMaOP problems.

Problem	M	D	MaOALO	ARMOEA	NSGA-III	MaOTLBO	RVEA
RWMaOP1	9	7	9.7836e-1 (4.53e-2)	1.6303e+1 (2.17e-1) =	3.6453e+0 (1.33e-1) =	1.0752e+1 (1.73e-1) =	3.9043e+0 (1.50e-1) =
RWMaOP2	4	10	1.3003e+1 (2.19e+0)	1.9725e+1 (5.81e-1) =	1.3517e+1 (1.66e-1) =	1.4689e+1 (1.99e-1) =	1.3873e+1 (1.05e+0) =
RWMaOP3	7	3	3.9490e+0 (1.94e-2) =	2.0184e+1 (1.83e+0) =	7.3674e-1 (5.41e-2)	9.7766e+0 (2.76e-1) =	4.2727e+0 (1.43e-1) =
RWMaOP4	5	6	4.5222e+0 (1.14e-1) =	1.4838e+1 (1.50e-1) =	1.0225e+0 (2.63e-2)	8.3520e+0 (6.93e-2) =	4.0717e+0 (3.87e-1) =
RWMaOP5	4	4	9.6614e-1 (4.40e-2)	1.4017e+1 (3.65e-1) =	3.9615e+0 (2.56e-1) =	6.6041e+0 (2.20e-1) =	3.7679e+0 (3.74e-1) =

Table 12
Results of IGD metric for various many-objective algorithms on DTLZ benchmark problems.

Problem	M	D	MaOALO	MaOABC-TA	DSAE	RL-RVEA	MaOEA-IH
DTLZ1	8	12	6.3397e-1 ± 5.02e-1	7.0418e-1 ± 1.14e-1	1.0596e+0 ± 1.90e-1	4.2723e-1 ± 6.70e-2	1.2849e+0 ± 8.66e-1
DTLZ2	8	17	4.0055e-1 ± 8.25e-3	5.1624e-1 ± 1.03e-1	3.9756e-1 ± 3.78e-3	3.9960e-1 ± 6.19e-4	5.6507e-1 ± 3.02e-1
DTLZ3	8	17	1.4267e+1 ± 6.73e+0	3.5594e+1 ± 1.39e+1	4.5461e+1 ± 1.26e+1	1.4521e+1 ± 3.17e+0	2.3619e+1 ± 6.07e+0
DTLZ4	8	17	4.1748e-1 ± 3.97e-4	4.4881e-1 ± 5.30e-2	4.5359e-1 ± 9.71e-2	4.6077e-1 ± 4.09e-2	7.4996e-1 ± 6.23e-2
DTLZ5	8	17	1.4991e-1 ± 1.17e-2	2.6120e-1 ± 3.89e-2	2.8604e-1 ± 5.27e-2	1.5006e-1 ± 8.42e-2	8.6605e-1 ± 4.95e-2
DTLZ6	8	17	2.2399e+0 ± 6.08e-1	3.7600e+0 ± 1.36e+0	3.3355e+0 ± 1.83e+0	4.1223e-1 ± 3.63e-1	1.7906e+0 ± 1.14e+0
DTLZ7	8	27	1.3067e+0 ± 1.11e-1	3.3902e+0 ± 1.63e+0	3.5954e+0 ± 1.08e+0	1.5781e+0 ± 8.76e-1	4.9069e+0 ± 9.60e-1

Table 13
Results of Friedman test, WRST and *p*-value based on IGD metric for various many-objective algorithms on DTLZ benchmark problems.

Problem	MaOALO	MaOABC-TA	DSAE	RL-RVEA	MaOEA-IH	*p*-value
DTLZ1	2.3	2.6	4.3	1.3	4.3	0.08
DTLZ2	3.3	4	2.6	2.6	2.3	0.71
DTLZ3	2	3.6	5	1.3	3	0.04
DTLZ4	1.3	3	2	2.6	5	0.16
DTLZ5	1.6	3.6	3.3	2.3	5	0.03
DTLZ6	3	4.3	4	1	2.6	0.08
DTLZ7	1.3	3.6	4	1.3	4.3	0.05

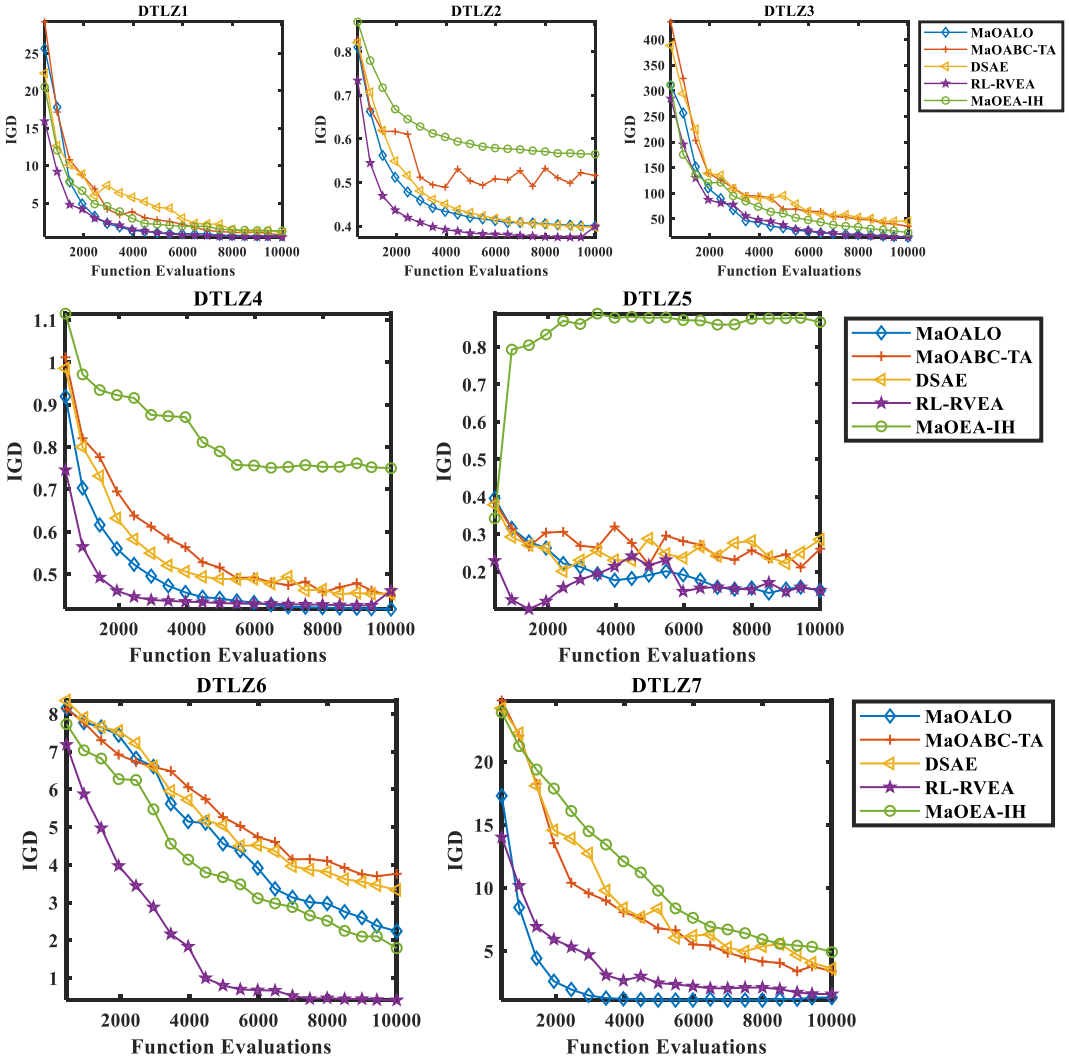

Fig. 7. Convergence curve based on the IGD metric for various many-objective algorithms on DTLZ problems.

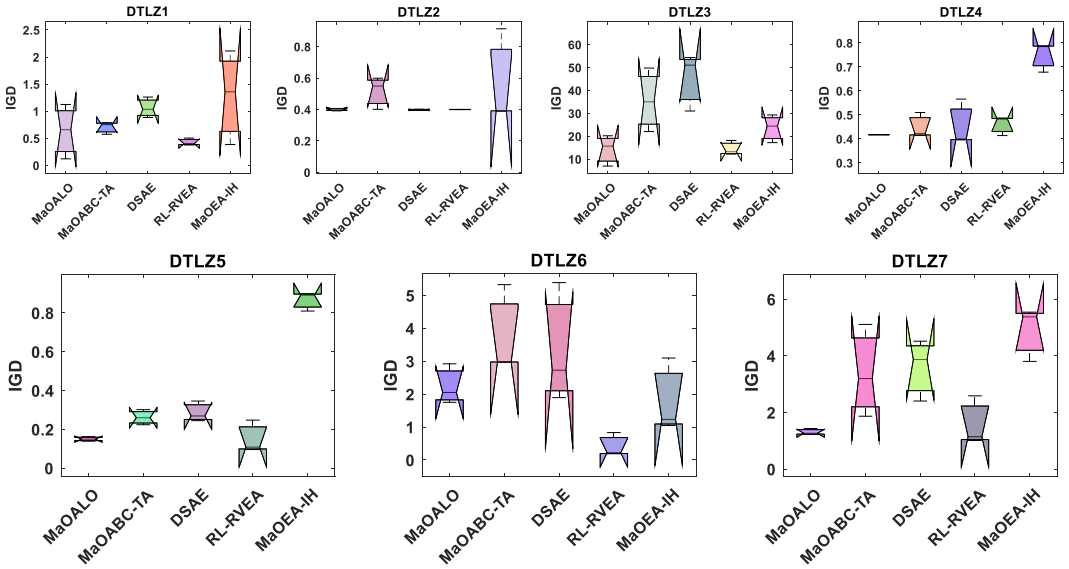

Fig. 8. Box plot based on the IGD metric for various many-objective algorithms on DTLZ problems.

Table 14
Results of HV metric for various many-objective algorithms on DTLZ benchmark problems.

Problem	M	D	MaOALO	MaOABC-TA	DSAE	RL-RVEA	MaOEA-IH
DTLZ1	8	12	3.2628e-1 ± 5.61e-1	2.1866e-3 ± 3.09e-3	0.0000e+0 ± 0.00e+0	1.0896e-1 ± 5.79e-2	1.3820e-1 ± 2.39e-1
DTLZ2	8	17	8.4184e-1 ± 4.78e-2	7.4069e-1 ± 1.01e-1	8.4293e-1 ± 1.89e-2	7.3216e-1 ± 2.12e-2	7.2074e-1 ± 2.43e-1
DTLZ3	8	17	0.0000e+0 ± 0.00e+0	0.0000e+0 ± 0.00e+0	0.0000e+0 ± 0.00e+0	0.0000e+0 ± 0.00e+0	0.0000e+0 ± 0.00e+0
DTLZ4	8	17	8.8624e-1 ± 1.38e-3	8.4278e-1 ± 3.43e-2	8.2532e-1 ± 7.15e-2	8.3894e-1 ± 1.37e-2	6.3771e-1 ± 6.12e-2
DTLZ5	8	17	3.1371e-2 ± 5.48e-3	3.1911e-2 ± 2.12e-2	5.3802e-2 ± 3.66e-3	9.5973e-2 ± 4.74e-3	0.0000e+0 ± 0.00e+0
DTLZ6	8	17	0.0000e+0 ± 0.00e+0	0.0000e+0 ± 0.00e+0	0.0000e+0 ± 0.00e+0	1.5409e-3 ± 2.63e-3	0.0000e+0 ± 0.00e+0
DTLZ7	8	27	2.9051e-2 ± 4.75e-2	4.5472e-2 ± 3.92e-2	1.0630e-2 ± 8.30e-3	2.2439e-2 ± 2.44e-2	7.5515e-2 ± 5.43e-2

Table 15
Results of Friedman test, WRST and *p*-value based on the HV metric for various many-objective algorithms on DTLZ benchmark problems.

Problem	MaOALO	MaOABC-TA	DSAE	RL-RVEA	MaOEA-IH	*p*-value
DTLZ1	5.3	3.2	1.7	4.3	2.5	0.26
DTLZ2	2.7	2.3	3.3	1.7	3	0.19
DTLZ3	3	3	3	3	3	1.00
DTLZ4	5	3	3	3	1	0.05
DTLZ5	2.7	2.3	4	5	1	0.02
DTLZ6	2.7	2.7	2.7	4.3	2.7	0.09
DTLZ7	2.3	4.3	2	2.3	4.6	0.23

- MaOALO consistently outperforms other algorithms in terms of runtime, demonstrating superior computational efficiency. The significantly lower RT values across all DTLZ problems indicate that MaOALO can solve MaOPs more quickly and efficiently than its counterparts.
- The efficiency of MaOALO can be attributed to its streamlined search process and effective use of computational resources, making it particularly suitable for large-scale optimization problems where computational time is a critical factor.

4.5. Strengths and limitations of MaOALO

The strengths of MaOALO lie in its superior convergence, diversity and computational efficiency, making it a robust tool for many-objective optimization challenges. Based on the extensive tests of MaOALO on benchmarks and real-world problems as well as its comparison with a host of peer algorithms, it is observed that—

- MaOALO consistently records lower mean GD and IGD values across test cases. This indicates that MaOALO is highly effective at approximating the Pareto front closely and maintaining high convergence and diversity of solutions.

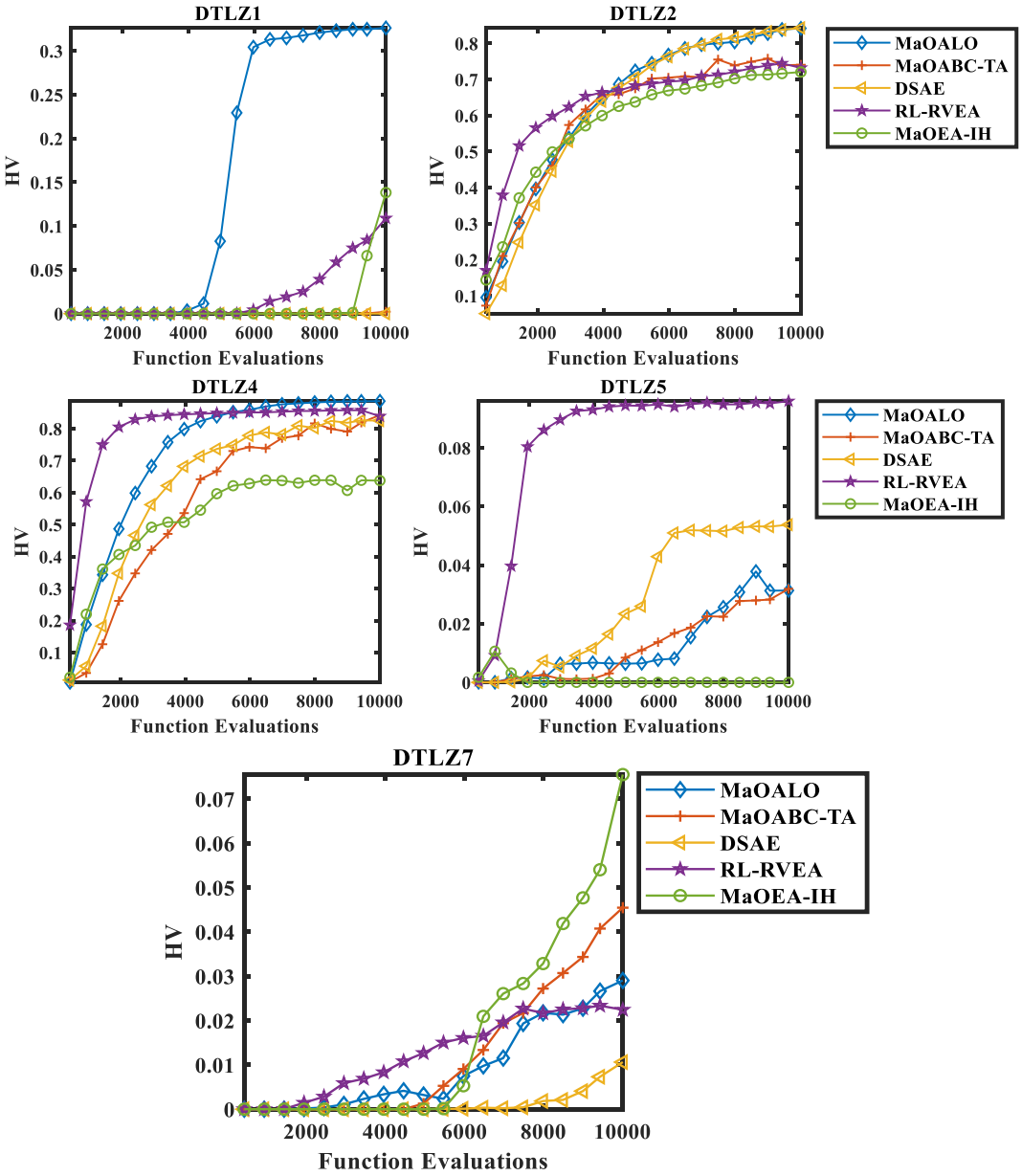

Fig. 9. Convergence curve based on HV metric for various many-objective algorithms on DTLZ problems.

- The SP and SD metrics demonstrate MaOALO ability to maintain a uniform distribution of solutions across the Pareto front. This uniform distribution is crucial in MaOPs, ensuring that all parts of the objective space are well-represented.
- MaOALO secures the best SP and SD results in a significant number of test problems, showcasing its robustness in maintaining solution diversity and comprehensive exploration of the Pareto front.
- MaOALO achieves higher HV values, indicating its ability to cover a larger volume in the objective space. This implies that the solutions found by MaOALO are not only diverse but also of high quality, closely approximating the true Pareto front.
- MaOALO consistently demonstrates shorter running times compared to its peers across various test problems. This superior computational efficiency makes MaOALO an attractive option for large-scale MaOPs.
- In RWMaOPs, MaOALO shows significant improvements in metrics such as SP and HV. This demonstrates its practicality and effectiveness in solving complex, real-world optimization problems.
- The consistent performance across a wide range of problems and configurations highlights MaOALO robustness. It efficiently handles diverse optimization challenges, making it a versatile and reliable tool for many-objective optimization tasks.

However, some limitations of MaOALO were also identified during the extensive tests. This could also be due to its being tested on a

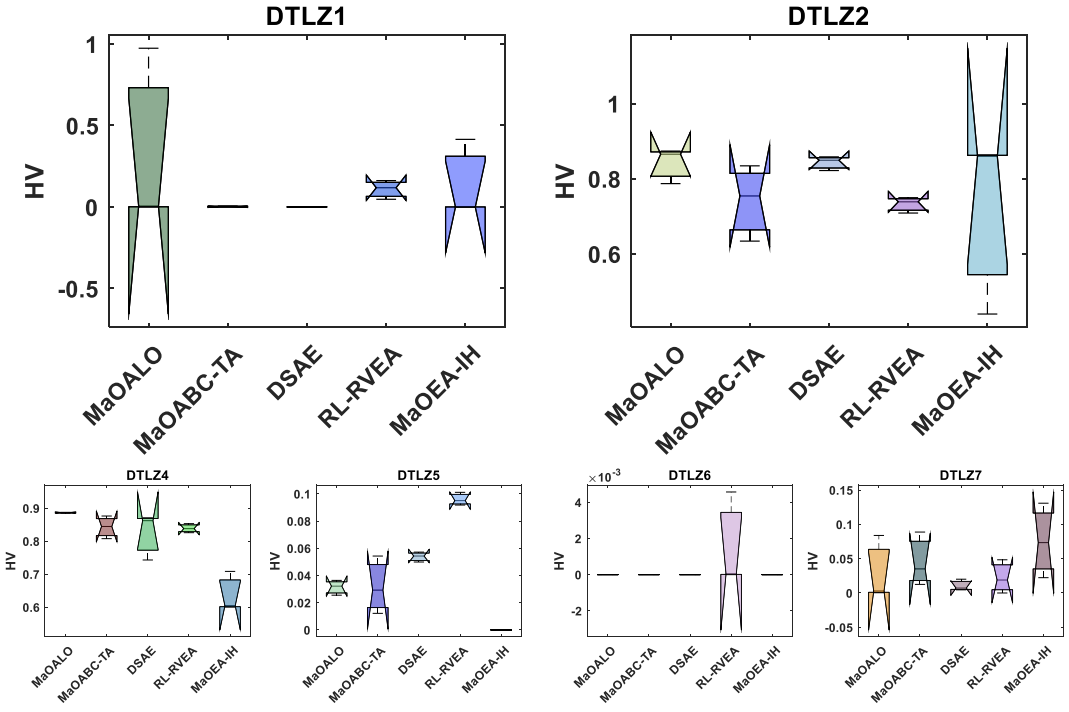

Fig. 10. Box plot based on the HV metric for various many-objective algorithms on DTLZ problems.

relatively small set of test problems, considering the endless variety of optimization problems that exists. Some of the limitations of MaOALO and this work are listed below—

- While MaOALO performs exceptionally well on a majority of test problems, there are instances where it does not achieve the best results. This suggests that the algorithm may need fine-tuning or hybridization with other methods to optimize its performance for specific problem types.
- The sophisticated mechanisms that contribute to MaOALO strengths, such as its ability to maintain a uniform distribution of solutions and fast computational speed, also make the algorithm complex to implement and understand. This complexity can be a barrier for novice practitioners who are not well-versed in advanced optimization techniques.
- Although MaOALO demonstrates efficiency in computational speed, its performance may still degrade with a very high number of objectives or decision variables, typical in real-world problems. Continuous assessment and enhancement of its scalability are necessary.
- MaOALO's ability to perform exceptionally well on benchmark problems could sometimes lead to overfitting, where the algorithm is finely tuned to specific test scenarios but may not generalize as well to new, unseen problems.

5. Conclusions

This paper introduces Many-Objective Ant Lion Optimizer (MaOALO) designed for tackling MaOPs. Initially, the reference point, niche preserve and information feedback mechanism concept are integrated into the ALO framework. MaOALO is tested on the MaF benchmark suite, encompassing 5, 9 and 14 objective scenarios and DTLZ benchmark with 8-objectives. These problems are characterized by complex frontiers with multimodal attributes and multiple local fronts, presenting significant challenges for optimization algorithms. MaOALO consistently demonstrates its efficacy by repeatedly obtaining well-converged and diverse solution sets across numerous trials on MaF and DTLZ problem set. MaOALO's performance is compared with several established algorithms like ARMOEA, NSGA-III, MaOTLBO, RVEA, MaOABC-TA, DSAE, RL-RVEA and MaOEA-IH. The comparative analysis revealed that MaOALO surpasses its peers, particularly in terms of GD, IGD, SP, SD, HV and RT metrics. It achieves superior results marked by lower GD, SP, SD, IGD values, greater HV stability, enhanced convergence and a faster convergence rate. Additionally, when applied to five real-world (RWMaOP1- RWMaOP5), MaOALO outshines four other methods in most test scenarios.

For subsequent initiatives, confirming the real-world applicability of our MaOALO through practical evaluations will be crucial. Additionally, investigating MaOPs that possess distinct features like large-scale dimensions, sparsity and constraints is vital, as these more accurately mirror real-life situations. Future efforts would be dedicated to improving and advancing MaOALO to ensure it delivers outstanding results for these types of challenges. The MaOALO source code is available at: https://github.com/kanak02/MaOALO.

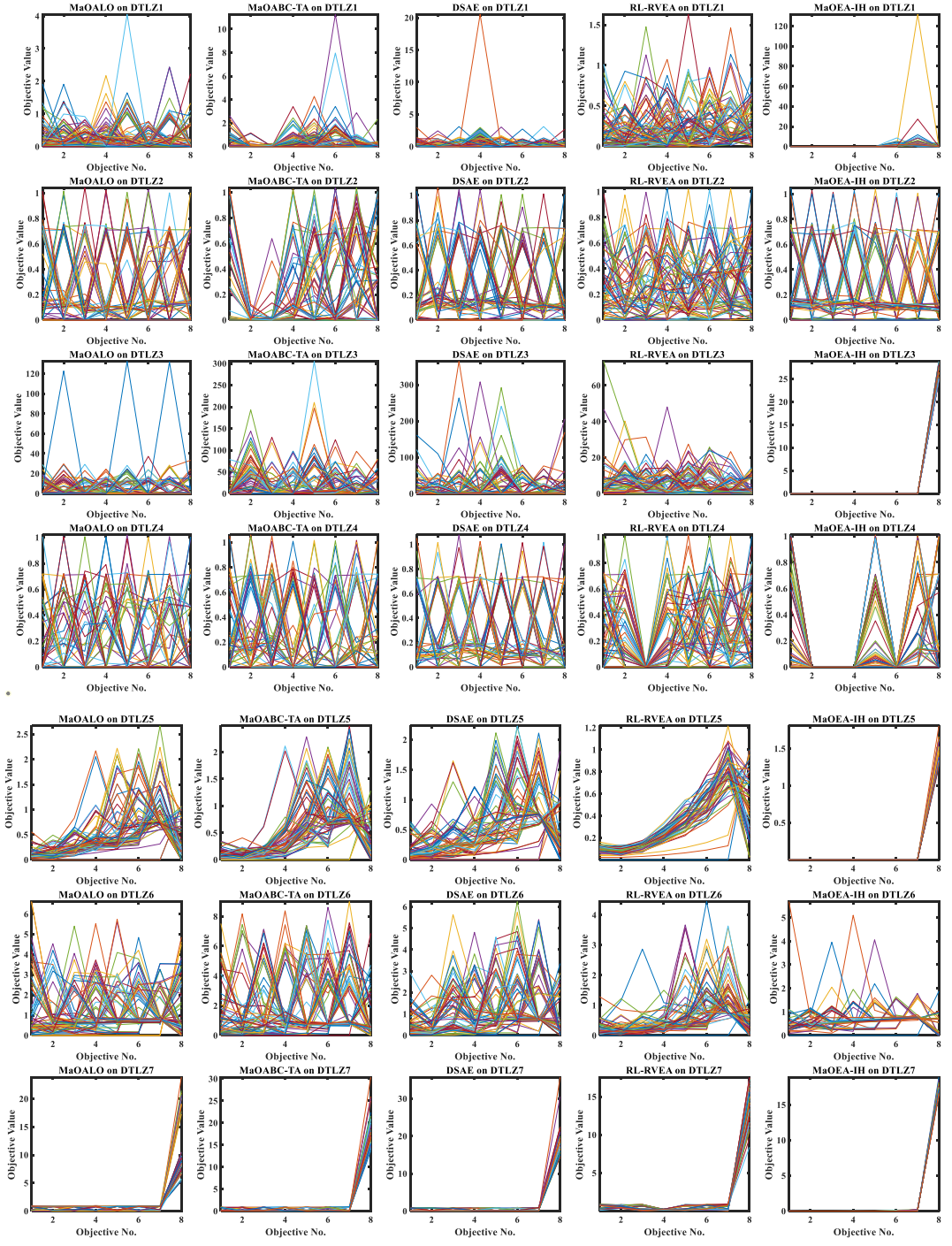

Fig. 11. Best Pareto optimal fronts obtained by various many-objective algorithms on DTLZ problems.

Funding

No Funding.

Institutional review board statement

Not applicable.

Table 16
Results of RT metric for various many-objective algorithms on DTLZ benchmark problems.

Problem	M	D	MaOALO	MaOABC-TA	DSAE	RL-RVEA	MaOEA-IH
DTLZ1	8	12	1.50	2.66	3.35	1.42E+01	9.47
DTLZ2	8	17	1.59	1.33	2.81	1.98E+01	1.27E+01
DTLZ3	8	17	1.42	2.64	4.46	1.64E+01	9.20
DTLZ4	8	17	1.72	2.81	3.08	3.24E+01	1.34E+01
DTLZ5	8	17	1.18	5.56	5.72	2.03E+01	1.24E+01
DTLZ6	8	17	1.35	2.52	2.86	2.00E+01	1.36E+01
DTLZ7	8	27	1.38	5.85	5.69	1.97E+01	1.45E+01

Informed consent statement

Not applicable.

Data availability statement

The data presented in this study are available through email upon request to the corresponding author.

CRediT authorship contribution statement

Kanak Kalita: Writing – review & editing, Writing – original draft, Visualization, Software, Methodology, Investigation, Formal analysis, Data curation, Conceptualization. **Sundaram B. Pandya:** Methodology, Investigation, Formal analysis, Data curation, Conceptualization. **Robert Čep:** Writing – review & editing, Resources, Project administration, Methodology. **Pradeep Jangir:** Writing – review & editing, Writing – original draft, Visualization, Software, Methodology, Investigation, Conceptualization. **Laith Abualigah:** Writing – review & editing, Supervision, Resources, Project administration, Methodology.

Declaration of competing interest

The authors declare that they have no known competing financial interests or personal relationships that could have appeared to influence the work reported in this paper.

Acknowledgments

This article was supported by the project Students Grant Competition SP2024/087, "Specific Research of Sustainable Manufacturing Technologies", financed by the Ministry of Education, Youth and Sports of Czech Republic and Faculty of Mechanical Engineering VŠB-TUO.

Appendix

Appendix A
Unconstrained Many-objective MaF test problems [55]:

Problem	Properties	Problem	Properties
MaF1	Linear	**MaF2**	Concave
MaF3	Convex, multimodal	**MaF4**	Concave, multimodal
MaF5	Convex, biased	**MaF6**	Concave, degenerate
MaF7	Mixed, disconnected, Multimodal	**MaF8**	Linear, degenerate
MaF9	Linear, degenerate	**MaF10**	Mixed, biased
MaF11	Convex, disconnected, nonseparable	**MaF12**	Concave, nonseparable, biased deceptive
MaF13	Concave, unimodal, nonseparable, degenerate	**MaF14**	Linear, partially separable, large scale
MaF15	Convex, partially separable, large scale		

Appendix B. Real World Many-objective engineering design Optimization Problems

B.1 RWMaOP1: Car cab design problem [56]

we consider the car cab design problem consisting of 11 decision variables and nine objectives. Among the decision variables, seven decision variables represent the thickness: B-Pillar inner (x_1), B-Pillar reinforcement (x_2), floor side inner (x_3), cross members (x_4), door beam (x_5), the door belt-line reinforcement (x_6) and roof rail (x_7). The remaining four variables are stochastic parameters that

indicate the material of B-Pillar inner (x_8), the material of floor side inner (x_9), the barrier height (x_{10}) and the barrier hitting position (x_{11}). real world many-objective car cab design optimization problem (RWMaOP1) as follows:

minimize

$$\text{weight of the car} = f_1(x) = 1.98 + 4.9x_1 + 6.67x_2 + 6.98x_3 + 4.01x_4 + 1.78x_5 + 0.00001x_6 + 2.73x_7$$

$$f_2(x) = \max\{g_1(x), 0\}$$

$$f_3(x) = \max\{g_2(x), 0\}$$

$$f_4(x) = \max\{g_3(x), 0\}$$

$$f_5(x) = \max\{g_4(x), 0\}$$

$$f_6(x) = \max\{g_5(x), 0\}$$

$$f_7(x) = \max\{g_6(x), 0\}$$

$$f_8(x) = \max\{g_7(x), 0\}$$

$$f_9(x) = \max\{g_8(x), 0\}$$

Subject to

$$g_1(x) = 1 - (1.16 - 0.3717x_2x_4 - 0.00931x_2x_{10} - 0.484x_3x_9 + 0.01343x_6x_{10}) \geq 0$$

$$g_2(x) = 0.32 - (0.261 - 0.0159x_1x_2 - 0.188x_1x_8 - 0.019x_2x_7 + 0.0144x_3x_5 + 0.8757x_5x_{10} + 0.08045x_6x_9 + 0.00139x_8x_{11} + 0.00001575x_{10}x_{11}) \geq 0$$

$$g_3(x) = 0.32 - (0.214 + 0.00817x_5 - 0.131x_1x_8 - 0.0704x_1x_9 + 0.03099x_2x_6 - 0.018x_2x_7 + 0.0208x_3x_8 + 0.121x_3x_9 - 0.00364x_5x_6 + 0.0007715x_5x_{10} - 0.0005354x_6x_{10} + 0.00121x_8x_{11} + 0.00184x_9x_{10} - 0.018x_2x_2) \geq 0$$

$$g_4(x) = 0.32 - (0.74 - 0.61x_2 - 0.163x_3x_8 + 0.001232x_3x_{10} - 0.166x_7x_9 + .227x_2x_2) \geq 0$$

$$g_5(x) = 32 - \left(\frac{URD * MRD * LRD}{3}\right) \geq 0$$

$$URD = 28.98 + 3.818x_3 - 4.2x_1x_2 + 0.0207x_5x_{10} + 6.63x_6x_9 - 7.77x_7x_8 + 0.32x_9x_{10}$$

$$MRD = 33.86 + 2.95x_3 + 0.1792x_{10} - 5.057x_1x_2 - 11x_2x_8 - 0.0215x_5x_{10} - 9.98x_7x_8 + 22x_8x_9$$

$$LRD = 46.36 - 9.9x_2 - 12.9x_1x_8 + 0.1107x_3x_{10}$$

$$g_6(x) = 32 - (4.72 - 0.5x - 4 - 0.19x_2x_3 - 0.0122x_4x_{10} + 0.009325x_6x_{10} + 0.000191x_{11}x_{11}) \geq 0$$

$$g_7(x) = 4 - (10.58 - 0.674x_1x_2 - 1.95x_2x_8 + .02054x_3x_{10} - .0198x_4x_{10} + .028x_6x_{10}) \geq 0$$

$$g_8(x) = 9.9 - (16.45 - 0.489x_3x_7 - 0.84x_5x_6 + 0.043x_9x_{10} - 0.0556x_9x_{11} - 0.000786x_{11}x_{11}) \geq 0$$

$$x_1 \in [0.5, 1.5]; x_2 \in [0.45, 1.35]; x_3 \in [0.5, 1.5]; x_4 \in [0.5, 1.5]; x_5 \in [0.875, 2.625]; x_6 \in [0.4, 1.2]; x_7 \in [0.4, 1.2];$$

B.2 RWMaOP2: 10-bar truss structure problem [57]

A mathematical programming problem of truss structure can be stated as follows. Find, $X = \{A_1, A_2, \ldots, A_m\}$ real world many-objective 10-bar truss structure optimization problem (RWMaOP2) To minimize the mass of truss, minimize compliance, maximize first natural frequency and minimize maximum buckling factor:

$$F_1(X) = \text{mass} = \sum_{i=1}^{m} A_i \rho L_i$$

$$F_2(X) = \text{compliance} = \delta^T * F$$

$$F_3(X) = \text{inverse of first natural frequency} = 1000000 * \left(\frac{1}{f_1}\right)$$

$$F_4(X) = \text{maximum buckling factor} = \max\left(\frac{\left|\sigma_j^{comp}\right|}{\sigma_j^{cr}}\right)$$

Subject to:

Behavior constraints:

$$g_1(X) : \textit{Stress constraints}, \frac{\max(|\sigma_j|) - \sigma_{\text{allowable}}}{\sigma_{\text{allowable}}} \leq 0$$

$$g_2(X) : \textit{Euler buckling constraints}, \max\left(\frac{\left|\sigma_j^{comp}\right| - \sigma_j^{cr}}{\sigma_j^{cr}}\right) \leq 0, \textit{where } \sigma_j^{cr} = \frac{kA_jE}{L_j^2}$$

Side constraints:

$$\textit{Cross} - \textit{sectional area constraints}, A_i^{\min} \leq A_i \leq A_i^{\max}$$

where.

A_i is a cross-section of i-th element
$A_i^{\min}$ is a minimum value of A
$A_i^{\max}$ is a maximum value of A
ρ is a density of truss material
L_i is a length of i-th truss member
δ is a displacement vector from finite element analysis
F is a load vector from finite element analysis
f_1 is the first natural frequency
σ_i^{comp} is compressive stress of i-th truss member
σ_i^{cr} is critical compressive stress of i-th truss member
i is an index of a compressive truss member
m is number of compressive truss members
j is an index of a degrees of freedom
n is number of degrees of freedom
k is Euler buckling coefficient which is set to 3.96
σ_i^{cr} is allowable buckling stress of i-th compressive member
E is the modulus of elasticity
A_i is the cross-section area of i-th compressive member.
L_i is the length of the i-th compressive member. Elemental cross-sections are assumed to be countable variables as beam regular sections It is assumed that the properties and permittable limits of all trusses are the same. Mass Density (ρ), elastic modulus (E) and permittable stress ($\sigma^{\max}$) are assumed as 7850 kg/m^3, 200GPa and 400MPa respectively.

B.3 RWMaOP3: Water and oil repellent fabric development [58]

One of the aims of the textile industry is to produce fabrics with high added value. Specifically, one of the most common alterations to textiles is the repellency of water and oil, feature known as hydrophobicity effect. Consequently, hydrophobicity can be assessed through seven criteria: the water ($f_1(\mathbf{x}) = -WCA$) and oil ($f_2(\mathbf{x}) = -OCA$) droplet contact angle; the air permeability ($f_3(\mathbf{x}) = -AP$), which measures the airflow through a woven fabric as a comforting property; the crease recovery angle ($f_4(\mathbf{x}) = -CRA$), which measures the ability of textiles to recover from creasing; the stiffness ($f_5(\mathbf{x}) = Stiff$), which is the cotton fabric comfort property; the tear strength ($f_6(\mathbf{x}) = -Tear$) of the finished fabric, which depends on the chemical finishing treatment applied to the fabric; and the tensile strength ($f_7(\mathbf{x}) = -Tensile$), which describes the fabric behavior under axial stretching load. The previous seven criteria can be considered as objective functions real world many-objective Water and oil repellent fabric development optimization problem (RWMaOP3) as follows:

minimize

$$f_1(\mathbf{x}) = -WCA = -\big(-1331.04 + 1.99 \times O\text{-}CPC + 0.33 \times K\text{-}FEL + 17.12 \times C\text{-}Temp - 0.02 \times O\text{-}CPC^2 - 0.05 \times C\text{-}Temp^2 \pm 15.33\big).$$

$$f_2(\mathbf{x}) = -OCA = -\big(-4231.14 + 4.27 \times O\text{-}CPC + 1.50 \times K\text{-}FEL + 52.30 \times C\text{-}Temp - 0.04 \times O\text{-}CPC \times K\text{-}FEL - 0.04 \times O\text{-}CPC^2 - 0.16 \times C\text{-}Temp^2 \pm 29.33\big).$$

$$f_3(\mathbf{x}) = -AP = -\big(1766.80 - 32.32 \times O\text{-}CPC - 24.56 \times K\text{-}FEL - 10.48 \times C\text{-}Temp + 0.24 \times O\text{-}CPC \times C\text{-}Temp + 0.19 \times K\text{-}FEL \times C\text{-}Temp - 0.06 \times O\text{-}CPC^2 - 0.10 \times K\text{-}FEL^2 \pm 413.33\big).$$

$$f_4(\mathbf{x}) = -CRA = -\big(-2342.13 - 1.556 \times O\text{-}CPC + 0.77 \times K\text{-}FEL + 31.14 \times C\text{-}Temp + 0.03 \times O\text{-}CPC^2 - 0.10 \times C\text{-}Temp^2 \pm 73.33\big).$$

$$f_5(\mathbf{x}) = Stiff = 9.34 + 0.02 \times O\text{-}CPC - 0.03 \times K\text{-}FEL - 0.03 \times C\text{-}Temp - 0.001 \times O\text{-}CPC \times K\text{-}FEL + 0.0009 \times K\text{-}FEL^2 \pm 0.22.$$

$$f_6(\mathbf{x}) = -Tear = -\big(1954.71 + 14.246 \times O\text{-}CPC + 5.00 \times K\text{-}FEL - 4.30 \times C\text{-}Temp - 0.22 \times O\text{-}CPC^2 - 0.33 \times K\text{-}FEL^2 \pm 8413.33\big).$$

$$f_7(\mathbf{x}) = -Tensile = -\big(828.16 + 3.55 \times O\text{-}CPC + 73.65 \times K\text{-}FEL + 10.80 \times C\text{-}Temp - 0.56 \times K\text{-}FEL \times C\text{-}Temp + 0.20 \times K\text{-}FEL^2 \pm 2814.83\big).$$

and $\mathbf{x} = (O-CPC, K-FEL, C-Temp)^T$, such that $10 \le O-CPC \le 50$, is the concentration of water and oil repellent finish in g/L, $10 \le K-FEL \le 50$, is the concentration of the crosslinking agent in g/L and $150 \le C\text{-Temp} \le 170$, is the curing temperature in $^\circ C$.

B.4 RWMaOP4: Ultra-wideband antenna design [59]

With the aim of designing a two-stopband ultra-wideband antenna, additionally to reaching the appropriate impedance features, high fidelity and gain uniformity are also expected. Such an antenna consists of a planar rectangular patch and one notch at each of two lower corners. Two U-shaped narrow grooves are cut in the monopole patch for each stopband. In order to design this antenna, ten parameters (lengths in mm) and five objective functions must be considered. More precisely, the objective functions to consider are the voltage standing wave ratio (VSWR) over the passband ($f_1(\mathbf{x}) = VPVP$), the VSWR over the WiMAX band ($f_2(\mathbf{x}) = -VWi$), the VSWR over the WLAN band $\big(f_3(\mathbf{x}) = -VWL\big)$, the E− and H-planes fidelity factor $\big(f_4(\mathbf{x}) = -FF\big)$ and the maximum gain over the passband $\big(f_5(\mathbf{x}) = PG\big)$. Hence, the real world many-objective Ultra-wideband antenna design optimization problem (RWMaOP4) is stated as:

minimize

$$f_1(\mathbf{x}) = VP = 502.94 - 27.18 \times ((w_1 - 20.0)/0.5) + 43.08 \times ((l_1 - 20.0)/2.5) + 47.75 \times (a_1 - 6.0) + 32.25 \times ((b1 - 5.5)/0.5) + 31.67 \times (a_2 - 11.0) - 36.19 \times ((w_1 - 20.0)/0.5) \times ((w_2 - 2.5)/0.5) - 39.44 \times ((w_1 - 20.0)/0.5) \times (a_1 - 6.0) + 57.45 \times (a_1 - 6.0) \times ((b_1 - 5.5)/0.5).$$

$$f_2(\mathbf{x}) = -VWi = -(130.53 + 45.97 \times ((l_1 - 20.0)/2.5) - 52.93 \times ((w_1 - 20.0)/0.5) - 78.93 \times (a_1 - 6.0) + 79.22 \times (a_2 - 11.0) + 47.23 \times ((w_1 - 20.0)/0.5) \times (a_1 - 6.0) - 40.61 \times ((w_1 - 20.0)/0.5) \times (a_2 - 11.0) - 50.62 \times (a_1 - 6.0) \times (a_2 - 11.0))(w_1 - 20.0)/0.5) - 78.93 \times (a_1 - 6.0) + 79.22 \times (a_2 - 11.0) + 47.23 \times ((w_1 - 20.0)/0.5) \times (a_1 - 6.0) - 40.61 \times ((w_1 - 20.0)/0.5) \times (a_2 - 11.0) - 50.62 \times (a_1 - 6.0) \times (a_2 - 11.0))130.53 + 45.97 \times ((l_1 - 20.0)/2.5) - 52.93 \times .$$

$$f_3(\mathbf{x}) = -VWL = -(203.16 - 42.75 \times ((w_1 - 20.0)/0.5) + 56.67 \times (a_1 - 6.0) + 19.88 \times ((b_1 - 5.5)/0.5) - 12.89 \times (a_2 - 11.0) - 35.09 \times (a_1 - 6.0) \times ((b_1 - 5.5)/0.5) - 22.91 \times ((b_1 - 5.5)/0.5) \times (a_2 - 11.0)).$$

$$f_4(\mathbf{x}) = -FF = -(0.76 - 0.06 \times ((l_1 - 20.0)/2.5) + 0.03 \times ((l_2 - 2.5)/0.5) + 0.02 \times (a_2 - 11.0) - 0.02 \times ((b_2 - 6.5)/0.5) - 0.03 \times ((d_2 - 12.0)/0.5) + 0.03 \times ((l_1 - 20.0)/2.5) \times ((w_1 - 20.0)/0.5) - 0.02 \times ((l_1 - 20.0)/2.5) \times ((l_2 - 2.5)/0.5) + 0.02 \times ((l_1 - 20.0)/2.5) \times ((b_2 - 6.5)/0.5)).$$

$$f_5(\mathbf{x}) = PG = 1.08 - 0.12 \times ((l_1 - 20.0)/2.5) - 0.26 \times ((w_1 - 20.0)/0.5) - 0.05 \times (a_2 - 11.0) - 0.12 \times ((b_2 - 6.5)/0.5) + 0.08 \times (a_1 - 6.0) \times ((b_2 - 6.5)/0.5) + 0.07 \times (a_2 - 6.0) \times ((b_2 - 5.5)/0.5).$$

and $\mathbf{x} = (a_1, a_2, b_1, b_2, d_1, d_2, l_1, l_2, w_1, w_2)^T$, such that $5 \le a_1 \le 7, 10 \le a_2 \le 12{,}5 \le b_1 \le 6{,}6 \le b_2 \le 7{,}3 \le d_1 \le 4{,}11.5 \le d_2 \le 12.5$,

$17.5 \leq l_1 \leq 22.5, 2 \leq l_2 \leq 3, 17.5 \leq w_1 \leq 22.5$ and $2 \leq w_2 \leq 3$.

B.5 RWMaOP5: Liquid-rocket single element injector design [60]

A four objective functions that proper injector design can achieve such goals. Therefore, for a desirable injector design, the maximum temperature of the injector surface ($f_1(\mathbf{x}) = TF_{\max}$), the temperature at three inches from the injector surface ($f_2(\mathbf{x}) = TW_4$), the maximum temperature at the tip of the injector post ($f_3(\mathbf{x}) = TT_{\max}$) and the objectives to be considered are— the distance from the inlet combustion ($f_4(\mathbf{x}) = X_{cc}$), where 99% of the combustion is complete. Thus, the real world many-objective Liquid-rocket single element injector design optimization problem (RWMaOP5) can be written as:

minimize

$$\begin{aligned} f_1(\mathbf{x}) = TF_{max} = {} & 0.692 + 0.477 \times \alpha - 0.687 \times \Delta HA - 0.080 \times \Delta OA - 0.0650 \times OPTT - 0.167 \times \alpha^2 - 0.0129 \times \Delta HA \times \alpha \\ & + 0.0796 \times \Delta HA^2 - 0.0634 \times \Delta OA \times \alpha - 0.0257 \times \Delta OA \times \Delta HA + 0.0877 \times \Delta OA^2 - 0.0521 \times OPTT \times \alpha \\ & + 0.00156 \times OPTT \times \Delta HA + 0.00198 \times OPTT \times \Delta OA + 0.0184 \times OPTT^2. \end{aligned}$$

$$\begin{aligned} f_2(\mathbf{x}) = TW_4 = {} & 0.758 + 0.358 \times \alpha - 0.807 \times \Delta HA + 0.0925 \times \Delta OA - 0.0468 \times OPTT - 0.172 \times \alpha^2 + 0.0106 \times \Delta HA \times \alpha \\ & + 0.0697 \times \Delta HA^2 - 0.146 \times \Delta OA \times \alpha - 0.0416 \times \Delta OA \times \Delta HA + 0.102 \times \Delta OA^2 - 0.0694 \times OPTT \times \alpha \\ & - 0.00503 \times OPTT \times \Delta HA + 0.0151 \times OPTT \times \Delta OA + 0.0173 \times OPTT^2. \end{aligned}$$

$$\begin{aligned} f_3(\mathbf{x}) = TT_{max} = {} & 0.370 - 0.205 \times \alpha + 0.0307 \times \Delta HA + 0.108 \times \Delta OA + 1.019 \times OPTT - 0.135 \times \alpha^2 + 0.0141 \times \Delta HA \times \alpha \\ & + 0.0998 \times \Delta HA^2 + 0.208 \times \Delta OA \times \alpha - 0.0301 \times \Delta OA \times \Delta HA - 0.226 \times \Delta OA^2 + 0.353 \times OPTT \times \alpha - 0.0497 \\ & \times OPTT \times \Delta OA - 0.423 \times OPTT^2 + 0.202 \times \Delta HA \times \alpha^2 - 0.281 \times \Delta OA \times \alpha^2 - 0.342 \times \Delta HA^2 \times \alpha - 0.245 \\ & \times \Delta HA^2 \times \Delta OA + 0.281 \times \Delta OA^2 \times \Delta HA - 0.184 \times OPTT^2 \times \alpha + 0.281 \times \Delta HA \times \alpha \times \Delta OA. \end{aligned}$$

$$\begin{aligned} f_4(\mathbf{x}) = X_{cc} = {} & 0.153 - 0.322 \times \alpha + 0.396 \times \Delta HA + 0.424 \times \Delta OA + 0.0226 \times OPTT + 0.175 \times \alpha^2 + 0.0185 \times \Delta HA \times \alpha \\ & - 0.0701 \times \Delta HA^2 - 0.251 \times \Delta OA \times \alpha + 0.179 \times \Delta OA \times \Delta HA + 0.0150 \times \Delta OA^2 + 0.0134 \times OPTT \times \alpha + 0.0296 \times OPTT \\ & \times \Delta HA + 0.0752 \times OPTT \times \Delta OA + 0.0192 \times OPTT^2. \end{aligned}$$

and $\mathbf{x} = (\alpha, \triangle HA, \triangle OA, OPTT)^T$, such that $0 \leq \alpha \leq 20$, is the hydrogen flow angle in degrees $(^\circ)$, $0 \leq \Delta HA \leq 25$, the hydrogen area increment, in percentage, with respect to the standard cross-sectional area (0.0186in^2) of the tube carrying hydrogen, $-40 \leq \Delta OA \leq 0$, is the oxygen area decrease, in percentage, regarding the standard cross-sectional area (0.0423in^2) of the tube transporting oxygen and $X'' \leq OPTT \leq 2X''$, is the oxidizer post tip thickness in in and X'' is the tip thickness with a standard value of 0.01in.

References

[1] Z. Xiao, J. Shu, H. Jiang, J.C.S. Lui, G. Min, J. Liu, S. Dustdar, Multi-objective parallel task offloading and content caching in d2d-aided MEC networks, IEEE Trans. Mobile Comput. 22 (11) (2023) 6599–6615, https://doi.org/10.1109/TMC.2022.3199876.

[2] B. Cao, J. Zhao, P. Yang, Y. Gu, K. Muhammad, J.J.P.C. Rodrigues, V.H.C. de Albuquerque, Multiobjective 3-D topology optimization of next-generation wireless data center network, IEEE Trans. Ind. Inf. 16 (5) (2020) 3597–3605, https://doi.org/10.1109/TII.2019.2952565.

[3] H. Ishibuchi, N. Tsukamoto, Y. Nojima, Evolutionary many-objective optimization: a short review, in: Proceedings of the IEEE Congress Evolutionary Computation, IEEE World Congress Computational Intelligence), Hong Kong, 2008, pp. 2419–2426, https://doi.org/10.1109/CEC.2008.4631121.

[4] B. Cao, J. Zhao, Y. Gu, Y. Ling, X. Ma, Applying graph-based differential grouping for multiobjective large-scale optimization, Swarm Evol. Comput. 53 (2020) 100626, https://doi.org/10.1016/j.swevo.2019.100626.

[5] L. Yin, M. Zhuang, J. Jia, H. Wang, Energy saving in flow-shop scheduling management: an improved multiobjective model based on grey wolf optimization algorithm, Math. Probl Eng. 2020 (2020) 9462048, https://doi.org/10.1155/2020/9462048.

[6] Q. Lin, J. Li, Z. Du, J. Chen, Z. Ming, A novel multi-objective particle swarm optimization with multiple search strategies, Eur. J. Oper. Res. 247 (3) (2015) 732–744, https://doi.org/10.1016/j.ejor.2015.06.071.

[7] Q. Zhang, J. Liu, X. Yao, An efficient many objective optimization algorithm with few parameters, Swarm Evol. Comput. 83 (2023), https://doi.org/10.1016/j.swevo.2023.101405.

[8] X. Wu, S. Dong, J. Hu, Z. Huang, An efficient many-objective optimization algorithm for computation offloading in heterogeneous vehicular edge computing network, Simulat. Model. Pract. Theor. 131 (2024), https://doi.org/10.1016/j.simpat.2023.102870.

[9] Q. Li, Z. Shi, Z. Xue, Z. Cui, Y. Xu, A many-objective evolutionary algorithm for solving computation offloading problems under uncertain communication conditions, Comput. Commun. 213 (2024) 22–32, https://doi.org/10.1016/j.comcom.2023.10.020.

[10] F. Ming, W. Gong, L. Wang, L. Gao, A constraint-handling technique for decomposition-based constrained many-objective evolutionary algorithms, IEEE Transactions on Systems, Man and Cybernetics: Systems 53 (2023) 7783–7793, https://doi.org/10.1109/TSMC.2023.3299570.

[11] W. Zhang, J. Liu, J. Liu, Y. Liu, H. Wang, A many-objective evolutionary algorithm based on novel fitness estimation and grouping layering, Neural Comput. Appl. 35 (34) (2023) 24283–24314, https://doi.org/10.1007/s00521-023-08950-x.

[12] Z. Shi, T. Zhao, Q. Li, Z. Zhang, Z. Cui, Workflow migration in uncertain edge computing environments based on interval many-objective evolutionary algorithm, Egyptian Informatics Journal 24 (4) (2023), https://doi.org/10.1016/j.eij.2023.100418.

[13] Z. Zhai, Y. Tan, X. Li, J. Li, H. Zhang, A composite surrogate-assisted evolutionary algorithm for expensive many-objective optimization, Expert Syst. Appl. 236 (2024), https://doi.org/10.1016/j.eswa.2023.121374.

[14] V. Palakonda, J.-M. Kang, Pre-DEMO: preference-inspired differential evolution for multi/many-objective optimization, IEEE Transactions on Systems, Man and Cybernetics: Systems 53 (12) (2023) 7618–7630, https://doi.org/10.1109/TSMC.2023.3298690.

[15] Y. Sun, Y. Cao, S. Cheng, J. Yang, W. Shi, A. Zhang, J. Ju, A many objective commercial recommendation algorithm via Game-Based core node extraction, Egyptian Informatics Journal 24 (4) (2023), https://doi.org/10.1016/j.eij.2023.100419.

[16] J. Cai, J. Yang, J. Wen, H. Zhao, Z. Cui, A game theory based many-objective hybrid tensor decomposition for skin cancer prediction, Expert Syst. Appl. 239 (2024), https://doi.org/10.1016/j.eswa.2023.122425.

[17] W. Wang, S. Zhang, W. Song, W. Ge, Preference-inspired coevolutionary algorithm with sparse autoencoder for many-objective optimization, Soft Comput. 27 (23) (2023) 17729–17745, https://doi.org/10.1007/s00500-023-09050-7.

[18] L.A. Márquez-Vega, J.G. Falcón-Cardona, E. Covantes Osuna, On the adaptation of reference sets using niching and pair-potential energy functions for multi-objective optimization, Swarm Evol. Comput. 83 (2023), https://doi.org/10.1016/j.swevo.2023.101408.

[19] T. Ye, H. Wang, T. Zeng, M.G.H. Omran, F. Wang, Z. Cui, J. Zhao, An improved two-archive artificial bee colony algorithm for many-objective optimization, Expert Syst. Appl. 236 (2024), https://doi.org/10.1016/j.eswa.2023.121281.

[20] Z. Liu, F. Han, Q. Ling, H. Han, J. Jiang, A many-objective optimization evolutionary algorithm based on hyper-dominance degree, Swarm Evol. Comput. 83 (2023), https://doi.org/10.1016/j.swevo.2023.101411.

[21] W. Zhang, J. Liu, J. Liu, Y. Liu, S. Tan, A dual distance dominance based evolutionary algorithm with selection-replacement operator for many-objective optimization, Expert Syst. Appl. 237 (2024), https://doi.org/10.1016/j.eswa.2024.124226.

[22] Y. Sun, J. Liu, Z. Liu, MaOEA/D with adaptive external population guided weight vector adjustment, Expert Syst. Appl. 242 (2024), https://doi.org/10.1016/j.eswa.2023.122720.

[23] C. Dai, C. Peng, X. Lei, A point crowding-degree based evolutionary algorithm for many-objective optimization, Memetic Computing 15 (4) (2023) 391–403, https://doi.org/10.1007/s12293-023-00398-9.

[24] M. Jameel, M. Abouhawwash, A new proximity metric based on optimality conditions for single and multi-objective optimization: method and validation, Expert Syst. Appl. 241 (2024), https://doi.org/10.1016/j.eswa.2023.122677.

[25] P. Liang, Y. Chen, Y. Sun, Y. Huang, W. Li, An information entropy-driven evolutionary algorithm based on reinforcement learning for many-objective optimization, Expert Syst. Appl. 238 (2024), https://doi.org/10.1016/j.eswa.2023.122164.

[26] Q. Liu, Y. Jin, M. Heiderich, T. Rodemann, G. Yu, An adaptive reference vectorguided evolutionary algorithm using growing neural gas for many-objective optimization of irregular problems, IEEE Trans. Cybern. 52 (5) (2022) 2698–2711, https://doi.org/10.1109/TCYB.2020.3020630.

[27] Z. Song, H. Wang, H. Xu, A framework for expensive many-objective optimization with Pareto-based bi-indicator infill sampling criterion, Memetic Computing 14 (2) (2022) 179–191, https://doi.org/10.1007/s12293-021-00351-8.

[28] C. Zhang, L. Zhou, Y. Li, Pareto optimal reconfiguration planning and distributed parallel motion control of mobile modular robots, IEEE Trans. Ind. Electron. 71 (8) (2024) 9255–9264, https://doi.org/10.1109/TIE.2023.3321997.

[29] C. Zhu, M. Wang, M. Guo, J. Deng, Q. Du, W. Wei, A. Mohebbi, An innovative process design and multi-criteria study/optimization of a biomass digestion-supercritical carbon dioxide scenario toward boosting a geothermal-driven cogeneration system for power and heat, Energy 292 (2024) 130408, https://doi.org/10.1016/j.energy.2024.130408.

[30] Y. Tian, H. Wang, X. Zhang, Y. Jin, Effectiveness and efficiency of non-dominated sorting for evolutionary multi- and many-objective optimization, Complex and Intelligent Systems 3 (4) (2017) 247–263, https://doi.org/10.1007/s40747-017-0057-5.

[31] K. Ikeda, H. Kita, S. Kobayashi, Failure of Pareto-based MOEAs: does nondominated really mean near to optimal?, in: Proceedings of the 2001 Congress on Evolutionary Computation, CEC IEEE Publications Congress on Evolutionary Computation, 2001, pp. 957–962, https://doi.org/10.1109/CEC.2001.934293 (Institute of Electrical and Electronics Engineers. Cat. No. 01TH8546).

[32] H. Sato, H.E. Aguirre, K. Tanaka, Improved S-CDAs using crossover controlling the number of crossed genes for many-objective optimization, in: Proceedings of the 13th Annual Genetic and Evolutionary Computation Conference, 2011, pp. 753–760, https://doi.org/10.1145/2001576.2001679. Dublin, Ireland.

[33] C. Zhu, L. Xu, E.D. Goodman, Generalization of Pareto-optimality for manyobjective evolutionary optimization, IEEE Trans. Evol. Comput. 20 (2) (2016) 299–315, https://doi.org/10.1109/TEVC.2015.2457245.

[34] S. Yang, M. Li, X. Liu, J. Zheng, A grid-based evolutionary algorithm for many-objective optimization, IEEE Trans. Evol. Comput. 17 (5) (2013) 721–736, https://doi.org/10.1109/TEVC.2012.2227145.

[35] M. Li, S. Yang, X. Liu, Shift-based density estimation for Pareto-based algorithms in many-objective optimization, IEEE Trans. Evol. Comput. 18 (3) (2014) 348–365, https://doi.org/10.1109/TEVC.2013.2262178.

[36] J. Bader, E. Zitzler, HypE: an algorithm for fast hypervolume-based manyobjective optimization, Evol. Comput. 19 (1) (2011) 45–76, https://doi.org/10.1162/EVCO_a_00009.

[37] J. Luo, X. Huang, Y. Yang, X. Li, Z. Wang, J. Feng, A many-objective particle swarm optimizer based on indicator and direction vectors for many-objective optimization, Inf. Sci. 514 (2020) 166–202, https://doi.org/10.1016/j.ins.2019.11.047.

[38] L. Li, G.G. Yen, A. Sahoo, L. Chang, T. Gu, On the estimation of pareto front and dimensional similarity in many-objective evolutionary algorithm, Inf. Sci. 563 (2021) 375–400, https://doi.org/10.1016/j.ins.2021.03.008.

[39] R. Cheng, Y. Jin, M. Olhofer, B. Sendhoff, A reference vector guided evolutionary algorithm for many-objective optimization, IEEE Trans. Evol. Comput. 20 (5) (2016) 773–791, https://doi.org/10.1109/TEVC.2016.2519378.

[40] Y. Yuan, H. Xu, B. Wang, X. Yao, A new dominance relation-based evolutionary algorithm for many-objective optimization, IEEE Trans. Evol. Comput. 20 (1) (2016) 16–37, https://doi.org/10.1109/TEVC.2015.2420112.

[41] H. Chen, Y. Tian, W. Pedrycz, G. Wu, R. Wang, L. Wang, Hyperplane assisted evolutionary algorithm for many-objective optimization problems, IEEE Trans. Cybern. 50 (7) (2020) 3367–3380, https://doi.org/10.1109/TCYB.2019.2899225.

[42] Y. Xiang, Y. Zhou, M. Li, Z. Chen, A vector angle-based evolutionary algorithm for unconstrained many-objective optimization, IEEE Trans. Evol. Comput. 21 (1) (2017) 131–152, https://doi.org/10.1109/TEVC.2016.2587808.

[43] J. Shen, P. Wang, X. Wang, A controlled strengthened dominance relation for evolutionary many-objective optimization, IEEE Trans. Cybern. 52 (5) (2022) 3645–3657, https://doi.org/10.1109/TCYB.2020.3015998.

[44] Q. Gu, Q. Xu, X. Li, An improved NSGA-III algorithm based on distance dominance relation for many-objective optimization, Expert Syst. Appl. 207 (2022) 117738, https://doi.org/10.1016/j.eswa.2022.117738.

[45] Q. Lin, S. Liu, Q. Zhu, C. Tang, R. Song, J. Chen, C.A.C. Coello, K. Wong, J. Zhang, Particle swarm optimization with a balanceable fitness estimation for many-objective optimization problems, IEEE Trans. Evol. Comput. 22 (1) (2018) 32–46, https://doi.org/10.1109/TEVC.2016.2631279.

[46] S.C. Liu, Z.H. Zhan, K.C. Tan, J. Zhang, A multiobjective framework for manyobjective optimization, IEEE Trans. Cybern. 52 (12) (2022) 13654–13668, https://doi.org/10.1109/TCYB.2021.3082200.

[47] Q. Lin, S. Liu, K.C. Wong, M. Gong, C.A.C. Coello, J. Chen, J. Zhang, A clustering-based evolutionary algorithm for many-objective optimization problems, IEEE Trans. Evol. Comput. 23 (3) (2018) 391–405, https://doi.org/10.1109/TEVC.2018.2866927.

[48] S. Liu, Q. Yu, Q. Lin, K.C. Tan, An adaptive clustering-based evolutionary algorithm for many-objective optimization problems, Inf. Sci. 537 (2020) 261–283, https://doi.org/10.1016/j.ins.2020.03.104.

[49] S. Liu, J. Zheng, Q. Lin, K.C. Tan, Evolutionary multi and many-objective optimization via clustering for environmental selection, Inf. Sci. 578 (2021) 930–949, https://doi.org/10.1016/j.ins.2021.08.054.

[50] S. Liu, Q. Lin, K.C. Wong, L. Ma, C.A.C. Coello, D. Gong, A novel multi-objective evolutionary algorithm with dynamic decomposition strategy, Swarm Evol. Comput. 48 (2019) 182–200, https://doi.org/10.1016/j.swevo.2019.02.010.

[51] S. Liu, Q. Lin, K.C. Tan, M. Gong, C.A.C. Coello, A fuzzy decomposition-based multi/many-objective evolutionary algorithm, IEEE Trans. Cybern. 52 (5) (2020) 3495–3509, https://doi.org/10.1109/TCYB.2020.3008697.
[52] S. Liu, Q. Lin, K.C. Wong, C.A.C. Coello, J. Li, Z. Ming, J. Zhang, A self-guided reference vector strategy for many-objective optimization, IEEE Trans. Cybern. 52 (2) (2020) 1164–1178, https://doi.org/10.1109/TCYB.2020.2971638.
[53] S. Liu, Q. Lin, J. Li, K.C. Tan, A survey on learnable evolutionary algorithms for scalable multiobjective optimization, IEEE Trans. Evol. Comput. (2023), https://doi.org/10.1109/TEVC.2023.3250350.
[54] S. Mirjalili, The ant lion optimizer, Adv. Eng. Software 83 (2015) 80–98, https://doi.org/10.1016/j.advengsoft.2015.01.010.
[55] R. Cheng, M. Li, Y. Tian, X. Zhang, S. Yang, Y. Jin, X. Yao, A benchmark test suite for evolutionary many-objective optimization, Complex and Intelligent Systems 3 (1) (2017) 67–81, https://doi.org/10.1007/s40747-017-0039-7.
[56] R. Tanabe, H. Ishibuchi, An easy-to-use real-world multi-objective optimization problem suite, Appl. Soft Comput. 89 (2020), https://doi.org/10.1016/j.asoc.2020.106078 article 106078.
[57] N. Panagant, S. Kumar, G.G. Tejani, N. Pholdee, S. Bureerat, Many-objective meta-heuristic methods for solving constrained truss optimisation problems: a comparative analysis, MethodsX 10 (2023) 102181, https://doi.org/10.1016/j.mex.2023.102181.
[58] N. Ahmad, S. Kamal, Z.A. Raza, T. Hussain, Multi-objective optimization in the development of oil and water repellent cellulose fabric based on response surface methodology and the desirability function, Mater. Res. Express 4 (3) (2017), https://doi.org/10.1088/2053-1591/aa5f6a article 035302.
[59] Y.-S. Chen, Performance enhancement of multiband antennas through a two-stage optimization technique, Int. J. RF Microw. Computer-Aided Eng. 27 (2) (2017), https://doi.org/10.1002/mmce.21064 article e21064.
[60] T. Goel, R. Vaidyanathan, R.T. Haftka, W. Shyy, N.V. Queipo, K. Tucker, Response surface approximation of Pareto optimal front in multi-objective optimization, Comput. Methods Appl. Mech. Eng. 196 (4–6) (2007) 879–893, https://doi.org/10.1016/j.cma.2006.07.010.
[61] C.A. Coello Coello, G.B. Lamont, D.A. Van Veldhuizen, Evolutionary algorithms for solving multi-objective problems. Genetic and Evolutionary Computation Series, second ed., Springer, 2007 https://doi.org/10.1007/978-0-387-36797-2.
[62] Y. Tian, R. Cheng, X. Zhang, F. Cheng, Y. Jin, An indicator-based multiobjective evolutionary algorithm with reference point adaptation for better versatility, IEEE Trans. Evol. Comput. 22 (4) (2018) 609–622, https://doi.org/10.1109/TEVC.2017.2749619.
[63] P. Jangir, P. Manoharan, S. Pandya, R. Sowmya, Objective teaching-learning-based optimizer for control and monitoring the optimal power flow of modern power systems, Int. J. Ind. Eng. Comput. 14 (2) (2023) 293–308, https://doi.org/10.5267/j.ijiec.2023.1.003. MaOTLBO.
[64] K. Deb, H. Jain, An evolutionary many-objective optimization algorithm using reference-point-based nondominated sorting approach, Part I: solving problems with box constraints, IEEE Trans. Evol. Comput. 18 (4) (2014) 577–601, https://doi.org/10.1109/TEVC.2013.2281535.
[65] S. Zhou, Y. Dai, Z. Chen, Dominance relation selection and angle-based distribution evaluation for many-objective evolutionary algorithm, Swarm Evol. Comput. 86 (2024) 101515, https://doi.org/10.1016/j.swevo.2024.101515.
[66] Z. Zhang, X. Shi, Z. Zhang, Z. Cui, W. Zhang, J. Chen, A many-objective evolutionary algorithm assisted by ideal hyperplane, Swarm Evol. Comput. 84 (2024) 101461, https://doi.org/10.1016/j.swevo.2023.101461.